Postaudit of Head and Transmissivity Estimates and Ground-Water Flow Models of Avra Valley, Arizona

U.S. GEOLOGICAL SURVEY
Water-Resources Investigations Report 96—4045

Prepared in cooperation with the
ARIZONA DEPARTMENT OF WATER RESOURCES
and CITY OF TUCSON

Postaudit of Head and Transmissivity Estimates and Ground-Water Flow Models of Avra Valley, Arizona

By R.T. HANSON

U.S. GEOLOGICAL SURVEY
Water-Resources Investigations Report 96—4045

Prepared in cooperation with the
ARIZONA DEPARTMENT OF WATER RESOURCES
and CITY OF TUCSON

Tucson, Arizona
1996

U.S. DEPARTMENT OF THE INTERIOR
BRUCE BABBITT, Secretary

U.S. GEOLOGICAL SURVEY
Gordon P. Eaton, Director

For additional information
write to:

District Chief
U.S. Geological Survey
Water Resources Division
375 South Euclid Avenue
Tucson, AZ 85719-6644

Copies of this report can be
purchased from:

U.S. Geological Survey
Open-File Section
Box 25286, MS 517
Denver Federal Center
Denver, CO 80225

CONTENTS

FIGURES

FIGURES—Continued Page

FIGURES—Continued Page

TABLES

CONVERSION FACTORS

Multiply	By	To obtain
foot (ft)	0.3048	meter
square mile (mi^2)	2.590	square kilometer
acre-foot (ft)	0.001233	cubic hectometer
foot per day per foot [(ft/d)/ft]	1	meter per day per meter
square foot (ft^2)	0.09294	square meter
foot squared per day (ft^2/d)	0.0929	meter squared per day
acre-foot per square mile (acre-ft/mi^2)	4.763	cubic meter per hectare
gallon per minute	0.06308	liter per minute
gallon per minute per foot [(gal/min)/ft]	0.2070	liter per minute per meter

WELL-NUMBERING AND NAMING SYSTEM

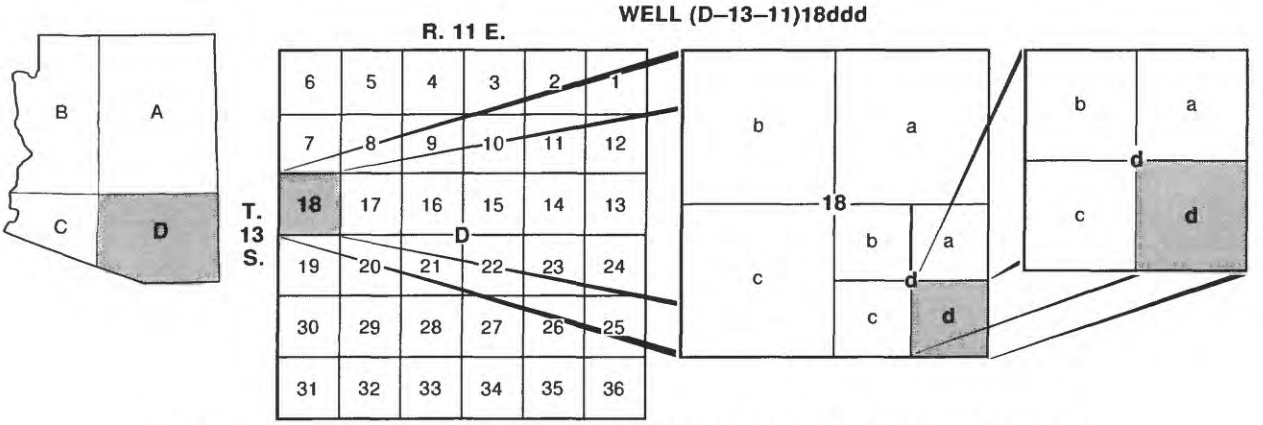

Quadrant D, Township 13 South, Range 11 East, section 18, quarter section d, quarter section d, quarter section d

The well numbers used by the U.S. Geological Survey in Arizona are in accordance with the Bureau of Land Management's system of land subdivision. The land survey in Arizona is based on the Gila and Salt River Meridian and Base Line, which divide the State into four quadrants that are designated by capital letters A, B, C, and D in a counterclockwise direction, beginning in the northeast quarter. The first digit of a well number indicates the township, the second the range, and the third the section in which the well is situated. The lowercase letters a, b, c, and d after the section number indicate the well location within the section. The first letter denotes a particular 160-acre tract, the second the 40-acre tract, and the third the 10-acre tract. These letters also are assigned in a counterclockwise direction, beginning in the northeast quarter. If the location is known within the 10-acre tract, three lowercase letters are shown in the well number. Where more than one well is within a 10-acre tract, consecutive numbers beginning with 1 are added as suffixes. In the example shown, well number (D–13–11)18ddd designates the well as being in the SE1/4, SE1/4, SE1/4, section 18, Township 13 South, and Range 11 East.

VERTICAL DATUM

Sea level: In this report "sea level" refers to the National Geodetic Vertical Datum of 1929—A geodetic datum derived from a general adjustment of the first order level net of the United States and Canada, formerly called "Sea Level Datum of 1929."

Postaudit of Head and Transmissivity Estimates and Ground-Water Flow Models of Avra Valley, Arizona

By R.T. Hanson

Abstract

Ground water from regional alluvial-aquifer systems is the main source of water in the alluvial basins of Arizona, such as Avra Valley. Ground-water flow models are used to assess ground-water availability and the effects of development on the regional ground-water resources. A postaudit of regional-head and transmissivity estimates and the ground-water flow models of Avra Valley was used to evaluate potential errors in the distribution of aquifer properties and recharge that can cause predictive errors in ground-water models. Simulations of predevelopment conditions in 1940 and historical development conditions for 1960–79 provided the basis of comparison for assessing predictive errors of historical conditions for two regional ground-water flow models. Potential errors in the estimation of the regional-head and transmissivity and alternate conceptual models were compared with an existing calibrated two-layer flow model for predevelopment (1940) and developed conditions (1940–85).

Measured heads can be subdivided into a north-central region and a region south of the basin constriction. A more variable regional-head surface typical of developed aquifer systems was indicated by kriged developed heads (1985) with about 50 percent more uncertainty than predevelopment heads (1940). Incorporating heads from adjacent basins at the ground-water inflow and outflow regions reduced uncertainty in kriged heads for these boundary areas. Universal cokriging of heads with the strongly correlated land-surface altitudes may improve regional-head estimates and model comparisons where head data are sparse.

Local transmissivity estimates can be subdivided into northern and south-central regions that are distributed along the valley axis and the Santa Cruz River. Regional geostatistical estimates of transmissivity, which are based solely on local estimates, are low in the northern part of Avra Valley and are high in the south-central part when compared with the head-conditioned model-derived estimates. These differences may be related to a systematic bias between aquifer-test conditions and methods of aquifer-test analysis. Cokriging transmissivities with specific capacity and silt-and-clay content provided the least uncertainty of all kriged estimates.

Predictive errors for the Avra Valley model are the result of a different combination of factors that become significant in the simulation of ground-water flow for the periods representing predevelopment, historical development, and future development conditions. Predictive errors for simulation of predevelopment conditions are caused by potential systematic errors in estimates of local transmissivity, uncertainty in long-term mountain-front recharge, and uncertainty in predevelopment heads along the margins of the basin where recharge and transmissivity estimates are constrained by heads during model calibration. Analog-model historical predictions of future development indicate changes to 1985 were as much as 50 to 100 feet different from actual

declines that were caused by errors in the spatial distribution and not the total amount of estimated future pumpage.

Predictive errors for simulation of historical development (1960–79) appear to be caused to a greater extent by combined errors in estimates of transmissivity and storage properties and to a lesser extent by estimates of net withdrawal and subsidence. Comparison of the two digital models resulted in differences in transmissivity of as much as 30,000 feet squared per day and differences in specific yield of as much as 0.1. In combination with some differences in net withdrawal, these model-parameter differences resulted in local differences in change in storage of as much as 4,000 acre-feet per square mile and are equivalent to historical predictive errors in water levels of as much as 40 feet. Areas with no differences in model parameters yield comparable simulated water-level declines that are similar to measured declines. The pattern of differences in transmissivity and storage parameters are similar to differences between model-derived estimates conditioned on heads and related geostatistical estimates derived from aquifer-test estimates.

A postaudit analysis of alternate conceptual models was explored on the basis of well-by-well comparisons of reductions in mean error and variance, and through the use of standardized calibration-error maps for predevelopment heads (1940) and developed heads (1985). Calibration-error maps provide a useful tool for exploring the spatial structure of model errors and the relative adequacy of model fit that is not available from traditional methods of model comparison. Calibration-error maps indicate estimated heads were too high in the southern part of Avra Valley, and estimated heads were too low in the northern part. Increased transmissivity in the southern part of the lower model layer; decreased hydraulic conductivity in the southwestern part of the upper layer; reduced ground-water inflow from Altar Valley; and increased recharge along the Tortolita Mountains, Tucson Mountains, and Brawley Wash yielded a significantly better model for predevelopment but not for developed conditions (1940–85). This may indicate that alternate conceptual models are different for different time periods or require analysis of time-varying model parameters for developed conditions, such as climatically variable recharge. Predictive errors for future simulations (1986–2025) also could potentially include errors of more than 40 ft from omission of subsidence from the simulation of regional ground-water flow in Avra Valley. Further refinement of the changing conceptual model of an aquifer system under continuing development and variable climate, such as Avra Valley, will require a variety of additional geophysical, geochemical, and hydraulic field data.

INTRODUCTION

Ground water is the main source of water for irrigation, public supply, and industry in the Tucson Active Management Area (TAMA) located in the Tucson basin and adjacent Avra Valley, southeastern Arizona (fig. 1). Since major ground-water development began in the 1940's, pumpage has exceeded estimates of recharge. Ground-water withdrawals have resulted in substantial water-level declines that, in turn, required active management of the ground-water resources to ensure long-term availability of ground water. Since enactment of the 1980 Groundwater Code (State of Arizona, 1980), the Arizona Department of Water Resources (ADWR) has been responsible for managing the ground-water resources in the active management areas of Arizona. Successful management of this resource requires accurate estimates of aquifer-system hydraulic properties and accurate estimates of recharge, withdrawals, and the resulting head surface that reflects the aquifer-system response to these inflows and outflows.

As of 1985, Tucson was one of the largest cities in the world that relied exclusively on ground

water for its water supply. The City of Tucson's Hydrology Section (herein called Tucson Water), which is in charge of managing the withdrawals for one of the largest water users in the TAMA, also requires this same information to minimize operating costs, maximize use of the ground-water resources, meet the per capita usage set by the ADWR in their first two of five 10-year management plans (1980–90 and 1990–2000), and achieve "safe-yield" by the year 2025 (Arizona Department of Water Resources, 1984, 1988). In addition to these existing constraints, the aquifer systems in the Tucson basin and Avra Valley also received sole-source designation in 1984 by the U.S. Environmental Protection Agency (1984).

Ground-water flow models are playing an increasingly important role in predicting the effects of development on regional-aquifer systems. Flow models that are used for evaluation and management of ground-water resources require simulation of the aquifer system under predevelopment conditions, historical development, and proposed future development. The successful application of ground-water flow models to regional-aquifer systems, in turn, requires regional estimates of aquifer properties and the pumpage and natural recharge and discharge (stresses) to yield adequate estimates of the response of water-level altitudes (heads) to the changing stresses caused by natural and human activities. Developing an adequate simulation of the regional-head surface also requires reliable comparison during model calibration between measured and simulated heads that are used to estimate the regional-head surface. In this report, the differences between any measured and simulated heads are referred to as predictive errors, and any combination of estimation and measurement errors are referred to as uncertainty in aquifer properties or model parameters.

Predictive errors and model uncertainty from regional ground-water flow models are caused by errors in data collection and interpretation, uncertainty in the conceptualization of the ground-water flow system, and errors in the mathematical representation of the regional-flow system. Commonly, the adequacy of a ground-water flow model during calibration is established in the context of predictive errors of head and flow, and a single statistic, such as the mean error

Figure 1. Location of study area.

between measured and simulated heads, is used as a system measure of adequacy. In regional models where the effects of aquifer properties and individual boundary conditions may be localized, a spatial measure of fit may be required to assess model adequacy within subregions and for the entire system. Therefore, objective and reproducible estimates of aquifer-system properties (transmissivity and storativity), estimates of regional-head surfaces, and regional estimates of uncertainty for these estimates are required to develop and properly evaluate an adequate simulation of the ground-water resources on a regional scale. In this study, geostatistical methods that involve uncertainty estimates in the regional-head surface will be used to make comparisons between simulated and estimated head surfaces so that a spatial measure of fit can be applied during the analysis of predictive errors.

The purpose of this study is to review the potential errors from the collection and interpretation of basic field data that affect regional estimates of transmissivity and head used with ground-water model simulations using Avra Valley as a relatively simple example of a regional-aquifer system. The Avra Valley field data and ground-

water models are used to compare these alternate methods for regional estimates and to apply them in the context of a historical postaudit of the existing ground-water flow models.

In 1986 the U.S. Geological Survey (USGS), in cooperation with ADWR (and as of 1988 also the cooperation of the City of Tucson), began to study alternate methods of estimating aquifer-system properties, head surfaces used for model comparison, and their collective effect on the predictive error of ground-water flow models. This study used the generally simple Avra Valley aquifer system in the TAMA (fig. 1). Avra Valley has been the site of many previous studies that lend additional insight in comparing methods of estimation and simulation. The data set is significantly large enough to allow application of most of the methods with few computational difficulties. Data used for point comparison of a trial-and-error calibrated-flow model, inverse modeling, and geostatistical estimates included predevelopment and developed hydraulic heads, transmissivities, specific capacities, vertically averaged silt-and-clay content of the upper Tinaja beds, and estimates of ground-water recharge to the aquifer system in Avra Valley.

This report presents (1) a brief description of the aquifer system, (2) the basic data used to estimate transmissivity and regional-head surfaces, (3) a description of regional-geostatistical estimates of transmissivity and heads, (4) comparisons with previous estimates of transmissivity and heads from predevelopment (1940) and developed (1985) conditions, and (5) a postaudit of published ground-water flow models.

Comparisons of regional estimates will include work completed in a concurrent study (Zimmerman and others, 1991). This parallel study evaluated techniques for estimating uncertainty and propagating these uncertainties in steady-state simulations of regional ground-water flow. In turn, these simulations were used to estimate the probability distribution of ground-water travel times, which is one of the major criteria used to evaluate the siting of High-Level Waste (HLW) repositories. Although a nuclear-waste repository most likely will never be sited in Avra Valley, this basin still provides a large data set in a typical regional setting that can be used to guide future investigators of basins where HLW repositories may be sited. Also, many of the model-development problems, such as comparison and estimation methods and evaluation of predictive errors and uncertainties related to simulation of regional ground-water flow at potential HLW repositories, are common to water-resource problems addressed by State and City agencies that use ground-water flow models to assess the development of regional-aquifer systems.

REGIONAL SETTING

The Regional Aquifer-System Analysis (RASA) program divided alluvial basins of Arizona into five generally contiguous subregions termed the central, southeast, west, Colorado River, and highland basins (Anderson, 1986, fig. 5). Avra Valley is along the east boundary between the west and central basins. The west basins, which include Avra Valley, have aquifer systems composed of upper and lower regional alluvium, small ground-water inflow, minor amounts of mountain-front recharge and stream-flow infiltration, predevelopment-head contours that are virtually straight lines normal to the basin axis, and ground-water pumpage from storage depletion (Anderson, 1986, p. 109).

Avra Valley is in the Basin and Range physiographic province, which is characterized by block-faulted mountains separated by sediment-filled basins. The mountains are composed of granitic, metamorphic, volcanic, and indurated sedimentary rocks of Precambrian to Tertiary age. Sediments of the basin consist of unconsolidated to indurated gravel, sand, silt, and clay of Tertiary and Quaternary age. Sediments generally are coarse grained along the margins of the basin and grade into finer-grained and evaporitic deposits in the central downfaulted parts of the basin.

Conceptual Model

In Avra Valley, the regional-aquifer system is composed of sediments that are saturated at depth. Water stored in the aquifer generally is unconfined to depths of 1,000 ft and moves in a northerly direction. Potential sources of water to the aquifer include ground-water inflow, mountain-front

recharge, infiltration of streamflow, and irrigation return flow. Discharge of water from the aquifer includes ground-water outflow and pumping. Ground-water pumping has greatly altered the natural-flow system and has caused widespread water-level declines, changes in horizontal-flow paths, development of vertical-hydraulic gradients and perched zones, and compaction of the aquifer.

Geology

Avra Valley is composed of a wide variety of igneous, metamorphic, and sedimentary rocks of Precambrian to Quaternary age. Rocks of primary interest to this study include the permeable sedimentary deposits of Tertiary and Quaternary age, referred to as alluvium (fig. 2). Bedrock that makes up the mountains (fig. 2) consists mainly of low-permeability crystalline rocks that impede the movement of ground water. Along the extreme edges of the valley, bedrock is overlain by a veneer of alluvium that generally is less than 100 ft thick. Bedrock in the center of the basin is overlain by more than 9,000 ft of alluvium (fig. 2).

The alluvium consists of several regionally extensive sedimentary units of diverse lithology (Anderson, 1989). In this report, the alluvium is subdivided into lower and upper units on the basis of geohydrologic characteristics (fig. 3). The lower alluvium consists of gravel and conglomerate to gypsiferous and anhydritic clayey silt and mudstone and is thousands of feet thick. The upper alluvium consists mainly of gravel, sand, and clayey silt and ranges from less than 100 to about 1,000 ft in thickness. The lower alluvium is equivalent to the Pantano Formation, lower Tinaja beds, and middle Tinaja beds described by Anderson (1987, 1988, and 1989) and the regional lower basin fill of Pool (1986). The upper alluvium is equivalent to the upper Tinaja beds and Fort Lowell Formation of Anderson (1987, 1988, and 1989) and the regional upper basin fill and stream alluvium of Pool (1986). Geologic and geophysical data indicate that the sediments of the upper alluvium generally are much more compressible compared with those of the lower alluvium and are more likely to compact from the withdrawal of ground water (Tucci and Pool, 1986; Anderson, 1989). Compaction environments within the upper alluvium include playa and alluvial-fan subregions and a zone where fan and playa sediments interfinger, herein referred to as the interfingered-zone subregion (Anderson and Hanson, 1987). Fan and playa environments generally are characterized by clay and silt concentrations of less than 20 and more than 60 percent, respectively. The interfingered-zone subregion generally contains 20–60-percent clay and silt. This subregion was subdivided into two adjacent zones with 20–40 and 40–60-percent clay and silt for subsidence evaluation (Anderson, 1989). The physical properties and evolution of Cenozoic deposits in Avra Valley and adjacent alluvial basins are described in more detail by Davidson (1973), Eberly and Stanley (1978), Allen (1981), Pool (1986), Tucci and Pool (1986), Anderson (1987, 1988, and 1989), and Hanson (1987, 1989a).

Hydrology

The lower and upper alluvium are saturated at depth and form a complex regional-aquifer system (fig. 3). The aquifer, which generally is unconfined to depths of 1,000 ft, is underlain and bounded on the east and west by bedrock of low permeability. Ground-water inflow to the aquifer occurs through gaps in the bedrock from Altar Valley and Tucson basin near Three Points and Rillito, respectively. Ground-water outflow from the aquifer occurs south of Picacho Peak. Estimates of ground-water inflow near Three Points range from 9,000 to 16,600 acre-ft/yr (Hanson and others, 1990; table 1). Estimates of ground-water inflow near Rillito range from 13,000 to 20,100 acre-ft/yr (Hanson and others, 1990; table 1). Estimates of ground-water outflow near Picacho Peak range from 19,000 to 34,700 acre-ft/yr (Hanson and others, 1990; table 1). On the basis of geochemical data, ground-water inflow is the primary source of recharge to the aquifer in the southern half of the valley (Conner, 1986). Areal recharge may be significant relative to ground-water inflow in the northern half of the valley (Hanson and others, 1990; table 1).

Areal recharge to the aquifer includes temporally variable amounts of mountain-front recharge and streamflow infiltration. Before 1965,

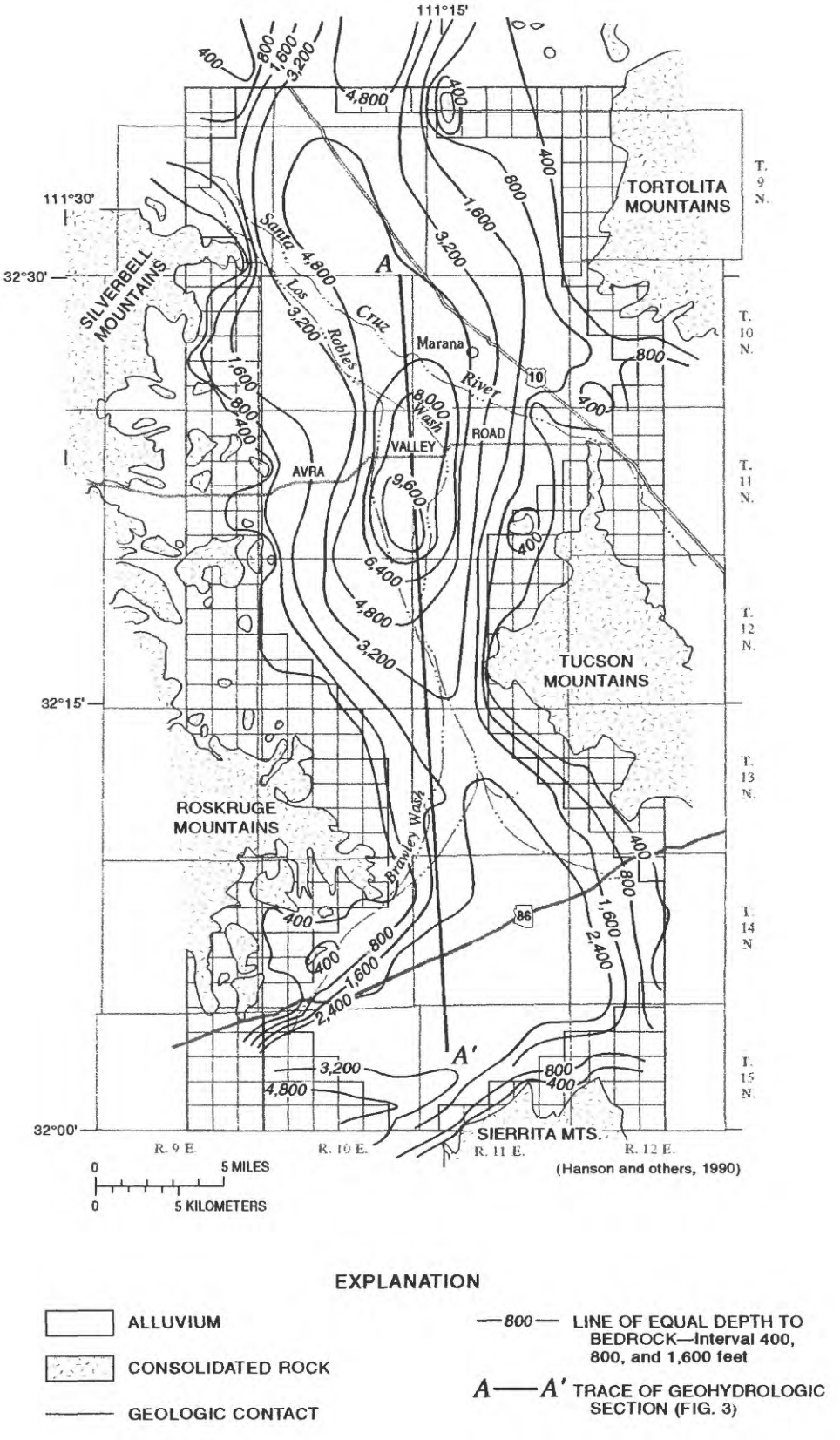

Figure 2. Extent of alluvium and depth to bedrock in Avra Valley, Arizona.

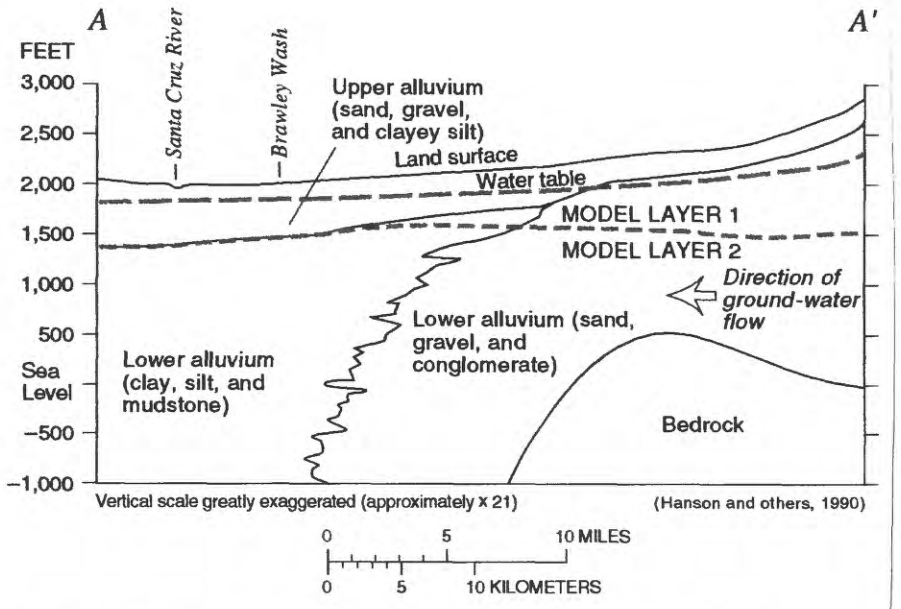

Figure 3. Generalized geohydrologic section of Avra Valley, Arizona.

areal recharge from combined sources probably was less than 15,000 acre-ft/yr (Hanson and others, 1990; table 1). Recharge through streamflow infiltration probably was greatest during the El Niño years, such as the record flows of 1978–79 and 1983–84 (fig. 4), and may increase through time from increased discharge and infiltration of sewage effluent. Discharge of sewage effluent into the Santa Cruz River near Tucson began after 1950, averaged 5,600 acre-ft/yr from 1951 through 1964, and increased to more than 49,000 acre-ft/yr by 1985 (Davis and Stafford, 1966; Dave Esposito, Environmental Planning Management, Pima County Wastewater Management Department, oral commun., 1988).

Ground-water movement generally is northward in the southern part of the valley and northwestward in the northern part. Movement and storage of ground water are controlled by the distribution of hydraulic head and by the transmissive and storage properties of the aquifer. Hydraulic properties of the lower and upper alluvium vary considerably from place to place, depending on lithologic factors such as sediment grain size, sorting, and cementation. In general, the lower alluvium has lower permeability than the upper alluvium but stores a much greater volume of water because of greater thickness.

Permeability of the aquifer is greatest in the upper alluvium along the channel of the Santa Cruz River and least in the mudstone of the lower alluvium. Hydraulic conductivity and transmissivity of the aquifer range from about 2 to 255 ft/d and 200 to 80,500 ft^2/d, respectively, on the basis of aquifer-test data. Hydraulic conductivity ranges from 20 to 50 ft/d in the lower alluvium, 30 to 40 ft/d in most of the upper alluvium, and 50 to 100 ft/d in the river gravels of the upper alluvium that underlie the channel of the Santa Cruz River. Transmissivity ranges from 1,000 to 50,000 ft^2/d in the lower alluvium and 1,500 to 40,000 ft^2/d in the upper alluvium. Estimates of composite transmissivities of the lower and upper alluvium, which were based on calibration of a one-layer flow model of the aquifer, generally range from 4,000 to 30,000 ft^2/d throughout most of the valley and exceed 40,000 ft^2/d along the Santa Cruz River (Moosburner, 1972).

Storage properties of the aquifer probably vary considerably and are difficult to determine from previous single-well, short-term aquifer tests. Estimates of storage properties generally are average values determined from water-budget calculations and model calibration. Estimates of specific yield in the upper part of the aquifer average about 0.15 (White and others, 1966; Anderson, 1972; Moosburner, 1972; Whallon, 1983; and Freethey and others, 1986). Storage coefficients for the confined parts of the aquifer probably average about $1x10^{-4}$. Estimates of the total volume of recoverable water stored in the aquifer range from 16.5 million acre-ft (White and others, 1966) to 24 million acre-ft (Freethey and Anderson, 1986).

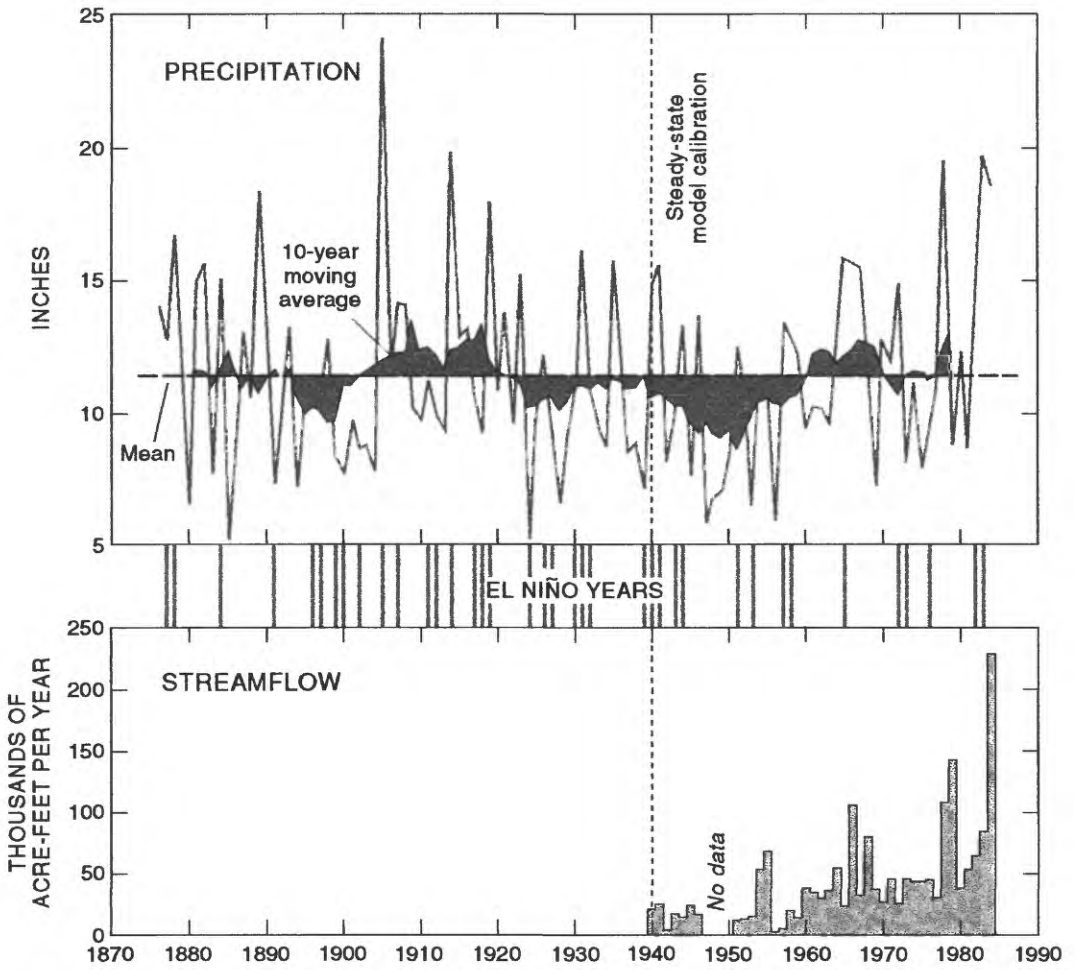

Figure 4. Annual streamflow in the Santa Cruz River at Cortaro, Tucson basin, 1940–84, and annual precipitiation from nearby Tucson, 1876–1988.

HEAD ESTIMATES

Regional-head estimates are used for initial pressure conditions for ground-water flow models and provide comparison surfaces for the calibration of ground-water flow models. The use of measured heads in model comparisons is becoming a more common practice for calibration of regional ground-water flow models but presently results in three fundamental problems. The first problem in using measured heads for model comparison is determining that the heads locally are representative of the vertical extent of the regional-aquifer system. The second problem is that measured heads may not coincide spatially with simulated heads. Horizontal interpolation of simulated heads to the location of the measured heads is usually employed for model comparison. This interpolation of simulated heads can introduce additional estimation error from the interpolator where gradients are large. The third problem is that comparison of simulated heads at selected points that represent the well sites precludes a spatial comparison over the entire regional surface. This well-by-well approach to model comparison results in a spatially limited and frequently biased comparison between measured and simulated heads.

In contrast to well-by-well comparisons for Avra Valley models (Hanson and others, 1990), heads from other Avra Valley models (Travers and Mock, 1984) are compared at all active cells. The resulting comparison is described in a single-system statistic such as average-model error. The interpolated regional-head surfaces used in cell-by-cell comparisons are frequently treated as

having equal certainty over the entire aquifer. The problem with this cell-by-cell approach is the potential for a biased estimate of model errors at any point in the time of simulation. If the data network used to estimate the regional-head surface changes through time, this bias in model-error comparisons also may change through time.

Regional estimates of head derived from kriging differ from these well-by-well and cell-by-cell approaches by providing a spatially variable estimate of the uncertainty that can be used to normalize the simulation errors and facilitate the comparison of errors from different conceptual models or different time periods. Although kriging is the best linear unbiased estimate, good regional-head estimates derived from kriging require enough head data that are spatially distributed to adequately estimate the regional head surface. The regional estimate also depends on the estimation and separation of any regional trend from the local random (stochastic) variation about the regional trend. In turn, the estimate of the random component depends upon the accuracy of the estimate of the spatial-autocorrelation structure. In addition, the spatial-autocorrelation structure should remain fairly constant over the entire region where the head surface is to be estimated. The random component also is affected by measurement and interpretation errors. Unlike other interpolation methods, kriging estimates can incorporate these spatially varying errors into the uncertainty of the kriging interpolator for the regional estimate.

The importance of measurement and interpretation errors in regional simulations of ground-water flow depends on the size, complexity, and objectives of the study. All geographic, geologic, and hydrologic data used for simulating ground-water flow are susceptible to these errors, and most regional estimates of these data can include this additional estimate of uncertainty. Previous studies of regional-flow systems have either considered measurement errors insignificant in comparison with numerical and conceptual-model errors (Waddell, 1982) or yielded such a large range as to require inclusion (Cooley and others, 1986; Weiss, 1991). Most studies that used measurement errors have treated them as independent components of error (additive) and have used ranking schemes for assignment of uncertainty.

Geostatistics have been used for regional-head estimates in alluvial-aquifer systems, such as parts of the developed Ogallala aquifer (Dunlap and Spinazola, 1981) and predevelopment conditions in part of Avra Valley (Clifton, 1981; Jacobson, 1985). In this study, the potential sources of uncertainties in head data are reviewed and geostatistical and hand-contoured regional-head estimates for predevelopment and developed conditions are compared and used to establish a basis for model comparisons with spatially variable uncertainty. These estimates will be used to compare simulation errors for predevelopment and developed conditions and for different conceptual models.

Uncertainties in Head Data

Measurement errors that carry over into the interpretation of heads include depth-to-water measurements, transient effects on water levels, location, and land-surface altitude errors. These measurement errors can be assumed to be independent and may be added together into a single intrinsic error estimate for each head measurement if they are determined to be uncorrelated. The degree of independence of measurement errors can be evaluated by estimating the correlation of measurement errors with the measured heads, land-surface altitudes, location, and their spatial autocorrelation.

Depth-to-water measurement errors are the primary field data that may affect model results through the comparison of measured and simulated heads. Depth-to-water measurements are prone to errors from the device used to estimate water levels in wells (an accuracy error), from the person making the measurement (human error), and from conditions in the well or in the measurement device or measurement method that make water-level measurements difficult to reproduce (precision error). Before the use of electric sounders in the 1950's, water levels commonly were measured with steel tapes and were reported to the nearest tenth of a foot. The measurements were taken in the winter (the nongrowing season) and were taken in shallow wells that commonly

represented water-table conditions and were less likely to be affected by cascading water, encrustation, or interference from other nearby producing wells. These early water-level measurements were collected by scientists who were familiar with the field conditions, were aware of the need to achieve reproducibility in the measurements, and ultimately were involved in the interpretation of the data. The early water-level data from Avra Valley are this type of data and probably are accurate to within 0.5 to 1 ft. More recent basin-wide surveys of water levels cover larger areas, many more wells, and are made with well sounders that can be affected by stretch in the steel or copper wire used. Although most sounders are calibrated periodically against steel tapes, comparison between sequential measurements made with different well sounders at the same well potentially can differ by as much as several feet. As basin development continues, use of ground water for industry and public supply can become more diverse. The simultaneous regional recovery of the whole aquifer system during the nongrowing season can be diminished in areas with industrial demands. For example, winter depth-to-water measurements made near an electric powerplant in northern Avra Valley (T. 10 S., R. 10 E., sec. 15) differed by as much as 32 ft between measurements made within 2 weeks of each other by separate field surveys.

Head measurements are susceptible to errors in the estimate of the location and land-surface altitude of the wells used for model comparisons. Well locations where heads are measured are point data that have the location attributes such as geographic coordinates (latitude and longitude or township and range) and land-surface altitude. The land-surface altitudes for most of the wells used for this study were surveyed and have an accuracy of about 0.1 ft. A few wellhead land-surface altitudes were estimated from topographic maps and have accuracies equal to one-half of the contour interval on the map (tables 5 and 6 at the back of the report).

Interpretation errors in measured heads can affect model comparison when the measured heads are not comparable to the heads represented by model layers. These errors are introduced from use of water levels that represent average regional-head or anomalous values from local perched systems or isolated layers within the aquifer system. Perched water levels commonly occur in regions where areal recharge, such as irrigation return flow or streamflow infiltration, are present. Anomalously high heads in shallow wells and cascading water in deeper wells with large completion intervals usually accompany these types of areal recharge. When these types of measurements are included with other adjacent, more representative head measurements, the result is a higher estimate in the uncertainty in the head surface. Conversely, when these measurements are used in place of more representative head measurements, uncertainty can be small locally; however, the regional-head surface may not be consistent with other parts of the aquifer system and, in turn, can lead to misestimation of aquifer parameters during the calibration of a regional-flow model.

Predevelopment Heads

Before the early 1940's, Avra Valley generally was undeveloped. In the Marana area, estimated pumpage was less than 10,000 acre-ft (White and others, 1966). Local seasonal changes occurred in storage; however, little to no regional change occurred in storage. Clifton's (1981) compilation of predevelopment heads is the data set commonly used to estimate the predevelopment head surface for Avra Valley. These 99 water-level altitudes were measured mostly between 1931 and 1948. An additional 19 water-level altitudes were found from this time period and included for this study. These data were compiled from the Agricultural Experiment Station and Water Resources Research Center of the University of Arizona and the U.S. Geological Survey (table 5 at the back of the report).

Land-surface altitudes and the measurement error for the land-surface altitudes are included with these water levels. Measurement errors at wells used to estimate predevelopment heads range from 0.1 to 25 ft. These altitudes represent a combination of survey measurements and estimates from topographic maps. Because most wells completed during early aquifer development are shallow, the error from depth-to-water measurements will be considered negligible. Prede-

velopment heads are strongly correlated with land-surface altitudes; measurement error from land-surface altitudes show little correlation with space, heads, or land-surface altitudes (table 1).

The regional predevelopment-head surface was estimated through universal kriging (Grundy and Miesch, 1987) with graphical fitting of the variogram model using measured predevelopment heads from Avra Valley (table 5 at the back of the report). The experimental variogram at wells where predevelopment heads and land-surface altitudes were measured appears to be parabolic (figs. 5*A* and 5*B*); whereas, the variogram for land-surface altitude-measurement errors appears to exhibit no spatial autocorrelation (fig. 5*D*). After removal of regional-quadratic drift, the residual variogram (fig. 6) was graphically fitted with a spherical variogram model with no nugget, a sill of 65 ft^2, and a range of 20,000 ft. The kriging of heads used a neighborhood of 8 mi or the 30 nearest neighbors. A summary of cross-validation measures (table 2) was estimated with hole-by-hole suppression (jackknifing). The predevelopment heads with 15 of the additional 19 data points retained demonstrate a typical parabolic semivariogram similar to Jacobson's variogram (1985, fig. 16). The kriging error from a second-order moving local neighborhood is

Table 1. Summary of descriptive statistics for data sets used from wells in Avra Valley, Arizona

[ft, foot; ft^2/d, foot squared per day; (gal/min)/ft, gallon per minute per foot. Dashes indicate no data]

Attribute	Mean	Standard deviation	Maximum	Minimum	Coefficient of variation	Number of samples	Correlations
Predevelopment head (ft)	1,870	167	2,381	1,611	0.09	112	[1]0.93
Predevelopment head land-surface altitude (ft)	2,090	215	2,630	1,759	.10	112	---
Predevelopment head measurement error[2] (ft)	5.3	7.4	25	.1	1.40	112	[3]-.04/.04
Developed head (ft)	1,849	265	2,567	1,253	.14	214	[1].933
Developed head land-surface altitude (ft)	2,181	275	3,096	1,739	.13	214	---
Developed head measurement error (ft)	2.8	5.1	25	.1	1.79	214	[3].02/.01
Log transmissivity[4] (ft^2/d)	4.03	.45	4.94	2.30	.11	169	[5].71/-.50
Measurement error[6] (ft^2/d)	.58	.49	1.02	0	.84	169	[7].23
Log specific capacity[4] [(gal/min)/ft]	1.50	.36	2.30	.40	.24	169	([8])
Average silt and clay content[9]	.38	.20	.80	.03	.53	151	([10])

[1]Correlation between head and land-surface altitude at well sites.

[2]Land-surface altitude-measurement error.

[3]First number is correlation between measurement error and head; second number is correlation between measurement error and land-surface altitude. Measurement-error correlation with spatial distance east and north are both 0.03 for predevelopment-measurement errors and -0.01 (east) and 0.04 for developed-measurement errors.

[4]Log-base 10 of samples used for statistics.

[5]Correlation between log-transmissivity and log-specific capacity (N=69); average silt-and-clay content (N=46).

[6]Measurement error is estimation error from linear-regression estimates of transmissivity with aquifer-test estimates assigned zero error.

[7]Correlation between measurement error and log transmissivity. Correlation with spatial distance east and north are -0.13 and 0.50, respectively.

[8]Correlation with spatial distance east and north are 0.09 and 0.28, respectively.

[9]Average silt-and-clay content is thickness-weighted average of sediment samples from the upper Tinaja beds.

[10]Correlation with spatial distance east and north are -0.38 and 0.25, respectively.

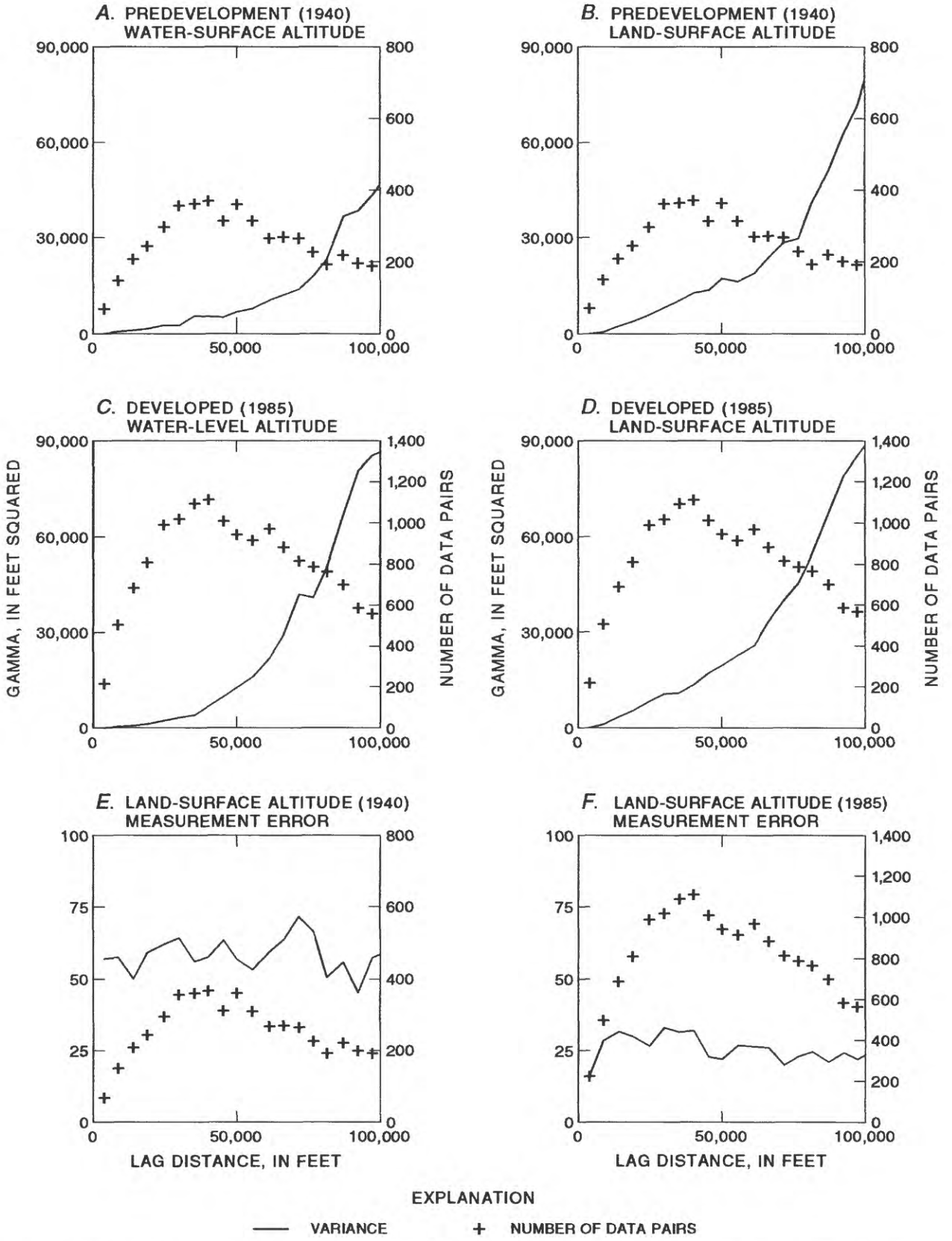

Figure 5. Semivariograms of predevelopment and developed heads, land-surface attitudes, and land-surface altitude-measurement errors.

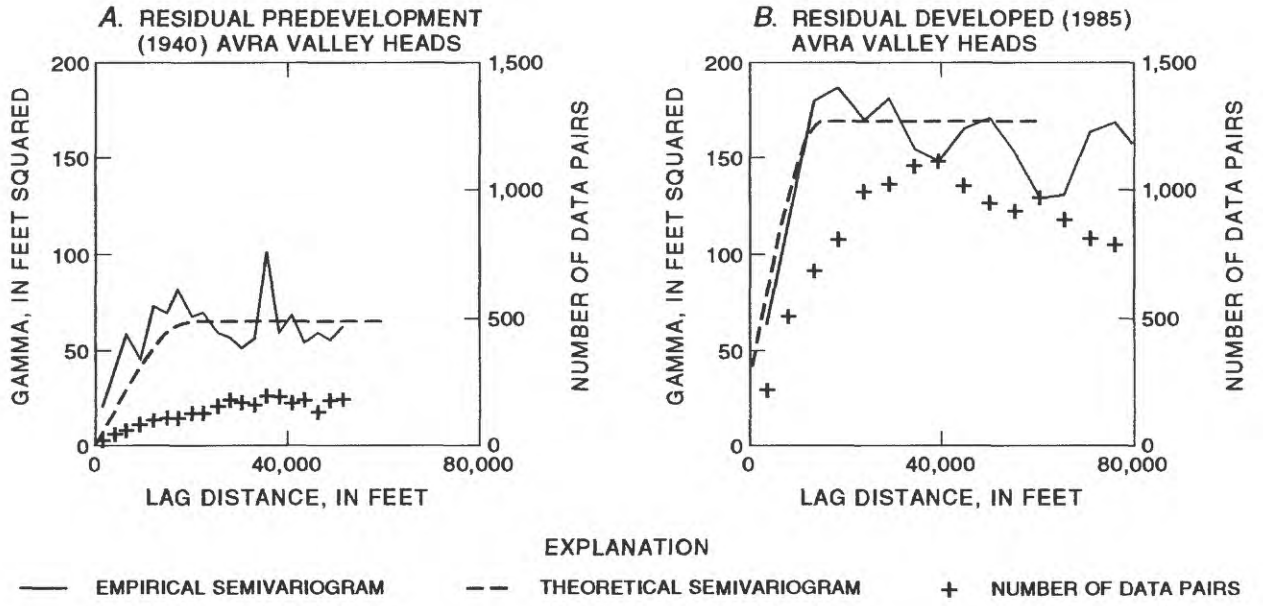

Figure 6. Empirical and theoretical residual semivariograms of head.

comparable to Jacobson's (1985) estimate that used a fourth-order polynomial for global drift. This indicates that a simpler model can yield a comparable error in the estimates. The kriged predevelopment heads are in close agreement with Moosburner's (1972) hand-contoured predevelopment heads (fig. 7) everywhere except near the Sierrita Mountains where data are sparse.

The additional 15 head data points reduced the kriging errors (fig. 8) in the northern and southern parts of the valley compared with the errors in the subregion between the Santa Cruz River and State Highway 85 presented by Jacobson (1985, fig. 22). Kriging errors generally range between 4 and 10 ft. The kriging errors become larger than one contour interval (50 ft) where data are lacking along the west flank of the Tortolita Mountains and northwest flank of the Sierrita Mountains. These areas indicate the critical need for "edge points" to reduce uncertainty (such as kriging errors) in head surfaces. A potential alternative to additional "edge points" would be universal cokriging of heads with the strongly correlated land-surface altitudes at the well sites (table 1) and additional land-surface altitudes along the edges and in other areas lacking head data.

When additional uncertainty is added from the error in land-surface altitude measurement, the kriging errors only increase in areas where the measurement errors are larger than a foot. This uncertainty occurs between the Santa Cruz River and the Tortolita Mountains and along the Silverbell Mountains and Roskruge Mountains. The overall increase generally is small because most land-surface altitudes were estimated through surveying; however, the few areas where discrepancies do occur illustrate the potential effect of errors from estimates made with topographic maps or digital-elevation model data.

Developed Heads

The use of a statistically based interpolation scheme, such as kriging, provides several advantages in repeated annual estimates of a regional-head surface. Kriging not only provides a map of the uncertainty of the estimate but also provides a technique that can be repeatedly applied to the same regions without additional bias from interpretations by different hydrologists. The regional estimation of developed heads are not only subject to the errors discussed for predevelopment heads but also includes errors from developed conditions. Errors from composite water levels, from interborehole flow or from

Table 2. Summary of cross-validation estimates for the head and transmissivity data sets used from wells in Avra Valley, Arizona

[Dashes indicate unavailable statistic. Modified from Zimmerman and others, 1991]

Aquifer property[1]	Average kriging error	Root-mean square error	Normalized root-mean square error
Predevelopment head[2]	0.18	13.03	1.37
Developed head[3]	-.10 .20	10.69 14.26	.94 1.00
Transmissivity $UK_{(T)}$[4]	-.03	.39	1.06
Transmissivity $GC_{(T)}$[5]	---	---	2.21
Transmissivity $CK_{(T,Sc)}$[6]	-0.006	0.60	1.62
Transmissivity $CK_{(T,Sc,F)}$[7]	---	---	---
Transmissivity $OK_{(T,T(Sc))}$[8]	-.002	.30	1.07

[1]Average kriging error and root-mean square error are in units of the aquifer properties and normalized root-mean square error is dimensionless.

[2]Error estimates made on 112 of the 114 data points.

[3]Error estimates made on 209 points (upper numbers) and on 214 points (lower numbers), which included edge points from Picacho and Tucson basins and Altar Valley.

[4]Universal kriging errors from aquifer-test transmissivities (N=69).

[5]Generalized covariance-error estimate from aquifer-test transmissivities (N=69).

[6]Cokriged-transmissivity errors from aquifer-test transmissivities (N=69) and specific capacities (N=169).

[7]Cokriged-transmissivity errors from aquifer-test transmissivities (N=69), specific capacities (N=169), and silt-and-clay content (N=205?). Cross-validation program malfunctioned for three attribute cases.

[8]Ordinary kriging with global linear-regression errors from aquifer-test transmissivities (N=69) and regression transmissivities from specific capacity (N=100).

transient water levels may be more important than measurement errors for kriging developed heads. Estimating these additional components of error can be difficult and deserve additional consideration; however, they are not addressed by this study.

A transition from predominantly seasonal agricultural pumping to nonseasonal industrial and public supply pumping reflects the evolution of water usage in many basins in the western United States. Thus, the condition of recovered winter water levels may not occur throughout a regional-aquifer system. In Avra Valley, this transition was marked by large purchases and retirement of farmland in the 1970's by the City of Tucson for the purpose of obtaining water rights in an adjacent basin. Following the acquisition of these water rights, the City of Tucson exports water from the southern part of the basin, and effluent is recharged in Tucson basin or flows back into the northern part of Avra Valley in the Santa Cruz River. Additional major industrial uses in Avra Valley include withdrawals for mining and electric-power generation in the northern part of the valley. Although these uses are small in volume, they affect the hydrologist's ability to contour heads that represent the regional-aquifer system. The most important water levels for determining the continued effect of pumping on subsidence occur during periods of maximum drawdown. Therefore, as an aquifer system is developed and uses evolve, the network of wells and timing of water-level measurements requires periodic re-evaluation and interagency coordination to make the data collected the most representative of regional conditions. Ultimately, continuous recorders or a dual set of maximum recovered water levels and maximum drawdown water levels may be needed to monitor all aspects of the aquifer system.

Regional-head contour maps of the aquifer system in Avra Valley have been produced by ADWR (Reeter and Cady, 1982; Travers and Mock, 1984), by Tucson Water on an annual basis (Babcock and others, 1982–89), and by the USGS

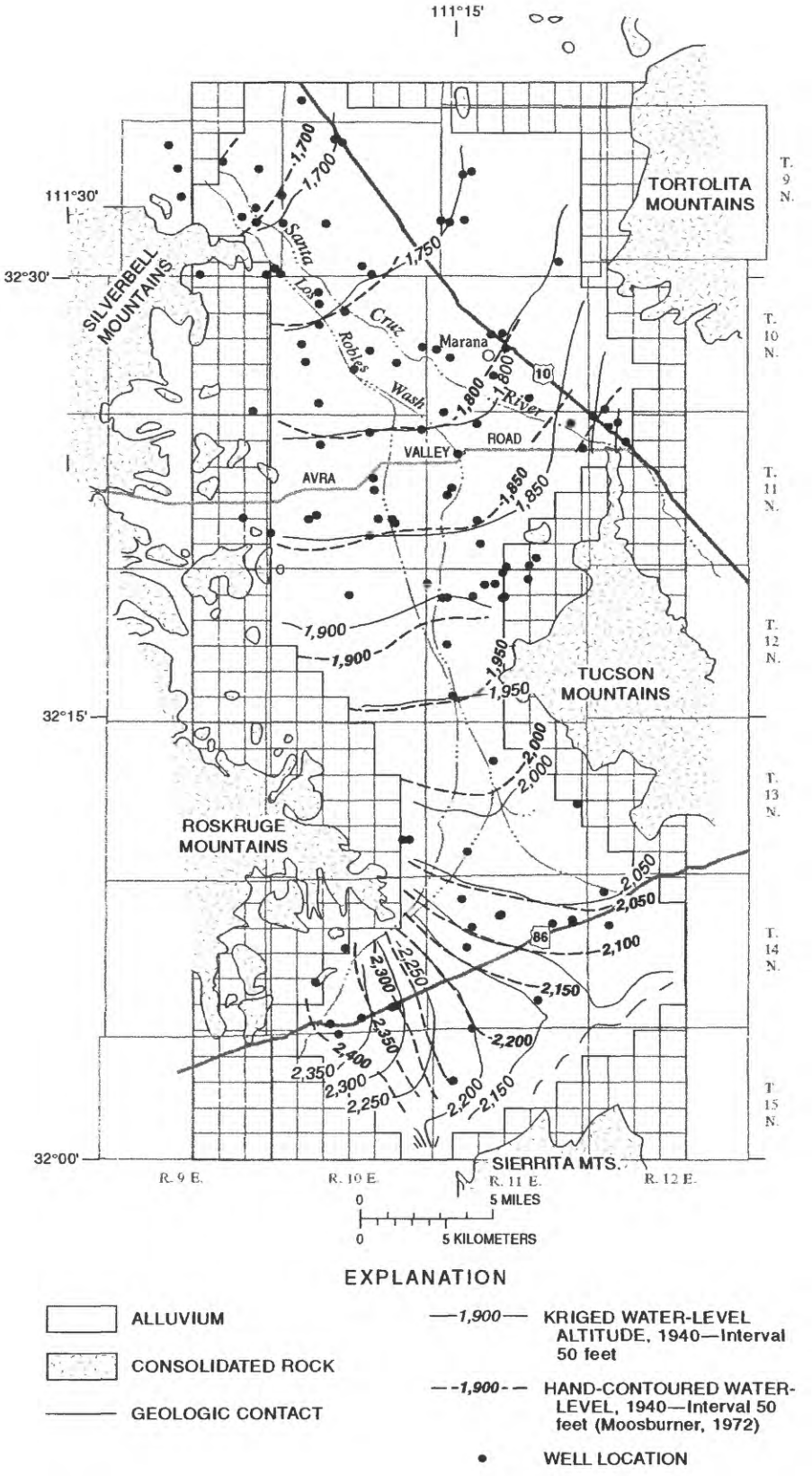

Figure 7. Kriged and hand-contoured predevelopment heads.

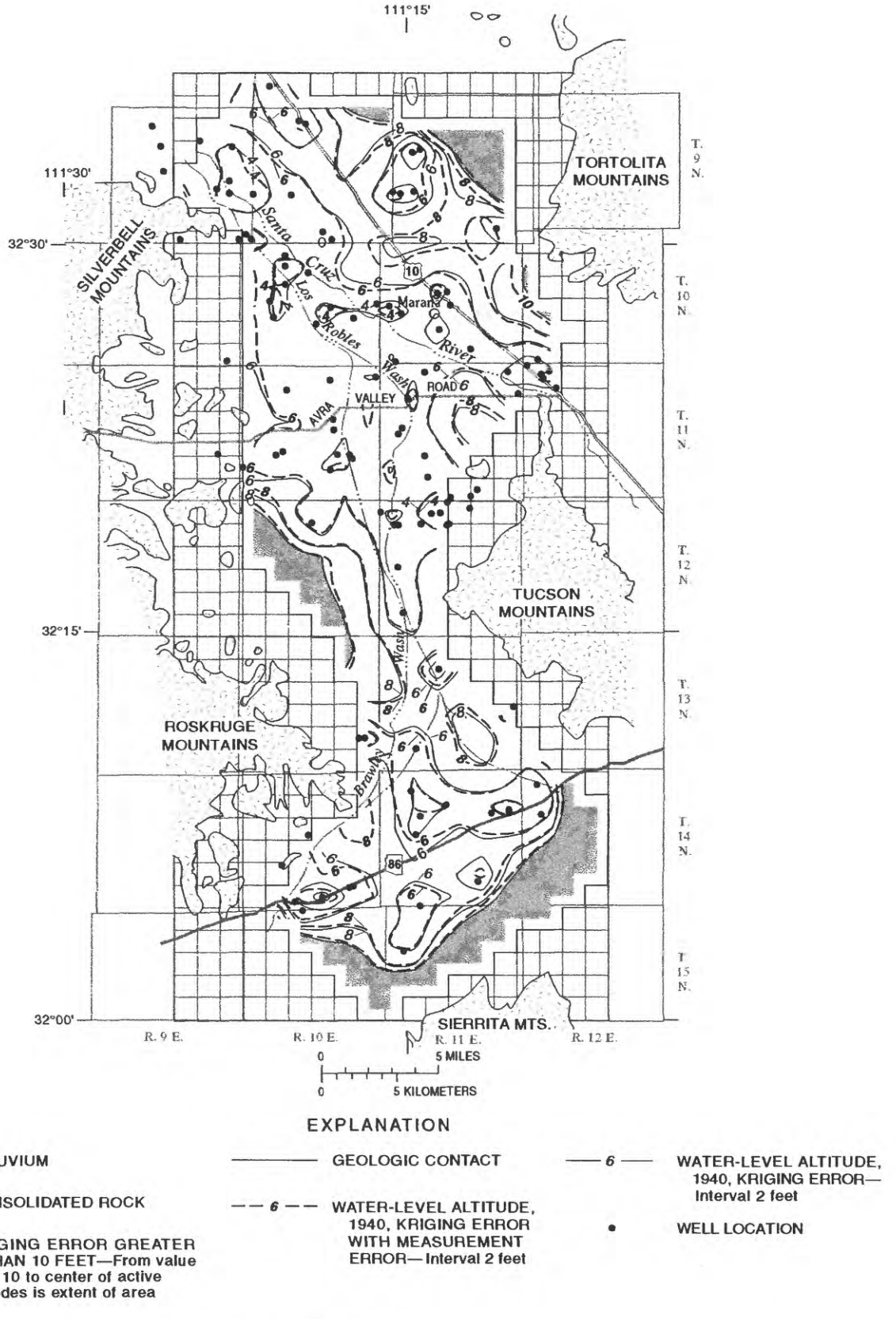

Figure 8. Kriging errors for predevelopment heads.

(Cuff and Anderson, 1987). The developed heads from the winter of 1984–85 were used with universal kriging to estimate the regional-head surface at the end of the transient-simulation period of the USGS ground-water flow model (Hanson and others, 1990).

The regional developed head surface was estimated through universal kriging (Grundy and Miesch, 1987) with graphical fitting of the variogram model using 1985 developed heads (table 6 at the back of the report). These data do not include wells suspected of being affected by perched water conditions. The experimental variograms at wells where developed heads were measured (fig. 5) are parabolic for the heads and land-surface altitudes and are lacking autocorrelation for measurement errors of land-surface altitude. After removal of regional quadratic drift, the residual variogram (fig. 6) was graphically fitted to a spherical theoretical variogram model with a nugget of 35 ft^2, a sill of 170 ft^2, and a range of 15,400 ft. The kriging of heads used a neighborhood of 8 mi or the 30 nearest neighbors. A summary of cross-validation measures (table 2) was estimated with hole-by-hole suppression (jackknifing). The kriged 1985 heads estimated from 214 heads are similar to the hand-contoured estimate (Cuff and Anderson, 1987) throughout the southern and central parts of Avra Valley (fig. 9).

The two sets of contours differ in the northern part of the valley where some different data were used north of the Pima County line. To reduce the estimation error along the edges of the valley where ground-water inflow and outflow occur, additional wells were selected from adjacent Altar Valley, Tucson basin, and Picacho basin. These points are considered a valid extension of the head surface in these inflow and outflow regions. As with the predevelopment heads, the developed heads show a strong correlation with land-surface altitude and almost no correlation with the measurement error of land-surface altitude (table 1). The variogram of land-surface altitude errors again indicates no spatial autocorrelation and is about half the error estimated for predevelopment well sites (fig. 5).

Kriging errors for the developed head surface range between 10 and 14 ft throughout most of the valley, and are the result of the estimated uncertainty of about 6 ft at distances of less than 1 mi. Thus, the developed head surface is estimated with about 50 percent more uncertainty, half the measurement error, and about twice as many points (table 1) as were used to estimate the predevelopment head surface. These attributes, in turn, may reflect the greater local variability in heads typical of developed aquifer systems. The addition of measurement error made little difference in kriging errors because of the accuracy in surveyed estimates of wellhead altitudes for most of the wells in Avra Valley (fig. 10). This error could potentially be larger if less exact methods were used to estimate altitudes or if subsidence of the land surface was more than several feet following earlier wellhead surveys. The advantage of adding only five edge points from adjacent basins is illustrated by the reduction of kriging errors on the order of tens of feet in the ground-water outflow area near Picacho Peak and by several feet for the ground-water inflow area between the Tortolita and Tucson Mountains.

TRANSMISSIVITY ESTIMATES

Over the last 20 years, hydrologists have estimated aquifer properties, simulated regional ground-water flow, and made predictions of the future state of the alluvial-aquifer system in Avra Valley. In addition to the many water-supply studies of Avra Valley, investigators have used data from Avra Valley to test and compare various techniques used to estimate transmissivities at a regional scale. Local and regional estimates of transmissivity were an integral part of many of these studies. A review of local transmissivity estimates made from aquifer tests, drillers' logs assignments, and regression estimates, and a review of regional-transmissivity estimates made by interpolation and inverse methods will provide a basis for comparison of the techniques used to make regional-transmissivity estimates. The trial-and-error model completed by Hanson and others (1990) will be used as a head-condition basis of comparison for the regional-transmissivity estimates.

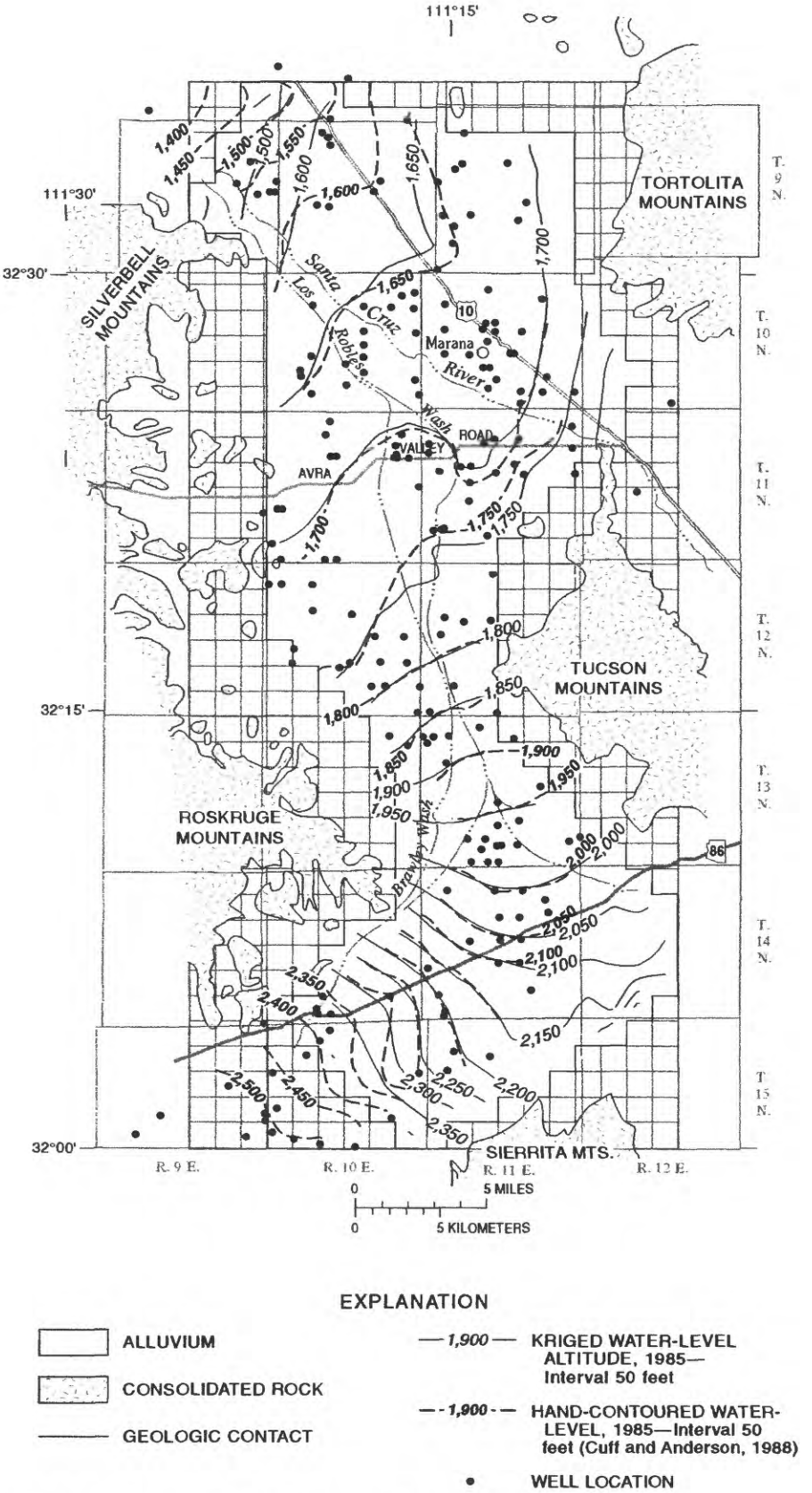

Figure 9. Kriged and hand-contoured developed heads.

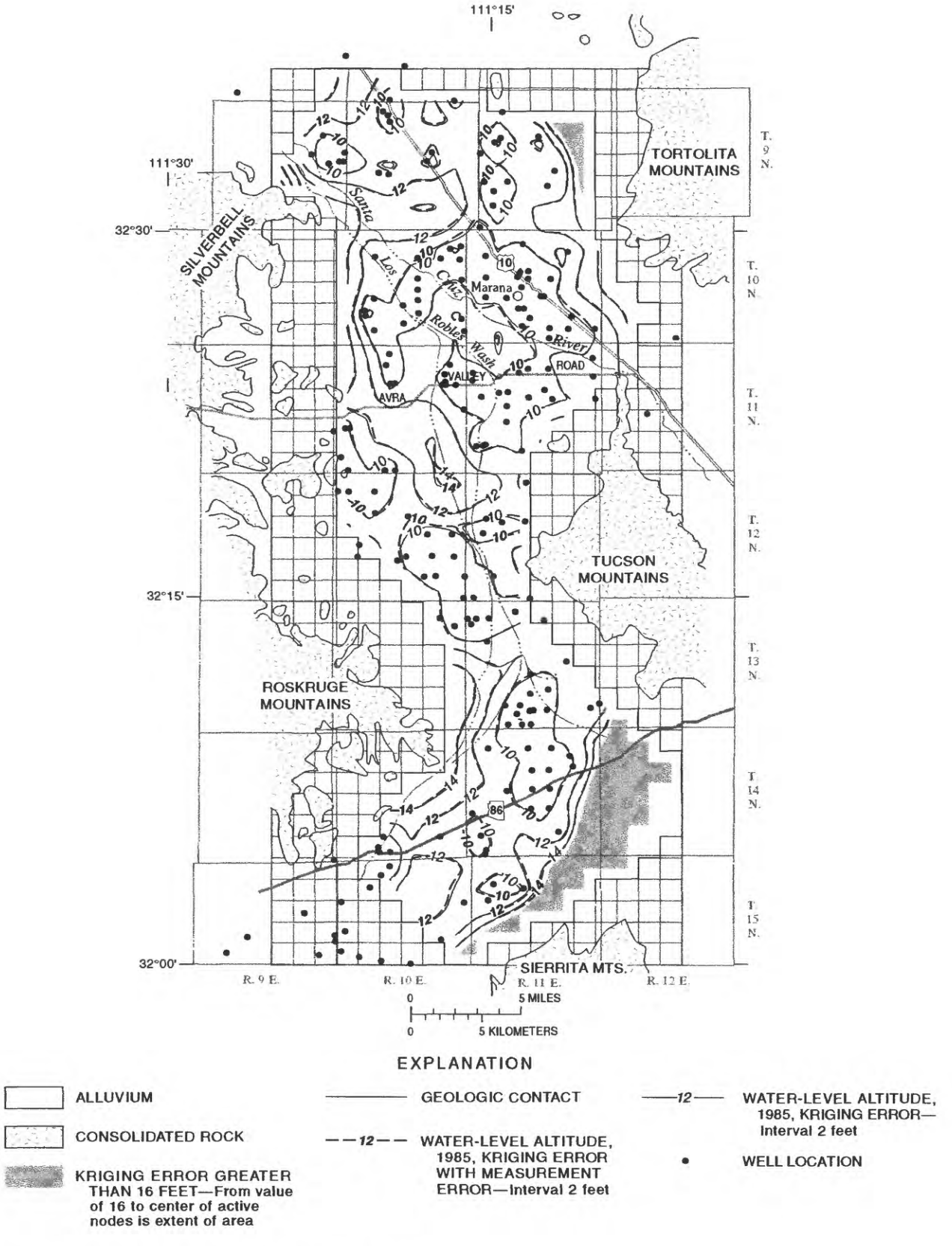

Figure 10. Kriging errors for developed heads.

Local Transmissivity Estimates

Transmissivities have been estimated at wells since the onset of development in Avra Valley. Aquifer-test transmissivities from 69 wells, specific capacities from an additional 100 wells, and average silt-and-clay content from an additional 67 wells were used to estimate regional transmissivities and were compared with regional ground-water flow-model estimates (fig. 11).

Values from the 1940's and 1950's are commonly higher than subsequent estimates and may often reflect well development and other less than ideal aquifer-test conditions. Clifton (1981) compiled 42 transmissivities from aquifer tests completed by Tucson Water during 1965–77 (table 7 at the back of the report). These tests were largely short-term drawdown tests followed by recovery measurements and were not supplemented with water-level measurements in nearby wells (Clifton, 1981). Clifton's estimates of transmissivity were made using a Cooper-Jacob approximation (Lohman, 1979). During 1977–87, additional transmissivities were estimated from aquifer tests by Johnson (1980) and Tucson Water (table 7 at the back of the report). Test conditions for these additional 27 values were similar to tests from the previous decade and estimates were made on the basis of a Cooper-Jacob approximation of recovery data.

Local transmissivity estimates are susceptible mainly to errors related to aquifer tests and related geologic data used to aid in construction of the wells tested. These estimates also are susceptible to errors in the conceptual model used to interpret the test data. Aquifer-test estimates of transmissivity depend on measurement errors, quality of test conditions, and alignment of the aquifer test with the assumed hydraulic model used to interpret the test. Measurement errors include head, time, and well-discharge errors. Quality-test conditions, however, require no interference from nearby pumping and require representative measurements, steady-state well losses, significant length of test, and a large enough stress to induce significant response from all sources contributing water to the wellbore within the aquifer system. Because most aquifer tests are performed with multiple sounders for water-level measurements, totalizing flowmeters for pump discharge, and are performed with relatively constant discharge conditions, measurement errors are assumed to be negligible compared to potential errors from model conceptualization.

An additional source of uncertainty in transmissivity estimates is from wells with varying degrees of efficiency and from wells with different saturated intervals from different total depths or from different time periods in the development of the aquifer system. For example, specific capacity, discharge, and pumping and static water levels for AV-5 (fig. 12) indicate a loss in well efficiency through time that is typical of several wells in the AV well field in southern Avra Valley (Sandy Elder, Tucson Water, written commun., 1987). The specific capacity and pumping water level generally were constant after an initial 6 years of decrease; however, the discharge rate and the static water level decreased throughout the 17 years of record. The pump was replaced in AV-5 in 1982, and the pump bowls were lowered 25 ft to a depth of 525 ft, which resulted in small increases in well performance and specific capacity.

Reduction of well efficiency and transmissivity also may be related to sequential desaturation of the major contributing layers within the aquifer system (fig. 12*B*) that are penetrated by wells such as AV-5. The reduction in efficiency and transmissivity generally requires resetting of the pump bowls at greater depths as was done for AV-5 but also indicates a general decrease in hydraulic conductivity and transmissivity at wells in alluvial-aquifer systems in areas of sustained development. Wellbore flow during pumping in AV-5 substantially decreases below a depth of 575 ft. This nonuniform distribution of wellbore flow may, in part, represent a reduction in hydraulic conductivity and transmissivity with depth owing to greater cementation and increased silt-and-clay content. Similarly, the flowmeter log from nearby AV-6 shows most of the water coming from shallow depths. In contrast to well AV-6, flowmeter logs indicate substantial contributions of water at depth from well AV-2, which is of comparable depth and about a mile south of AV-6. This difference may reflect the spatial variability of facies and cementation in the middle Tinaja beds. Under ideal conditions, aquifer tests used for regional-transmissivity estimates should only include tests that reflect the same major

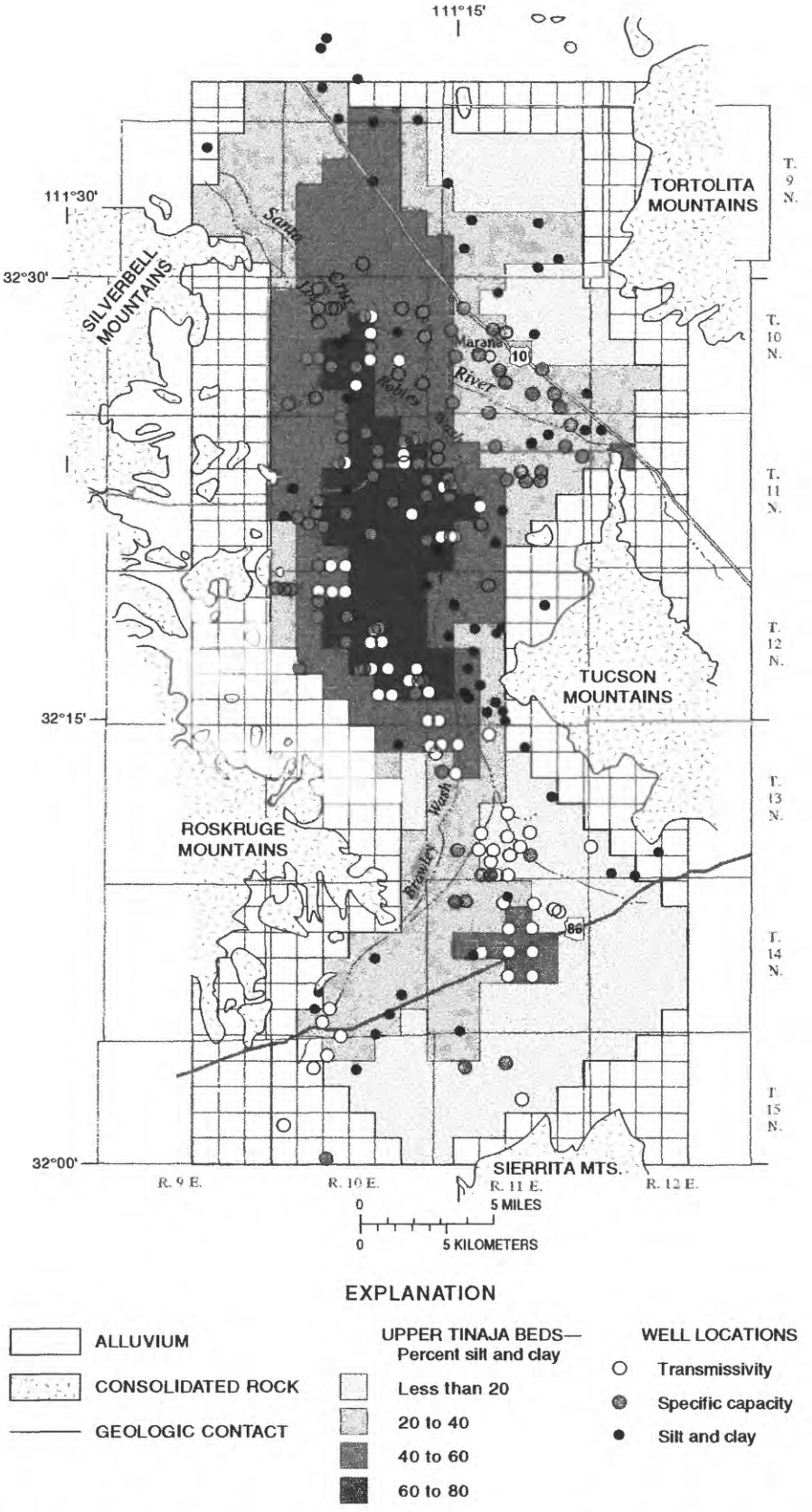

Figure 11. Location of wells with transmissivity, specific-capacity, and silt-and-clay estimates.

contributing layers in the flow system. Under conditions of sustained dewatering, early tests and more recent tests may not represent the same contributing layers. Thus, flowmeter logs can be used to delineate major contributing layers and to verify that all wells that are grouped together for statistical analysis are receiving water from the same layers.

Old wells may reflect substantially different well efficiencies than new wells because of well construction and related developing or deteriorating well conditions. For example, Clifton (1981) suggested that the older irrigation wells maintained an efficiency (ratio of theoretical water-level drawdown to drawdown measured in the field times 100) of about 60 percent in Avra Valley. These wells generally were drilled with cable-tool rigs with casing driven during drilling and casing perforation after completion. Clifton also suggested that newer screened wells drilled with rotary rigs and completed with screens or louvers and gravel packing were only about 20-percent efficient. The specific capacities of the less efficient wells were adjusted by Clifton (1981, equation 116) before estimating the log-log relation between specific capacity and transmissivity. Initial estimates of entrance losses from the louvers in AV-5 ranged between 11 and 17 percent of discharges for 690 to 1,210 gal/min. The history of specific capacity at a well, such as AV-5 (fig. 12), indicates that this well is not one of the 19 wells adjusted by Clifton (1981). The differences in specific capacity between older and newer wells also may be the result of factors other than the type of perforations.

The length of aquifer tests is significant especially in alluvial-aquifer systems where delayed yield and layering can affect the estimates of drawdown or the hydraulic model used for interpretation. Many tests overestimate transmissivity with respect to specific capacity (fig. 13) when compared with an envelope of "ideal" Theis conditions for a range of storage coefficient between 0.1 and 1.0×10^{-4} and assumed conditions of 1-foot radius and 1 day of pumping. The grouping of wells by decades or drilling method only segregates a suite of wells in the AV well field that appears to have large transmissivity relative to specific capacity. These wells were rotary drilled by Tucson Water in the 1970's and completed with louvers or screens (fig. 13). A clustering of potentially overestimated transmissivities (or under-

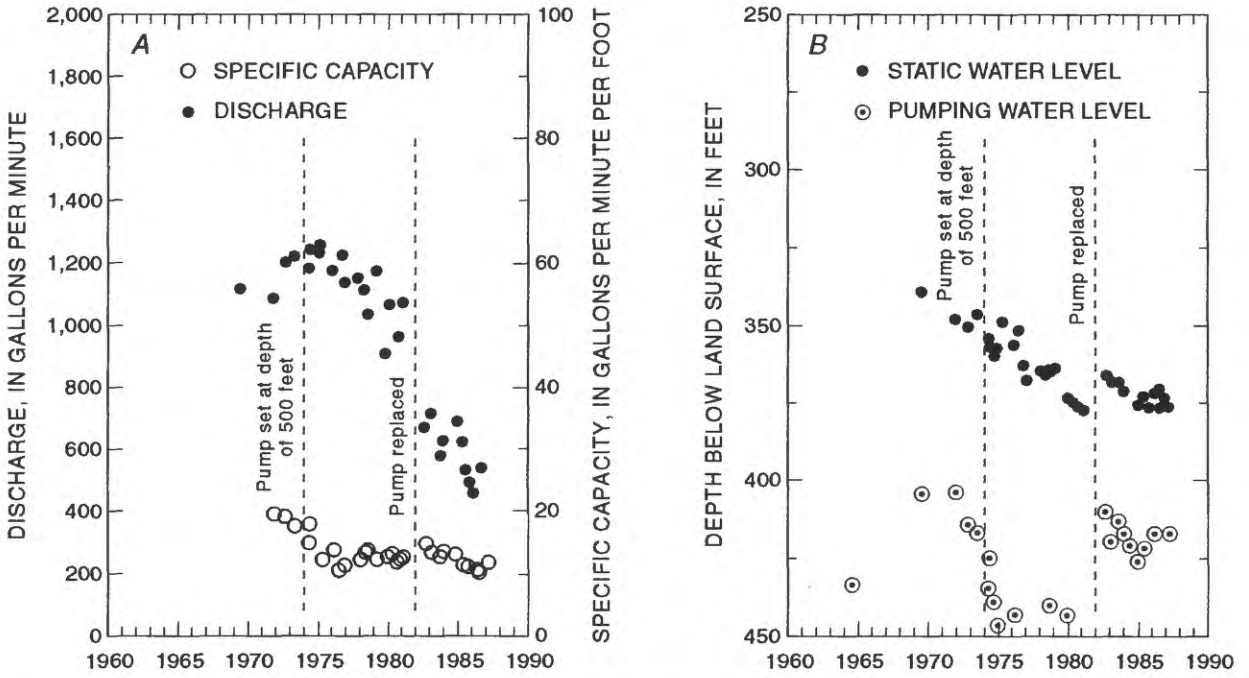

Figure 12. Discharge, specific capacity, and water levels through time for well AV-5 (D-11-10)27cdc.

estimated specific capacities) generally related to wells drilled in the 1960's and 1970's are in the south-central part of Avra Valley. A less distinct clustering of potentially underestimated transmissivities (or overestimated specific capacities) generally is related to wells drilled in the 1950's. This factor is coincident with a zone of suspected perched ground water in the north-central part of Avra Valley (fig. 14). The AV wells drilled in the 1960's exhibit distinctly lower specific capacity and transmissivity. Conversely, AV wells drilled in the 1970's exhibit larger specific capacity and transmissivity and also may include some of the screened wells that Clifton (1981) claimed to be less efficient with underestimated specific capacity.

In general, short pumping periods may be more prone to underestimation of specific capacity because of well inefficiency; whereas, seasonal estimates may be more prone to overestimation because of delayed yield decreasing the seasonal drawdown. Because step-drawdown data were unavailable for almost all the wells used in this study, no detailed analysis of well efficiencies was possible. Future studies, however, may need to address well efficiency and whether seasonal and short-term specific capacities are consistent estimates before collectively using them to supplement regional estimates of transmissivity.

Comparison of Regional-Transmissivity Estimates

Regional-estimation techniques can be subdivided into methods that use local transmissivity estimates alone or incorporate other

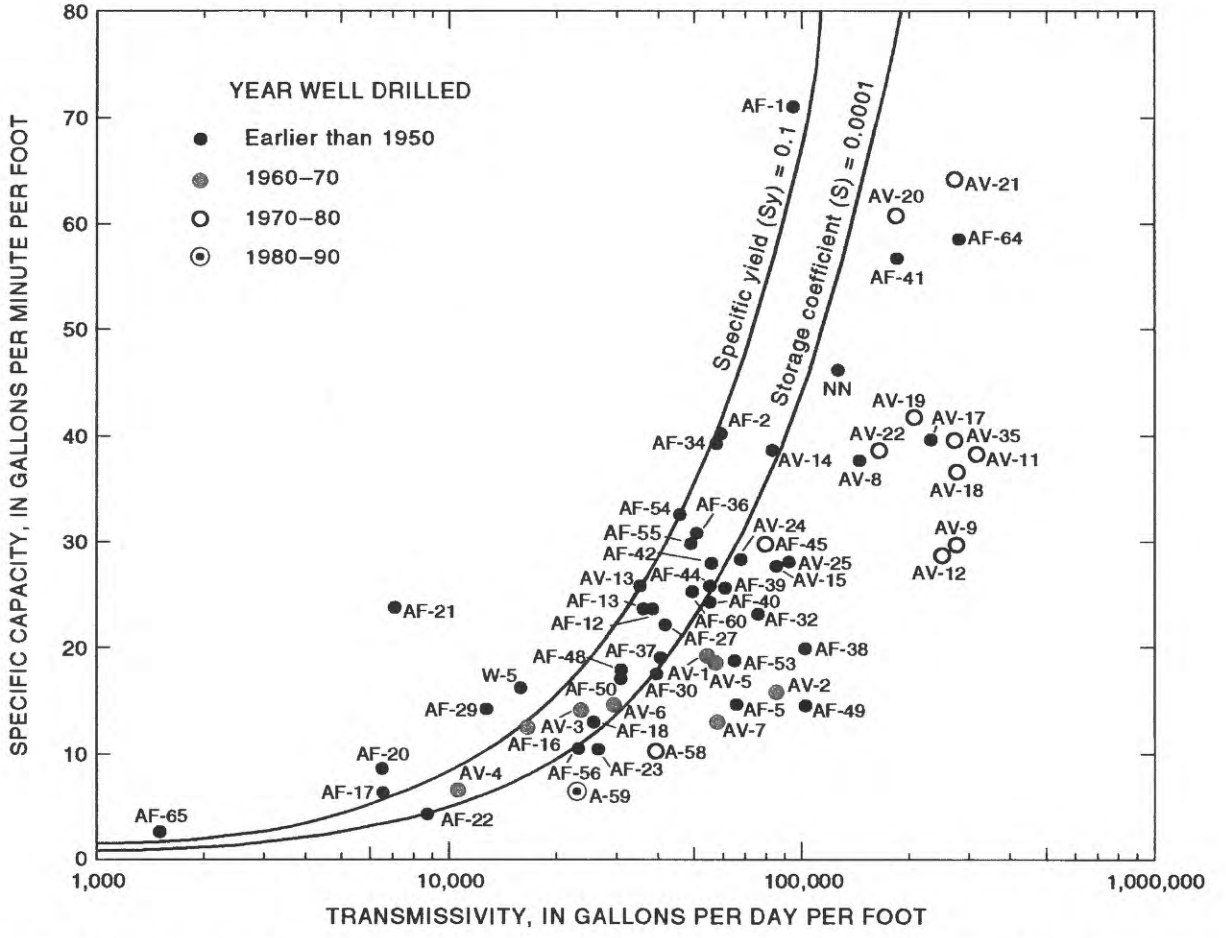

Figure 13. Aquifer-test transmissivity and specific-capacity values with respect to potential Theis conditions.

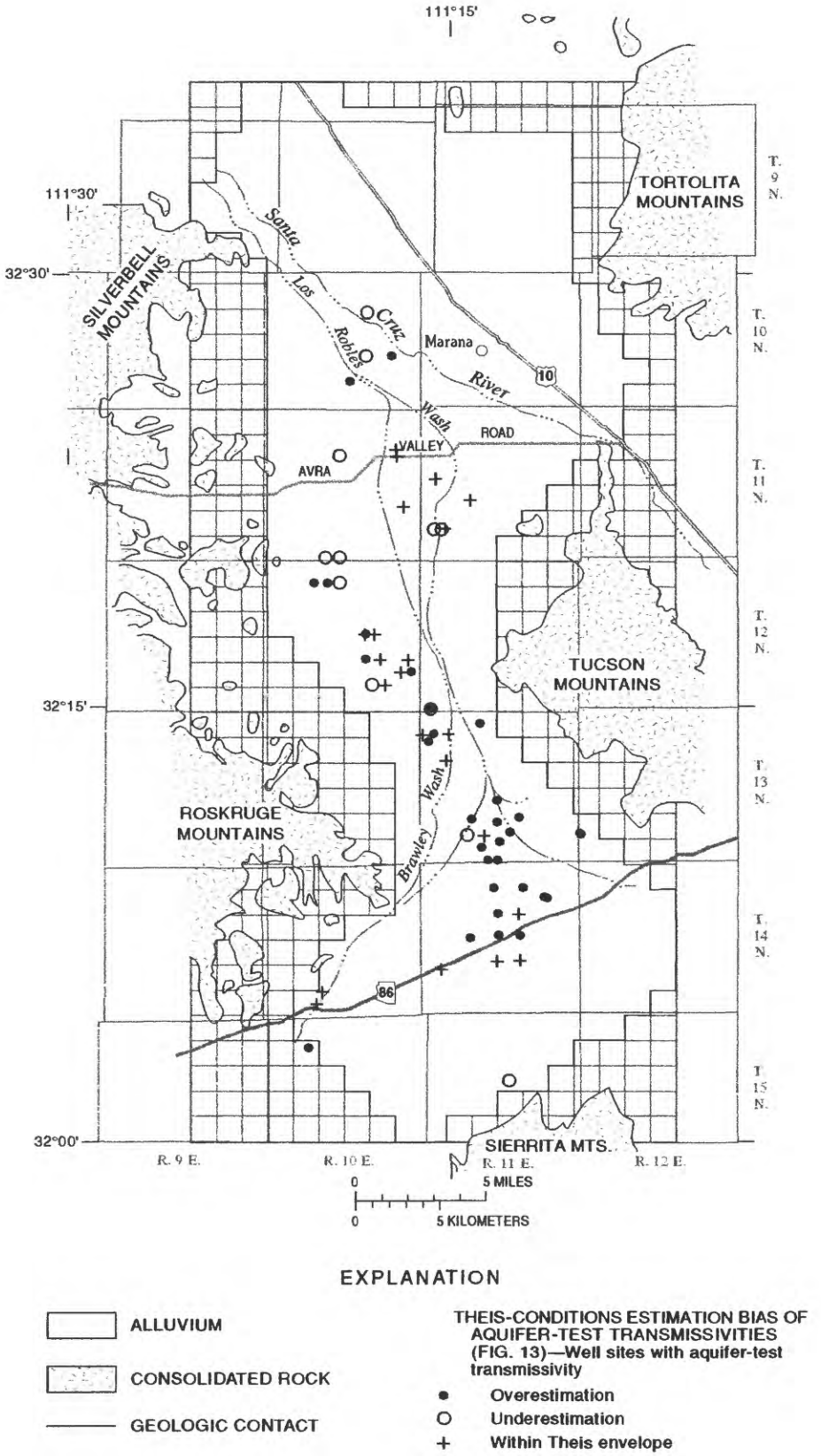

Figure 14. Wells with aquifer tests and potential bias with respect to Theis conditions.

indirect information. Local transmissivity estimates are commonly used as point values to generate regional estimates and help establish the overall uncertainty of regional estimates. Because transmissivity estimates are not primary field measurements, these values can be affected by measurement and interpretation errors discussed in the previous sections by the spatial extent and distribution of local estimates and by the method used to estimate regional values. To overcome poor spatial distributions, indirect information is commonly included through coestimation with supplementary covarying attributes such as specific capacity, sand or silt-and-clay content, and geophysical signatures. Similarly, inverse or head-conditional regional estimates supplement the local estimates on the basis of comparisons between measured and simulated heads. For the purposes of comparison, a choice was made to use the head-conditional estimate of regional transmissivity from the trial-and-error model (Hanson and others, 1990) as the basis of comparison with interpolated and other head-conditioned inverse estimates of regional transmissivity. Through a somewhat arbitrary choice, this basis of comparison has the additional indirect constraint of matching measured heads, which is not present in most interpolation methods.

Regional-transmissivity estimates of Avra Valley were made by several investigators (Moosburner, 1972; Clifton, 1981; Travers and Mock, 1984; Jacobson, 1985; Hanson and others, 1990; and Zimmerman and others, 1991) using hand-contouring, geostatistical estimates, and inverse techniques. All these geostatistical and ground-water model-derived regional estimates are based on all or part of the aquifer tests (tables 7, 8, and 9 at the back of the report) done prior to 1990. This section reviews selected comparisons of the geostatistical and inverse estimates and related uncertainty.

Geostatistical Estimates

Interpolation of the regional estimate at unknown locations is derived from weighted values of local transmissivity estimates at surrounding known locations. Only wells in a local neighborhood are used to make an estimate at an unknown point. The geostatistical technique of kriging is a local estimator; whereas, trend surface and hand contouring are considered global estimators. Hand contouring, inverse-distance-squared regression, dip projection, area-weighted, and zonal assignments are methods used to make regional estimates. Inverse-distance, dip projection, area-weighted, local zonation, and hand contouring all yield regional estimates but do not provide information about the uncertainty of the estimate or the correlation structure over the entire region. Trend-surface analysis provides a scalar measure of goodness-of-fit, R^2 (coefficient of determination), which describes the overall fit of the surface with respect to known data points. Trend-surface analysis, however, does not represent a spatially varying estimate of uncertainty or an estimate of the covariance. Similarly, packages such as SURFACE III (Sampson, 1988) provide cross-validation techniques for methods such as inverse-distance and dip projection but do not yield an estimate of the spatially varying uncertainty of the estimate or the spatial correlation of the estimate. Hand contouring takes advantage of "soft information" such as knowledge of the geology, hydrology (especially boundary conditions), and any perceived trends or discontinuities in the regional-transmissivity field. Hand contouring, however, is not quantitative nor exactly reproducible by different hydrologists. In contrast, kriging yields reproducible estimates, the uncertainty of the estimator, and the overall correlation structure. Universal kriging (UK), generalized covariance (GC), cokriging (CK), and ordinary kriging (OK) with linear regression were used to obtain regional-transmissivity estimates for Avra Valley (Zimmerman and others, 1991). This study will review these estimates and compare them with the trial-and-error inverse estimate of regional transmissivity (Hanson and others, 1990). The choice of the trial-and-error model, while somewhat arbitrary, provides a consistent basis of comparison with a head-conditioned estimate of regional transmissivity.

Universal Kriging—Examples of regional-transmissivity estimates for alluvial aquifers include OK (Palumbo and Khaleel, 1983) for the Mesilla bolson, New Mexico, and two-domain OK for Avra Valley (Clifton, 1981). However, most sets of local transmissivity estimates do not exhibit

a stationary mean and variance that allow the application of OK. Clifton identified two subregions (fig. 15*A*) with about half the variance and three times the geometric mean for the northern part of Avra Valley in comparison to south-central Avra Valley on the basis of a combined transmissivity and specific-capacity data set (Clifton, 1981, figs. 10 and 11). Clifton kriged the transmissivities in the northern part of Avra Valley separately from the south-central part of the valley. As with Avra Valley, sets of aquifer-test estimates commonly are too small (less than 30) to split into multiple domains without using supplementary data such as specific capacities. Regional estimation of transmissivity using UK that accounts for a regional trend was applied to the alluvial aquifer in the upper Santa Cruz River basin (Williams, 1987).

Zimmerman and others (1991) used a single-domain UK estimate with first-order northerly drift (fig. 16*A*) and a spherical variogram model with a nugget of 0.04, a range of 18,000 ft, and a sill of 0.12 from the 69 aquifer-test log transmissivities for Avra Valley. The residual variogram for log transmissivities (Zimmerman and others, 1991, fig. 5–4) is similar to the southern-central valley variogram estimated by Clifton (1981, fig. 11) because most of the aquifer-test estimates are in the south-central part of the valley. Log transmissivities (Zimmerman and others, 1991, plate 1*A*) from UK with first-order northerly drift removed is similar to the two-domain OK estimate made by Clifton (1981, fig. 16) for southern and central Avra Valley. Kriging errors also are comparable to Clifton's (1981, fig. 15) estimate (Zimmerman and others, 1991, plate 1*B*) in the south-central part; however, errors are higher in the northern part of the basin where data are sparse and where Clifton used supplemental data.

The UK estimate is considerably higher than the trial-and-error model estimate in the northeastern part of the valley where extrapolation occurred and was higher in the AV well field. The UK transmissivities were lower in the central valley along the Santa Cruz River and southeast of the Silverbell Mountains and were similar to the flow-model estimate in the southern part of Avra Valley (fig. 16*A*). A continuous northerly trend in transmissivity values in the northern part of the valley compared to transmissivity values in Clifton's two-region approach cannot be addressed statistically without data from additional aquifer tests. The presence of high-permeability sediments along the Santa Cruz River and the silt-and-clay distributions (Anderson, 1989, figs. 4 and 5), however, collectively indicate that the basin has several transmissivity subregions of different spatial extent in the upper alluvium that represent different depositional environments.

Generalized Covariance—Kriging in the presence of trends ordinarily involves identification and removal of the trend before the kriging of residuals and is a time-consuming and computationally intensive process (Neuman and Jacobson, 1984). An alternative to this approach is to use the theory of intrinsic random fields (IRF; Matheron, 1975) where the drift is removed by differencing the data, and kriging is carried out using generalized covariances that are generalizations of variograms for the differenced field.

The GC estimate of transmissivity (Zimmerman and others, 1991, plate 1*B*) used an IRF-1 with $K(h) = -2.213 \times 10^{-6} |h|$, where h is the distance between transmissivity locations used to estimate transmissivity at unknown locations. As with all the kriging techniques, the related estimation errors are higher along the margins of the basin where data are sparse (Zimmerman and others, 1991, plate 1*B*). The difference between trial-and-error and GC estimates (fig. 16*B*) is similar to the UK differences but is considerably more in the northern part of the valley where GC was allowed to expand the search radius to satisfy a minimum number of nearest neighbors (fig. 11). As with the UK, a linear northerly trend in the transmissivity distribution remains unresolved because there are so few estimates from the northern part of the valley.

Cokriging—Cokriging was initially used in the mining industry to solve the "undersampled" problem where two attributes were sampled; however, many samples lack the attribute of interest at most sample locations. Cokriging assumes that a statistical relation exists between the covarying attributes that represent some complex physically based relation. Ahmed and DeMarsily (1987) have compared cokriging of transmissivity with specific capacities using other techniques of parameter estimation for a

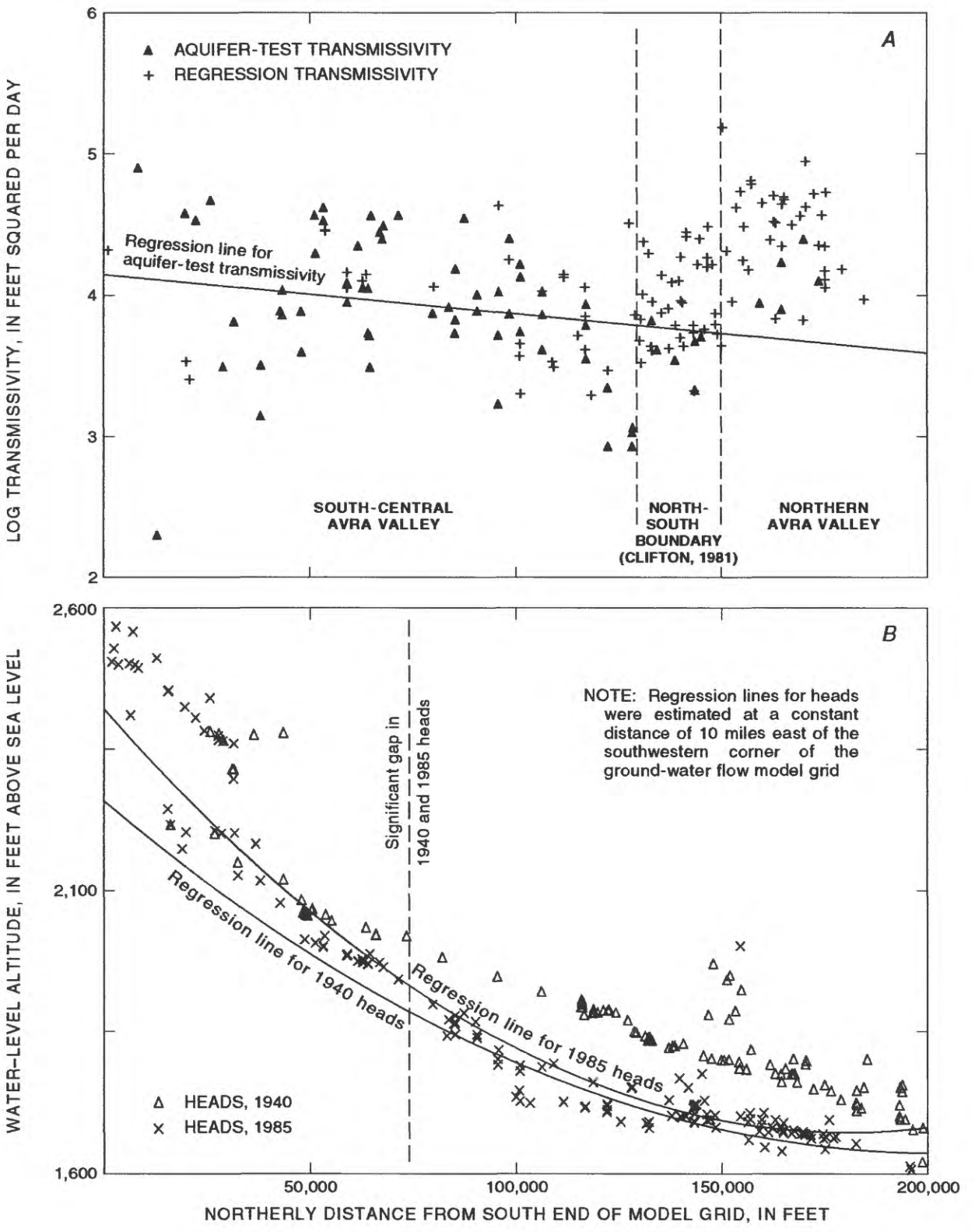

Figure 15. Heads and log transmissivity with northerly distance along the model grid, Avra Valley, Arizona. *A,* Log transmissivity from aquifer tests and specific-capacity values. *B,* Predevelopment and developed heads with respect to northerly distance.

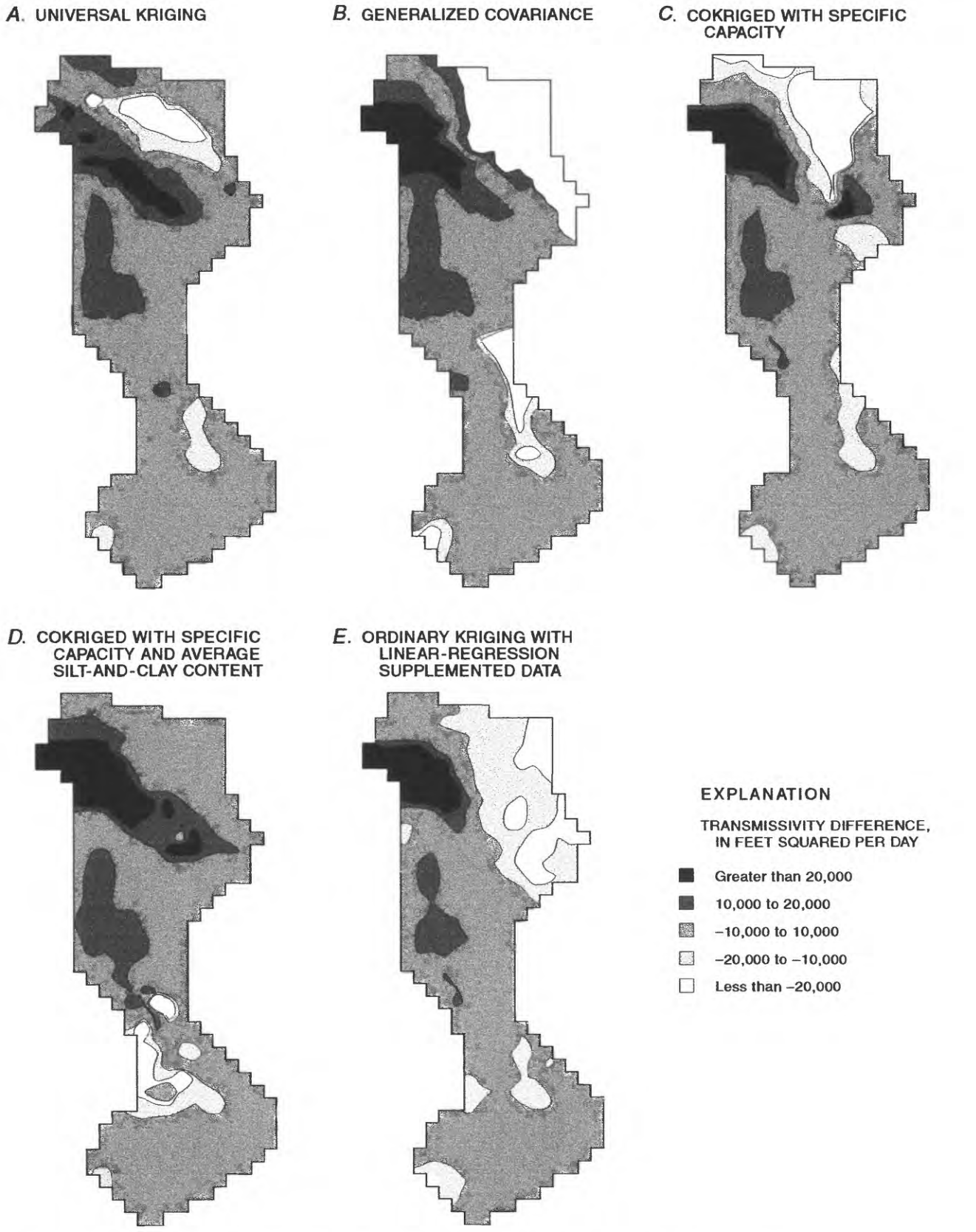

Figure 16. Difference between trial-and-error and geostatistical estimates of transmissivity.

regional-aquifer model. The CK estimates of transmissivity also were made for other regional alluvial aquifers such as the Yolo basin, California (Aboufirassi and Marino, 1984), and the southern part of the upper Santa Cruz River basin, Arizona (Williams, 1987). More recently, Yates and Warrick (1987) used CK of soil-water content with percent-sand content, and Ahmed and others (1988) used CK of transmissivity with electrical properties.

Cokriging also can reduce the kriging error by cokriging attributes that are correlated. Yates and Warrick (1987) note that the reduction in kriging errors and cross-validation error occurred for attributes with more than a 0.5 correlation. Correlation coefficients are 0.7 between log transmissivity and log specific capacity and only -0.5 between log transmissivity and silt-and-clay content data for Avra Valley (table 1). The moderate degree of correlation between transmissivity and specific capacity is typical of estimates for data from other alluvial aquifers in southeastern Arizona and will reduce the uncertainty in the regional-transmissivity estimate. The low degree of correlation between transmissivity and silt-and-clay content is weaker than expected considering the empirical relation between permeability and silt-and-clay content estimated by Anderson and others (1992, fig. 9) but can still potentially reduce the uncertainty in the regional-transmissivity estimate. The correlation between log specific capacity and silt-and-clay content was poor at -0.2.

Coestimation of regional transmissivities from local transmissivity estimates and covarying attributes, such as specific capacity and average silt-and-clay content, is another way of supplementing the sparse distribution of aquifer-test transmissivities in Avra Valley. The CK method requires the additional theoretical semivariogram models for the cross covariance of any pair of attributes (Myers, 1982). The undersampled attribute, transmissivity, and covarying attributes need to be sampled together at a set of locations to estimate the cross covariance. For Avra Valley, there are 69 sites with transmissivity and specific-capacity values, 46 sites with transmissivity and silt-and-clay content values, and 84 sites with specific-capacity and silt-and-clay content values for estimating the cross covariance. Anderson's (1989) vertically averaged silt-and-clay percentages for the upper Tinaja beds were used to represent the silt-and-clay content of the saturated part of the upper alluvium. An additional 13 silt-and-clay percentages were estimated for the upper Tinaja beds from test-hole drilling along the Central Arizona Project canal alignment (Wrege and others, 1985) and from basic data from Tucson Water. These values, along with Anderson's 109 values, were assigned to wells that were within a 0.5-mile proximity, were within the same textural subarea mapped by Anderson (1989, fig. 4), and had transmissivity or specific-capacity estimates (table 7 and 8 at the back of the report). An additional 67 wells with particle-size data and no estimates of specific capacity or transmissivity are in the northeastern, western, and southwestern parts of the valley (fig. 13, table 10). Silt-and-clay content data show a small negative correlation with easterly distance and suggest a general coarsening of the upper Tinaja beds to the east (fig. 11).

The variogram models used for CK are fitted graphically to the experimental variogram data of log transmissivity, log specific capacity, average silt-and-clay content, and the respective pseudo-variables (fig. 17). Spherical semivariograms with a common range of 50,000 ft were used to satisfy the Cauchy-Schwartz inequality as was done by Ahmed and De Marsily (1987).

Zimmerman and others (1991) made CK estimates of log transmissivity with log specific capacity (two properties) and additionally with average silt-and-clay content (three properties). Because of the difference in magnitude and resulting large differences in variance between these covarying attributes, each data set was normalized to a standard mean ($\mu = 0$) and variance ($\sigma^2 = 1$) for estimation and then denormalized for presentation of the estimate. The addition of silt-and-clay content to CK transmissivity with specific capacity improved the estimate and estimation error (Zimmerman and others, 1991, pls. 1 and 2) in the northeastern part of the valley where only silt-and-clay data exist (fig. 11). The cokriged transmissivities are similar to Clifton's inverse-model estimates of transmissivity in the northern part of Avra Valley (Clifton, 1981, figs. 24 and 30) and are in alignment with the sedimentary facies of the upper Tinaja beds (Anderson, 1989, fig. 4).

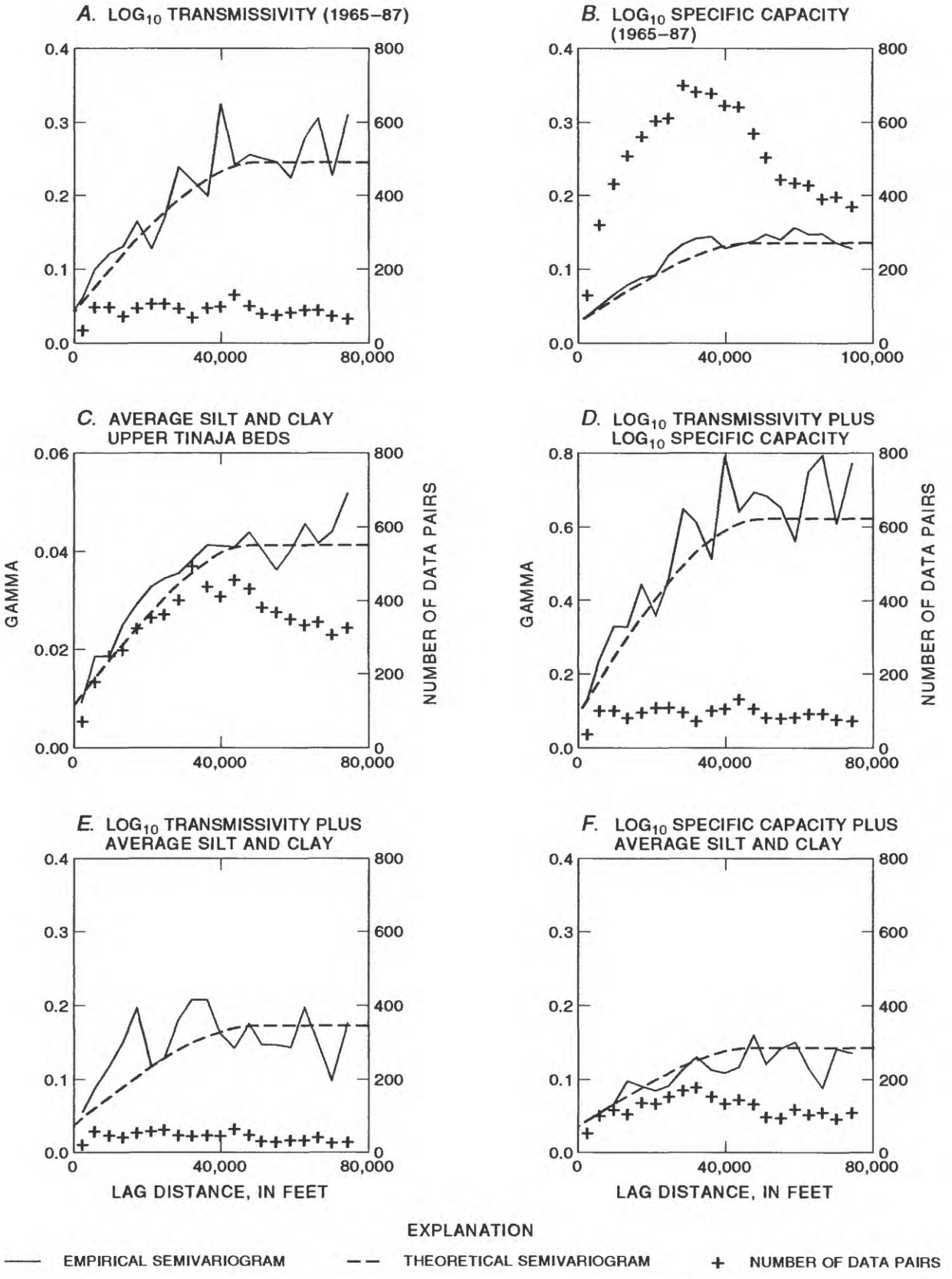

Figure 17. Experimental and pseudovariable semivariograms of transmissivity, specific capacity, and average silt and clay with theoretical curves. Determination of gamma is variable.

Log transmissivity cokriged with log specific capacities (fig. 16*C*) and cokriged with log specific capacities and silt-and-clay content (fig. 16*D*) show large underestimations of transmissivity with respect to the trial-and-error model along the Santa Cruz River and overestimation in the AV well field. The overestimation and poor correlation of silt-and-clay content with transmissivity and specific capacity may be poor in part because the upper Tinaja beds are unsaturated to partly saturated in the southern part of the valley where most of the aquifer-test transmissivities were obtained. As with the other kriging estimates, the two-property cokriging also overestimated transmissivity in the northeastern part of the valley. The major difference in this northeastern part of the basin where some silt-and-clay data occur was that transmissivity values were nonexistent and specific-capacity estimates were sparse. In this part of the valley, the three-property estimate is more in alignment with the flow-model transmissivity estimate (fig. 16*D*) than the other estimates. The three-property estimate also produces one of the lowest estimates of uncertainty in the regional-transmissivity estimate, which included the largest reductions of uncertainty occurring in the northeastern part of the basin where transmissivity values were nonexistent.

Ordinary Kriging with Linear Regression—Transmissivity estimates from regression relations between specific capacity and transmissivity commonly are used to supplement sparse distributions of aquifer-test transmissivities. Specific capacities were estimated at a large number of additional wells in Avra Valley (fig. 11 and table 8 at the back of the report). As with transmissivities, estimates made on wells shortly after drilling characteristically are higher than more recent values. Estimates were made for different time periods that included a few hours during pump-efficiency tests, a few days during aquifer tests, and a few months during seasonal pumping (table 9 at the back of the report). For longer pumping periods, the elapsed time greatly exceeds the aquifer time constant (T/r^2S) resulting in a closer fit to the Cooper-Jacob approximation. Thus, seasonal estimates of specific capacity may be better than estimates from shorter (aquifer test) time periods for confined aquifers but also may include the effects of delayed yield for unconfined aquifers. Clifton (1981) compiled 106 values for 1940–77 from basic-data files and published reports (White and others, 1966; Matlock and Morin, 1976). Most of these estimates represent seasonal water-level drawdowns. In order to expand the number of log transmissivities available for kriging, Clifton used 37 sites where both specific-capacity (*SC*) estimates, in gallons per minute per foot of drawdown, and transmissivity (*T*) estimates, in feet squared per day, were available to establish a log-log regression equation:

$$\log T = 2.36 + 1.07\,(\log SC). \qquad (1A)$$

Of the original 106 values, 14 represent sites having additional transmissivities. An additional 8 specific-capacity values from 1977–87 were included with the remaining 92 values (table 8 at the back of the report). These additional values are from shorter time periods such as aquifer tests and well-efficiency tests. Even with this increase to 69 aquifer-test sites, the small number and poor spatial distribution of transmissivity estimates yielded a log-log regression equation:

$$\log T = 2.34 + 1.13\,(\log SC) \qquad (1B)$$

that is similar to Clifton's model (equation 2*A*) because most of the additional estimates of transmissivity are still in a central corridor of the valley and in the southern part of the valley. Estimation errors from the log-log linear regression of transmissivity and specific capacity show some correlation with estimated values and slightly more correlation with northerly distance along the valley. The regression model derived from these data results in spatial extrapolation from a model using transmissivity estimates predominantly from wells completed in the alluvial-fan sediments in the south and from wells completed in playa and interfingered playa and alluvial-fan sediments in the central part of Avra Valley. Specific-capacity values from wells in the northern part of the valley, in turn, largely represent shallow fluvial and deeper playa sediments (figs. 11 and 15*A*). The resulting error in the log-log regression estimator increases to the north for both models. The spatial extrapolation

with the regression model and the consistency of the specific-capacity values in the northern part of the valley, however, yield a large number of estimates that are potentially biased and yield a regional estimate of uncertainty that is relatively smaller than differences between these and other head-conditioned estimates of transmissivity. These characteristics are exemplified by Clifton's transmissivity variogram (1981, fig. 10) for the northern part of Avra Valley, which shows half the variance of the transmissivity variogram for south-central Avra Valley and represents transmissivities that largely are derived from specific capacities. Clifton's two-domain regional-transmissivity estimate is extrapolated from a regression model that largely represents only the south-central part of the valley. This limitation is a problem that reflects the typically poor spatial distribution in many alluvial aquifers that can yield lower variance in some regions that are, in part, an artifact of this regression-model approach to supplementing the transmissivity data set.

The 69 log transmissivities were supplemented with the 100 log specific capacities using equation 1*B*. Because of the poor spatial distribution of these data, the valley again was treated as a single domain for estimation of the regional-transmissivity distribution. A regional trend was estimated with these 169 transmissivities using a global step-forward regression. Ordinary kriging was applied to the residuals with all estimates treated with equal certainty. The regional trend was added back into the kriged residuals for the estimate of regional transmissivity. As with the other kriging methods, OK resulted in relative overestimation in the northeast and at the AV well field and underestimation along the Santa Cruz River and southeast of the Silverbell Mountains (fig. 16*E*). The estimation error was reduced in the northern part of the valley relative to UK and GC estimates by the indirect inclusion of the specific-capacity derived transmissivities. The error, however, was not as low as the CK estimates.

Inverse Estimates

Methods of estimating transmissivity, selected boundary conditions, and related uncertainty for steady-state ground-water flow included trial-and-error calibration of the digital-flow model, Monte Carlo methods, nonlinear-regression estimates, and conditioned inverse techniques. Previous models of Avra Valley, which include electric-analog trial-and-error (Moosburner, 1972), finite-difference trial-and-error (Travers and Mock, 1984; Hanson and others, 1990), and finite-element Jacobson/Neuman method (Clifton, 1981; Jacobson, 1985), are all inverse estimates of the regional-transmissivity distribution. Regional estimates from flow models that are conditioned on heads and estimates of boundary conditions are different from the geostatistical estimates that are based solely on interpolation of the local transmissivities. Conditioning the regional-transmissivity estimate can substantially reduce the uncertainty in the estimate of regional heads (Clifton and Neuman, 1982) and can potentially result in regional-transmissivity estimates that are different from geostatistical estimates (Clifton, 1981; Zimmerman and others, 1991).

Regional transmissivities from trial-and-error calibration of a digital-model simulation of the aquifer system (Hanson and others, 1990) were derived (fig. 18*A*) from the electric-analog model estimate (Moosburner, 1972), which in turn, generally is in alignment with the sedimentary facies and the cokriged estimate of transmissivity. Exceptions to this alignment appear to occur in the north-central part of the valley where the aquifer system is thickest (Anderson, 1989, fig. 3; Hanson and others, 1990, fig. 2) and is more layered (Hanson, 1989a, fig. 23).

A pattern of differences (fig. 18*A*) similar to the geostatistical differences occurs when aquifer-test estimates are subtracted from the regional estimate during trial-and-error model calibration. These groupings also are roughly coincident with the overestimations to the south in the AV well field and underestimations to the north along the Santa Cruz River as shown for departure from ideal "Theis conditions" (fig. 14) and may collectively suggest that short-term aquifer tests interpreted on the basis of Theis conditions yield systematic error in regional-transmissivity estimates. This systematic error may be due, in part, to the short-term tests used to estimate transmissivity and a more pronounced effect from delayed yield at early time for many of the tests performed in the less layered southern part of the valley. These

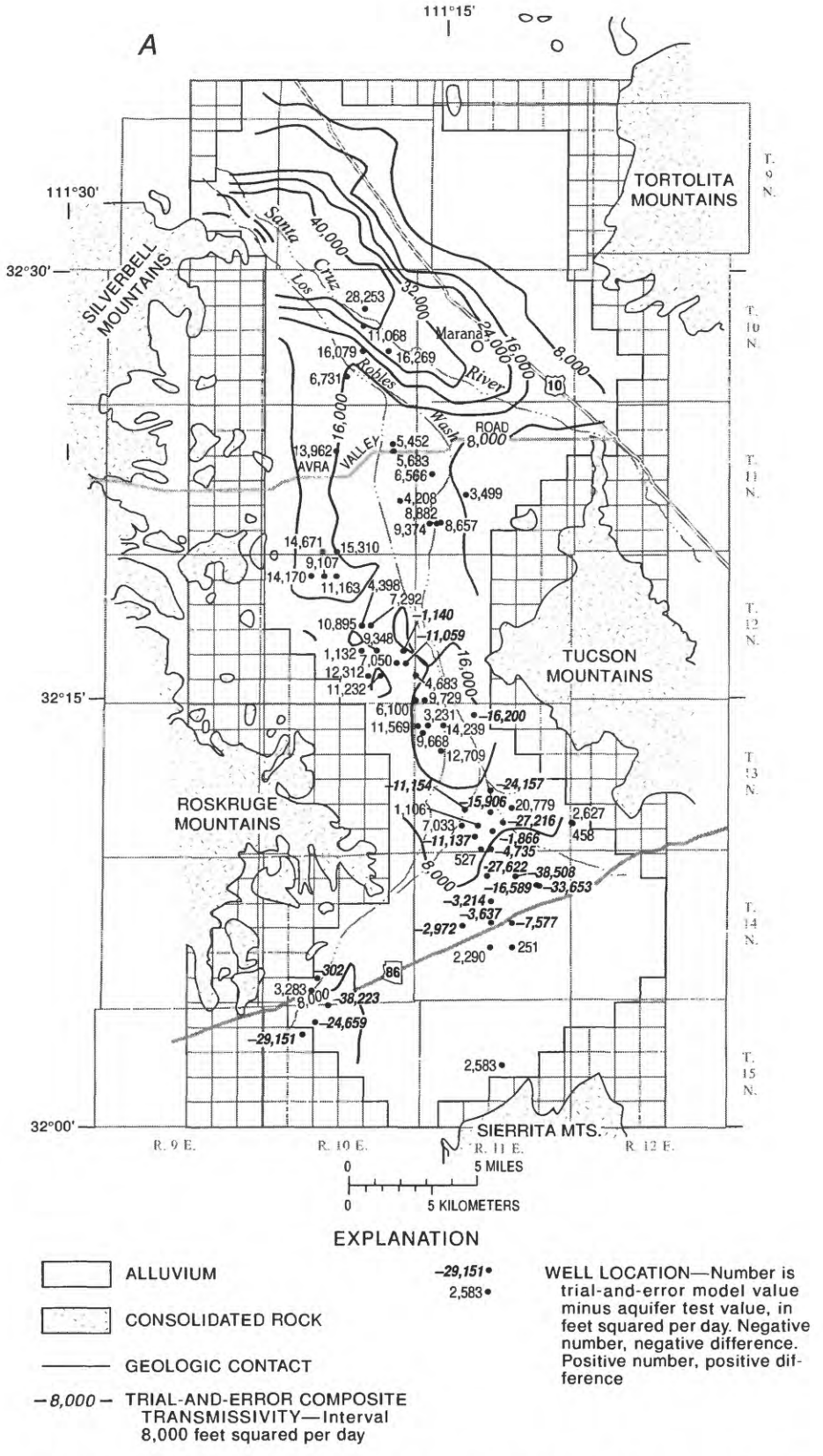

Figure 18*A*. Trial-and-error composite transmissivity and difference between trial-and-error and aquifer-test transmissivities.

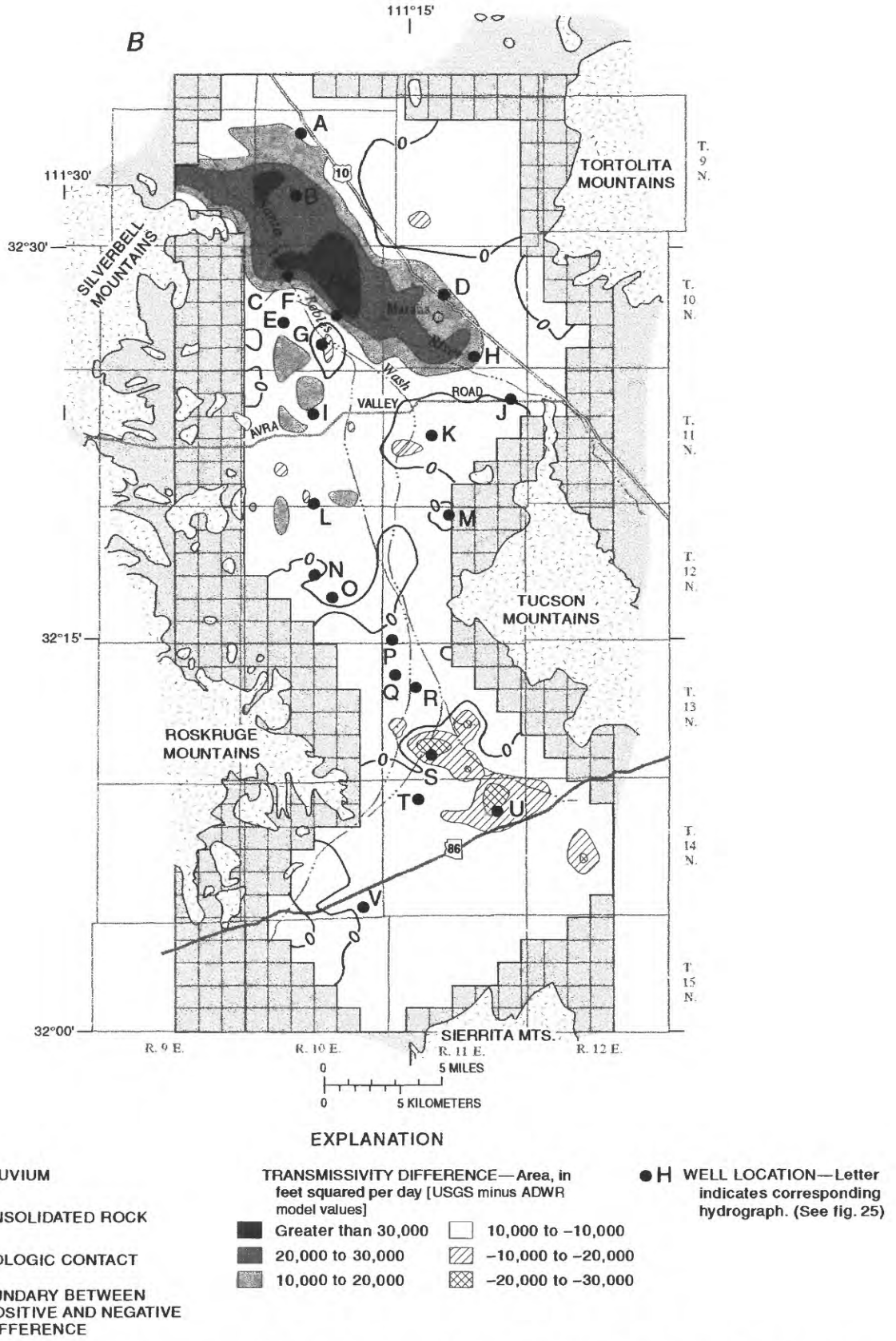

Figure 18*B*. Difference between two-layer and one-layer trial-and-error model estimates of transmissivity.

factors, in turn, may indicate the importance of the effective thickness and layering on the regional-transmissivity distribution. The effective thickness of the flow system is the permeable and saturated parts of the hydrostratigraphic units that are penetrated by wells or exposed to natural recharge or discharge. The model-derived transmissivities also are not in alignment with the textural facies (figs. 11 and 18*A*), which may indicate that the correlation between sediments within model layers and within the textural facies may not be valid in all parts of the valley.

Travers and Mock (1984) calibrated a trial-and-error model over a 20-year historical transient period (1960–79) using the drillers' log method for initial estimates of regional transmissivities for Avra Valley and the Tucson basin. Drillers' log assignments commonly are used to supplement sparse distributions of aquifer-test transmissivity estimates. This approach depends on the assignment made between rock type and hydraulic conductivity. The empirical relation between hydraulic conductivity and particle size is nonlinear (Anderson and others, 1992, fig. 9) making the method sensitive to the assumed values. This approach also depends on geometric means of the assigned estimates over the correct thickness of the effective-flow system. Because the effective-flow system in many alluvial basins may not include deeper and less permeable layers penetrated by some wells, the general tendency is underestimation of transmissivity with this method. Although not used by Travers and Mock (1984), this method also can yield an estimate of the uncertainty at each well.

This model is different from the other trial-and-error models in the choice of boundary conditions, calibration of hydraulic properties (transmissivity and storage), and natural inflows and outflows in transient simulations. The transmissivity values were altered along with specific yield during the first 10 years of transient-state simulation to match the spatial distribution of heads in 1970 and "verified" in the subsequent 10-year period to match heads in 1980. A pattern similar to the kriging estimates is indicated (fig. 18*B*) when the trial-and-error model transmissivities are subtracted from transmissivities from this model.

When the geostatistical estimates made by Clifton and Neuman (1982, figs. 9 and 15) and Jacobson (1985, figs. 12 and 34) are compared with their final inverse solutions, the same pattern of increased transmissivities in the Santa Cruz River region and decreased transmissivities in the south-central AV well field region is apparent. A marked difference exists between these two inverse estimates because Jacobson computed larger transmissivities in the central part of the basin and in the AV well field. These differences are from a solution that was based on a combination of measured and kriged heads that gave better spatial distribution of head comparison during the inverse solution. Both inverse solutions yielded transmissivity distributions similar to the trial-and-error models (Moosburner, 1972; Hanson and others, 1990) that had low average errors between measured and simulated head.

POSTAUDIT OF GROUND-WATER MODELS

Numerical models of ground-water flow systems are useful tools for assessing the aquifer-system response to changing stresses. Models, however, are only an approximation of the actual flow system and are based on average and estimated conditions. The accuracy with which a model can simulate aquifer response is related directly to the accuracy of the input data, the amount of detail that can be simulated at the scale of the model, and the model discretization of time and space. The accuracy of a model is inversely related to the duration, magnitude, and distribution of pumping and recharge simulated by the model. Additionally, the trial-and-error approach to model calibration is inexact and commonly is compounded by variable uncertainty and sensitivity of the aquifer-parameter and boundary-condition estimates during the simulation of changing stress conditions such as climatic cycles and variable pumping.

Predictive errors and model uncertainty from regional ground-water flow models are caused by errors in data collection and interpretation, uncertainty in the conceptualization of the ground-water flow system, and errors in the mathematical

representation of the regional-flow system. Konikow (1986) suggested that differences between measured and predicted water levels from regional ground-water flow models of alluvial basins may be caused by a combination of factors that include large errors in the assumed total pumpage during the prediction period, two-dimensional representation of a three-dimensional system, and the lack of consideration of land subsidence. The largest source of predictive error commonly is the assumed amount and distribution of future pumpage.

Before the sources of predictive-model errors can be understood and quantified, a study of historical simulation errors is needed to rank and segregate errors due to potential errors or uncertainty in pumpage, and from errors due to systematic errors in estimates of aquifer properties and boundary conditions. Analysis of predevelopment and historical simulations can be used to determine if systematic errors in the aquifer-property distributions or boundary conditions are identifiable and are large in relation to errors in pumping estimates. Postaudit comparisons of steady-state and transient-state simulations were studied to address the potential effects of boundary conditions and aquifer properties on historical prediction errors. If prediction errors caused by boundary conditions or hydraulic properties used in the flow model are systematic, then some spatially distributed measure of model fit may yield additional information about the source of the error. Unfortunately, errors in estimating pumpage, boundary conditions, and aquifer properties commonly are linked. Thus, errors in one component are compensated by errors in the other components to achieve a model that compares favorably with measured heads.

Errors related to the mathematical representation of the system include the discretization of time and space, the mathematical approximation of the flow equation, and related interpolation of aquifer properties required by the discretized model formulation. A concurrent study (Goode and Appel, 1992) of alternate forms of the interpolated estimates of intercell transmissivity used by the MODFLOW ground-water flow model (McDonald and Harbaugh, 1988) produced differences that were small compared to calibration errors for the Avra Valley model (Hanson and others, 1990). Although errors related to time and space discretization can be significant, model errors related to the mathematical representation generally are assumed to be small for the Avra Valley model and are not specifically addressed in this report.

Steady-State Models

Previous steady-state simulations of predevelopment conditions in Avra Valley include an electric-analog model (Moosburner, 1972), two inverse models (Clifton, 1981; Jacobson, 1985), and a two-layer model (Hanson and others, 1990). Comparisons of values used for steady state include reviews of predevelopment boundary conditions and transmissivity distributions. Geostatistical estimates of transmissivity consistently indicate values smaller than the trial-and-error model along the Santa Cruz River and southeast of the Silverbell Mountains and values larger than the trial-and-error model in the northeastern part of the valley and in the AV well field in the southern part of the basin (figs. 15*A–E*). The electric-analog model and inverse models show a similar pattern of differences. The two inverse models resulted in transmissivities that differed as much as 100 percent from initial geostatistical estimates. These inverse models started with geostatistical estimates of transmissivity that indicated a low uncertainty in the regions of the largest differences. Large differences from initial estimates along with the departures from Theis conditions (figs. 14 and 16), similar distribution of differences between Theis conditions and trial-and-error model transmissivities (fig. 18), and low kriging errors in areas with the largest differences between model and kriged transmissivities collectively indicate that biases are occurring in the aquifer-test transmissivities and specific-capacity estimates that are consistent in the northern, central, and southern parts of the valley. In turn, these field estimates result in geostatistical transmissivity estimates that are markedly different from head-conditioned estimates.

A good model fit requires the absence of any systematic errors in the steady-state model. Systematic errors may result from incorrect estimates of the boundary conditions and aquifer

parameters or from an incorrect conceptual model. Overall model fit usually is assessed with a single-error statistic, such as average-absolute error or root-mean-square error, and some analysis of residual-head differences, such as the correlation between simulated and measured head throughout the model area. The correlation and Weibull-probability plot for the two-layer model indicates an approximate normal distribution with some overestimation of simulated heads at higher altitudes, which generally occur in the southern part of Avra Valley (Hanson and others, 1990, fig. 11). This overestimation of heads in the southern part of the valley may be the result of underestimation of model transmissivities in the southern or central part of the valley or overestimation of ground-water inflow in the two-layer model.

Correlation and autocorrelation structures can give additional insight as to whether systematic errors are occurring. The spherical variogram of log transmissivities indicates that trial-and-error transmissivities are correlated to as much as 50,000 ft (Zimmerman and others, 1991, fig. 4–5), which is identical to the estimated range used for cokriging. When a regional trend was estimated for the model using a second-order polynomial, the residual log transmissivities indicate no correlation at any distance intervals. Because universal kriging and generalized covariance indicated an apparent linear northerly trend in transmissivities (fig. 15*A*), the presence of a second-order drift in the distribution of calibrated trial-and-error transmissivities may be an artifact of conditioning on the heads, which showed second-order drift (fig. 15*B*). Head residuals from the trial-and-error model indicate a weak but significant inverse correlation ($r^2 = -0.33$ at $\rho = 0.01$) with the measured heads. Similarly, head residuals show weak but significant correlation ($r^2 = 0.48$ at $\rho = 0.05$) with the northerly direction. These weak correlations again may collectively indicate that the largest residuals generally occur at higher altitudes in the southern part of Avra Valley. A spherical variogram of predevelopment-head error residuals indicates spatial autocorrelation over a range of about 20,000 ft (fig. 19) and a sill of about 100 ft^2, which is similar to the estimated range and about 1.5 times the sill of the spatial residuals of measured predevelopment heads. The residual semivariogram also indicates a growth in variance with distance for distances greater than about 50,000 ft. Thus, the autocorrelation structure of head-error residuals shows a similar correlation length and 50-percent larger variability than the measured head residuals used to condition the trial-and-error model. The autocorrelation structure also indicates a larger-scale increase in variance at a distance just greater than the correlation length of the trial-and-error transmissivities. Head-error residual-correlation lengths that are half the model-transmissivity correlation lengths and a weak but significant correlation ($r^2 = 0.27$ at $\rho = 0.05$) between head-error residuals and model transmissivities would appear to indicate that there may be a small basin-wide systematic error in the model-derived transmissivity field. This systematic error could result in increases in head errors with increasing transmissivity. Correlations between measured and simulated heads, head-residual correlations with measured head and northerly distance, and the residual-head variogram, however, appear to collectively indicate that there is no basin-wide monotonic type of systematic error in the regional simulated heads. Instead these indicators appear to allow inference of some sort of local systematic error. Systematic error representing model subregions can be addressed through spatial analysis of model error.

When spatial comparisons are made between simulated heads from a ground-water flow model and regional-contour maps of head, no qualification generally is given to the spatial variability of uncertainty in the contour maps. All segments of estimated contours are treated with the same level of confidence, and all simulated heads are given the same weight in any set of summary statistics that describe the match between measured and simulated heads. Delhomme (1976) demonstrated an alternate approach that helps to account for the uncertainty in the contour map derived from measured heads. His standardized calibration-error map provides a map of normalized differences from the difference between kriged and simulated heads divided by the kriging error. This type of map results in contours of the differences between kriged and simulated heads that are multiples of the local uncertainty in the kriged heads. The utility of this approach as an indicator of regional or local systematic errors is strongly dependent on

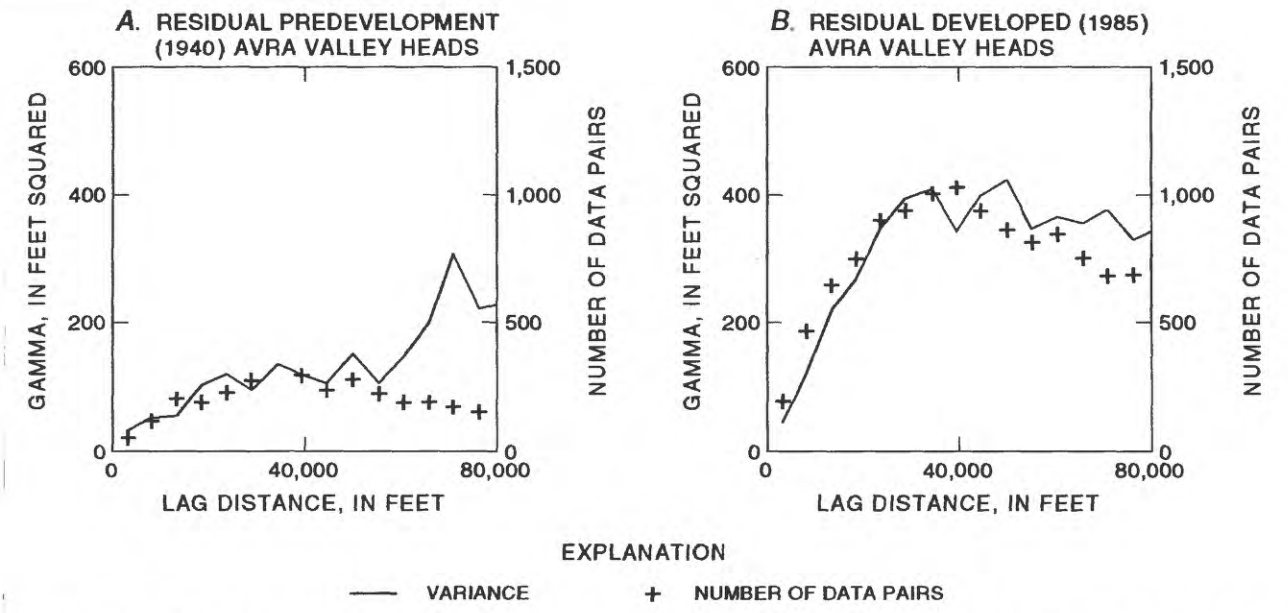

Figure 19. Semivariograms for residual errors between measured and simulated heads for predevelopment and developed conditions.

the quality of the kriged map and related distribution of field data. On the basis of Chebyshev's inequality, 65 percent of the values of a random variable should occur within one standard deviation of the mean, 95 percent within two standard deviations, and 99.5 percent within three standard deviations. If potential outliers are assumed to represent any values more than twice the local kriging error away from the local mean (kriged-head value), potentially unacceptable errors would occur when the difference between kriged and simulated heads are more than twice the kriging error. The contours of standardized-calibration errors for the predevelopment (steady-state) simulation of Avra Valley (fig. 20) indicate errors less than twice the kriging error throughout most of the north and central parts of the model area. Areas where the simulated heads are less than the kriged estimate occur along the northeastern boundary with the Tucson basin and Tortolita Mountains, in several small regions along the Roskruge Mountains, and in one small area along Brawley Wash. The areas along the model boundaries have kriging errors of more than 8 ft and could be related to incorrect boundary conditions or transmissivity estimates. The two isolated regions where simulated heads underestimate kriged heads (positive error) are related to areas with less than 8 ft of kriging error and may be related to suspect data points or unachievable match between the kriged and simulated surfaces for a regional-scale model. Simulated heads overestimate kriged heads (negative error) by more than twice the kriging error in the southern part of the model and in two central regions. The southern region is an area with large kriging errors (10 to 60 ft) because of the few number of measured heads and larger hydraulic gradients. This area may reflect a poor estimation of kriged heads (fig. 8), underestimation of transmissivity, and overestimation of ground-water inflow from Altar Valley. The isolated areas of overestimation in the northern part of the model simulation may reflect areas of unachievable low uncertainty (less than 6 ft) in the kriged head surface (fig. 8). The other notable feature of the standardized error map is the lack of differences greater than twice the kriging errors along other parts of the flow-model boundary where uncertainty in the kriged-head surface commonly is largest.

Two-dimensional simulation of three-dimensional flow generally results in overestimation of transmissivity in areas where upward flow is a significant source (inflow) of ground

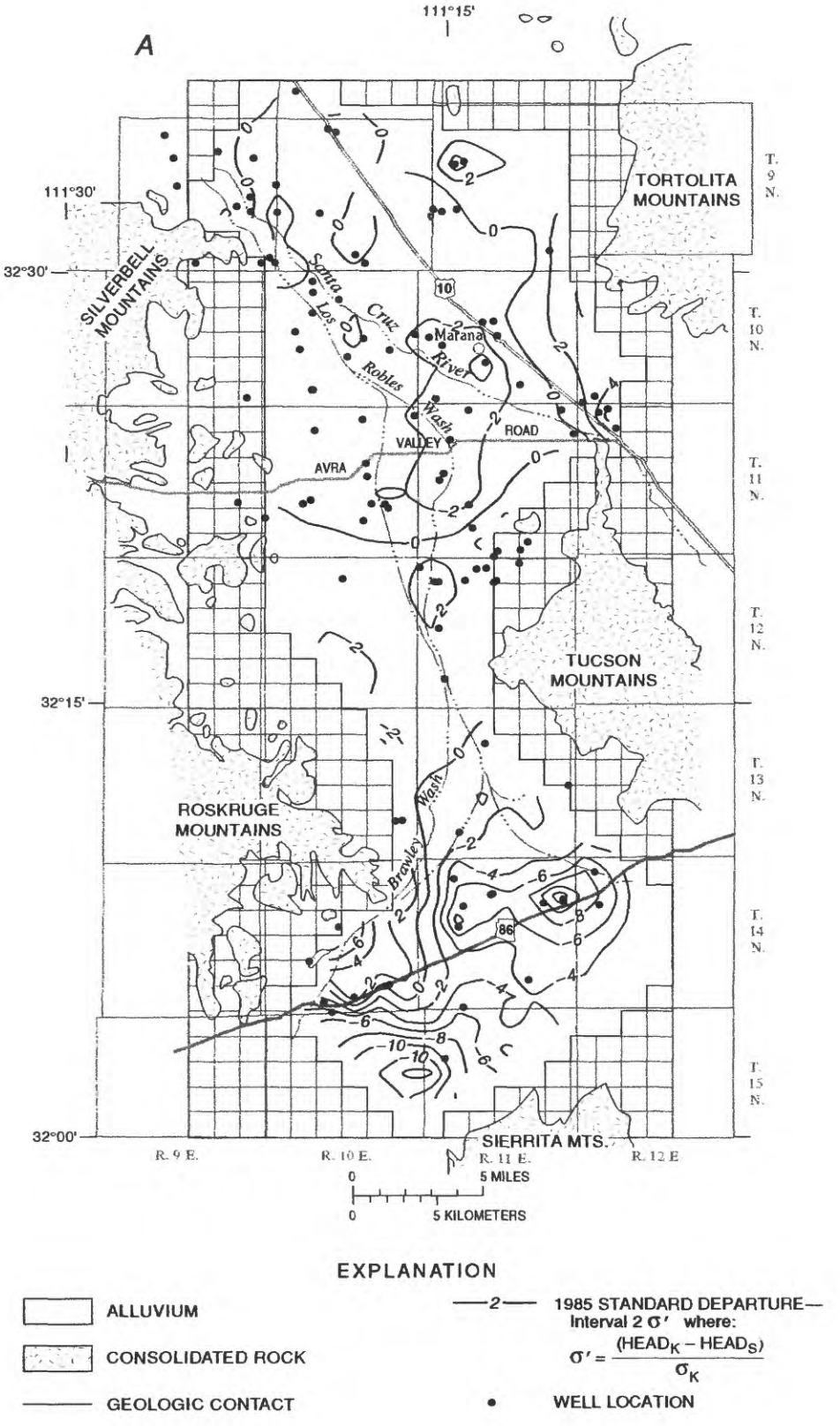

Figure 20*A*. Standardized steady-state calibration errors.

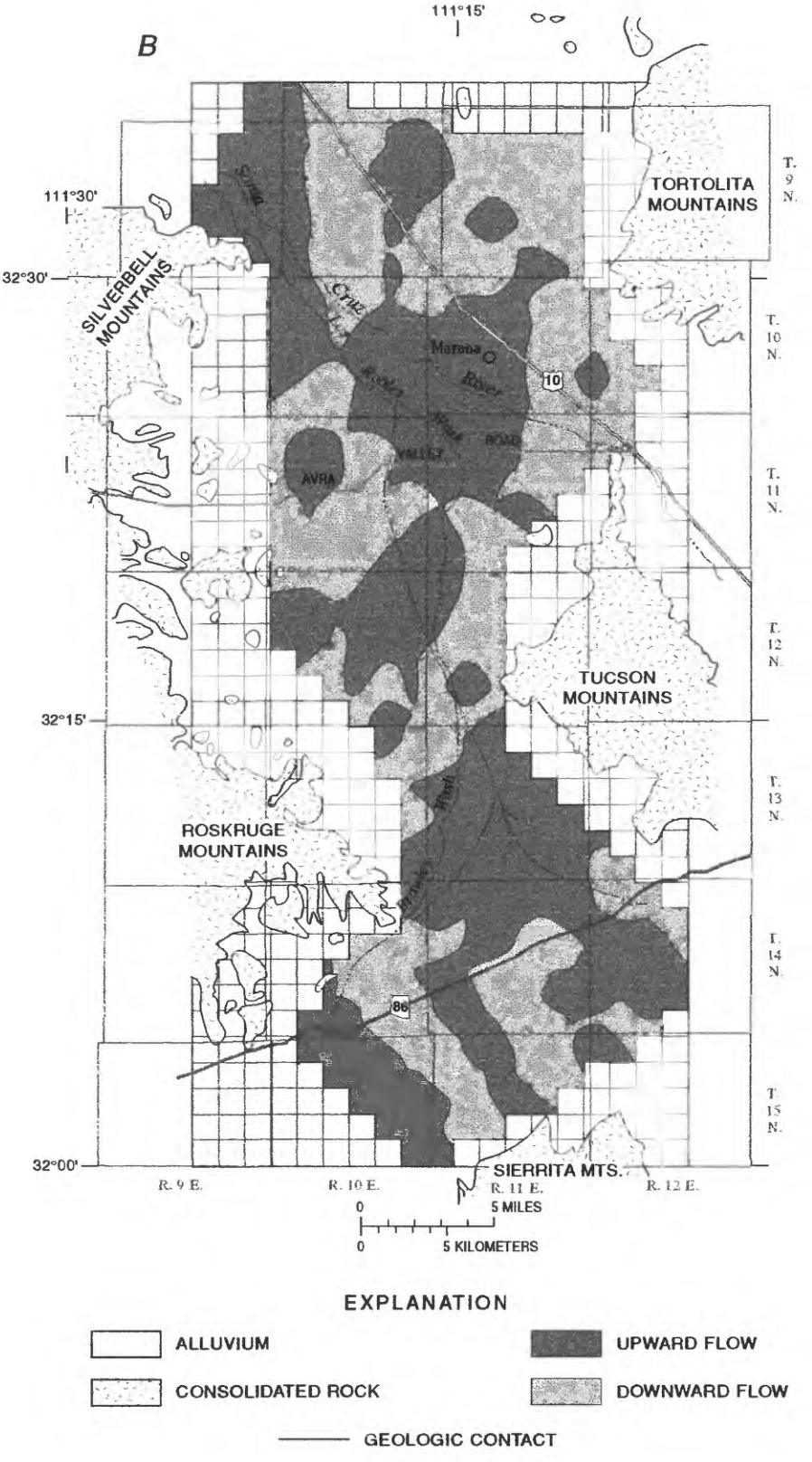

Figure 20*B*. Distribution of vertical flow between layers in the two-layer, steady-state, predevelopment-flow model.

water and results in underestimation of transmissivity where downward flow is a significant loss (outflow) from the horizontal flow of ground water. The distribution of vertical flow between layers in the trial-and-error model indicates that flow is largely rejected from the lower layer along a diagonal across the basin constriction (fig. 20*B*). Vertical flow is aligned with the transmissivity distribution of the lower layer with 15 percent of the total basin flow occurring as upward flow south of the basin constriction. This pattern of upward flow also is in alignment with a statistically significant ($\rho = 0.01$) gap in the distribution of 1940 and 1985 heads (fig. 15*B*). When the trial-and-error model was simulated as a one-layer model, the mean error was almost doubled; however, the difference between mean error and slight reduction in variance were not significant at the 95-percent confidence level (table 2). These statistical indicators suggest that three-dimensional flow is potentially important locally but not important with respect to all the measured heads for predevelopment and developed conditions over the entire valley. The largest upward flows also are coincident with the areas of underestimation of model transmissivity with respect to field transmissivities. The regions of negative standardized error (fig. 20*A*) also are coincident with several areas of upward flow (fig. 20*B*). These patterns of model error could collectively indicate underestimation of model transmissivity in the two-layer model and overestimation in the one-layer model.

Six alternate boundary-condition cases of the steady-state model were evaluated for a significant reduction in mean errors and reduction in the variance of errors with respect to the calibrated conceptual model (Hanson and others, 1990). Three alternate transmissivity distributions also were evaluated for the southern part of the model. These errors were evaluated on the basis of the 100 measured heads (table 3). The six alternate boundary conditions, three alternate transmissivity distributions, and composite cases that were evaluated are:

(1) Arizona Department of Water Resources model values of recharge (Osterkamp, 1973; Travers and Mock, 1984) and predevelopment pumpage (D.R. Pool, hydrologist, USGS, written commun., 1989);
(2) Clifton's (1981) mountain-front recharge, Tucson Mountains;
(3) Hanson and others (1990) proposed mountain-front rechage, Sierrita Mountains;
(4) Hanson and others (1990) proposed Brawley Wash streamflow infiltration;
(5) A composite of cases 2, 3, and 4;
(6) Mountain-front recharge along the southeast flank of the Tortolita Mountains;
(7) Increased hydraulic conductivity in the upper layer for the southern part of Avra Valley and holding Altar Valley inflow constant;
(8) Increased transmissivity in both layers in the southern part of Avra Valley;
(9) Decreased hydraulic conductivity in the upper layer in the southwestern part of Avra Valley and holding Altar Valley inflow constant; and
(10) A composite of cases 2, 4, 6, 8, and 9.

Cases (1) through (6) used constant-head ground-water inflow and outflow cells and the transmissivity and leakance distributions of the trial-and-error model (Hanson and others, 1990). Cases (7), (8), and (9) used changes in transmissivities with the boundary conditions from the two-layer model and ground-water inflow held constant. Cases (2), (4), and (6) were based on areas of large positive differences in the standardized calibration-error map (fig. 20*A*) for predevelopment conditions.

An alternate transmissivity distribution for the southern part of Avra Valley was based on the mutual regions of large negative standardized error for steady-state (fig. 20*A*) and transient-state (fig. 24) conditions for cases (7), (8), and [(9); fig. 21)]. On the basis of the model difference with aquifer tests and the ADWR model, hydraulic conductivity was doubled in the south-central part of the valley [case (7)]. An additional increase in transmissivity was assessed for case (8) by doubling transmissivity in the lower layer in this region along with the increased hydraulic conductivity from case (7). On the basis of the standardized-error maps, the case (9) simulation used transmissivities that were reduced by about

Table 3. Summary of alternate boundary conditions used for analysis of alternate conceptual models

[acre-ft/yr, acre-foot per year; ft/d, foot per day; ft^2/d, foot squared per day]

Boundary-condition name	Initial estimate per cell	Number of cells	Boundary-condition name	Initial estimate per cell	Number of cells
Mountain-front recharge (acre-ft/yr)					
Silverbell-Waterman	124	17	Tucson–west	100	5
Roskruge	75	16	Tucson–northwest	167	3
Sierrita	133	9	Tortolita–southwest	333	3
Tucson–southwest	12	7	Tortolita–west	266	6
Streamflow infiltration (acre-ft/yr)					
Santa Cruz River–southwest	650	9	Brawley Wash	150	16
Santa Cruz River–northwest	545	11	Los Robles Wash	73	15
Average predevelopment pumpage (acre-ft/yr)					
(D-10-9)	707	2	(D-11-11)	970	8
(D-11-10)	866	7			
Hydraulic conductivity (ft/d)					
South-central	4	61	Southwest–upper layer	7	34
Transmissivity (ft^2/d)					
South-central–lower layer	2,150	55			

half in the southwestern part of Avra Valley except along Brawley Wash.

Mean errors were not significantly different for any additional recharge except for recharge along Brawley Wash (table 4). Mean errors and standardized-calibration errors, however, were less for recharge along the Tucson and Tortolita Mountains (fig. 22). The greatest reduction in variances occurred when transmissivity was increased in the upper layer. Variances were slightly reduced when recharge was simulated in the Tucson and Tortolita Mountains. Mean errors were closest to zero for increases in transmissivity. On the basis of these simulations, a composite simulation [case (10)] was assessed with recharge in the Tucson and Tortolita Mountains, streamflow infiltration along the southern half of Brawley Wash, altered transmissivities, and redistribution of ground-water inflow from Altar Valley. This case also included reduced transmissivity in the southwestern part of Avra Valley because the composite errors were improved with the reduced values. This simulation resulted in a mean error close to zero that was significantly different from the calibrated model and resulted in a 20-percent reduction in the variance. The standardized calibration-error map shows a reduction of overestimated heads in south-central Avra Valley, and a better fit along the Tucson and Tortolita Mountains (fig. 22); however, the simulated heads overestimate the regional-head surface near the ground-water inflow boundary. These errors are larger than those in the original model (fig. 20*A*) in the southwestern part of Avra Valley where hydraulic conductivities were decreased, ground-water inflow was decreased by about 2,000 acre-ft/yr, and streamflow infiltration along Brawley Wash was added.

The composite case is a good example of an alternate conceptual model where the fit relative to the original trial-and-error model is better in some regions and worse in others but results in an overall

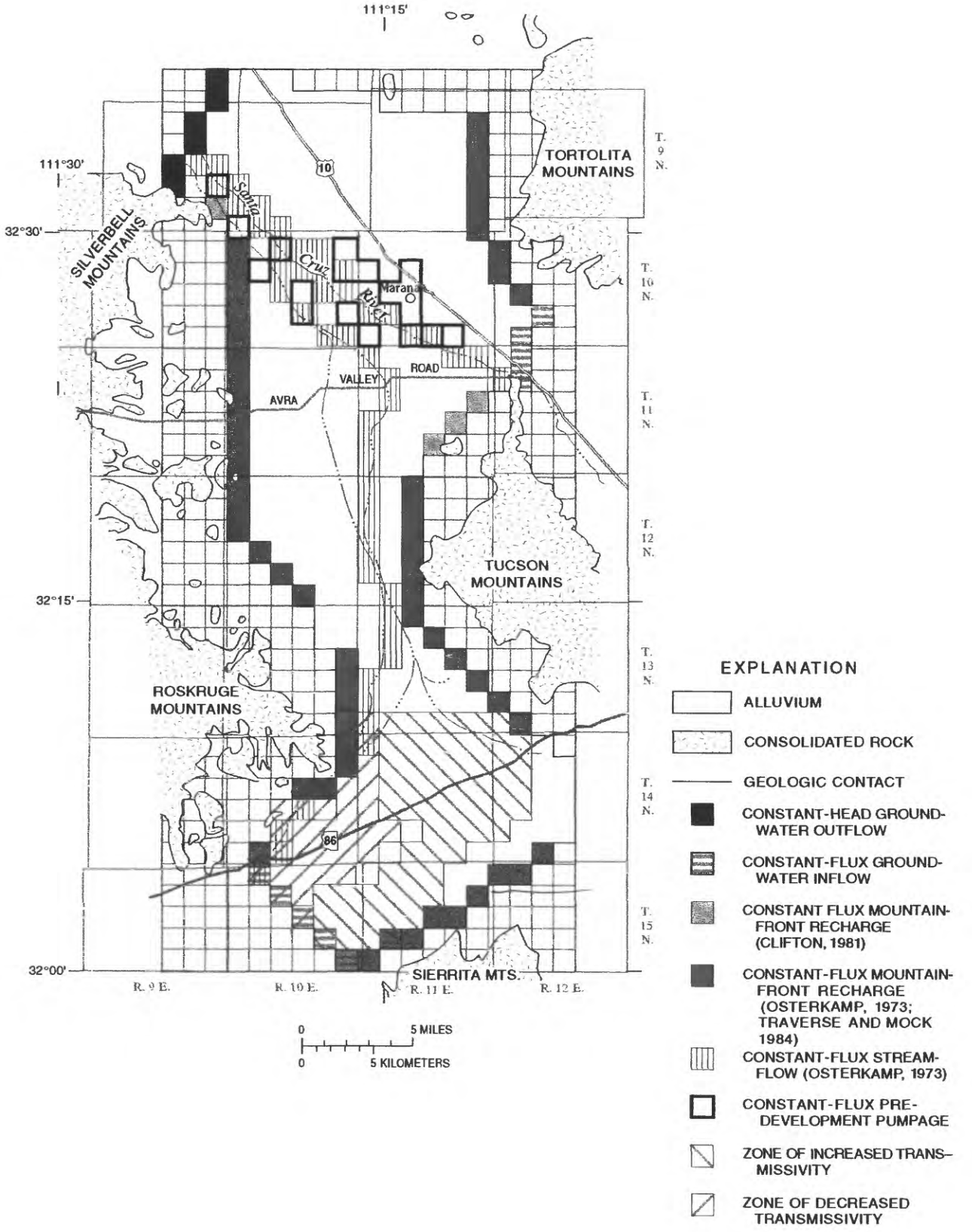

Figure 21. Ground-water flow model finite-difference grid with alternate conceptual-model boundary conditions used for this study.

Table 4. Summary of conceptual-model analysis with respect to the trial-and-error calibrated, two-layer model

[ft, foot; ±, plus minus. Dashes indicate statistic not calculated. From Hanson and others (1990)]

Model alteration	Null hypothesis	Mean error (ft)[1]	Root-mean square error (ft)	Differences of means (ft)[2]	Ratio of variance[2]
Trial-and-error calibrated model	---	-5.98 (±14.86)	15.95	---	---
One-layer model	One layer same as two-layer model	-3.43 (±14.59)	14.92	[3][-2.55] [(-2.78)]	[3][0.96] [(1.01)]
(1) Pumpage and total boundary recharge	Pumpage and additional recharge in two-layer model	-25.25 (±24.36)	35.00	19.27	2.69
(2) Recharge, Tucson Mountains	Additional recharge in two-layer model	-5.93 (±14.19)	15.32	[-.05]	[.91]
(3) Recharge, Sierrita Mountains	Additional recharge in two-layer model	-8.64 (±17.30)	19.26	[2.66]	[1.36]
(4) Streamflow recharge, Brawley Wash	Additional recharge in two-layer model	-13.09 (±16.99)	21.38	7.11	[1.31]
(5) Composite of options 2, 3, and 4	Additional recharge in two-layer model	-18.60 (±20.67)	27.73	12.62	1.93
(6) Recharge, Tortolita Mountains[4]	Additional recharge in two-layer model	-6.60 (±14.09)	15.49	[.62]	[.90]
(7) Increased hydraulic conductivity, upper layer (1)[5]	Double the values in south-central part of two-layer model	-.96 (±14.56)	14.52	-5.02	[.04]
(8) Increased transmissivity in southern part	Double the values in both layers of two-layer model	1.20 (±18.88)	18.82	-7.18	1.61
(9) Decreased hydraulic conductivity, upper layer (1)[5]	Half the values in southwestern part of two-layer model	-12.41 (±29.16)	31.56	6.43	3.85
(10) Composite of recharge and transmissivity[6]	Additional recharge and different transmissivity in two-layer model	.02 (±13.31)	13.25	-5.96	[.80]

[1]Number in parentheses is standard deviation of sample (N=100).

[2]Acceptance region is based on the 95-percent confidence of accepting the null hypothesis. Differences in brackets are not significantly different.

[3]Upper number is for steady-state model (N=100), and lower number in parentheses is for transient-state model (N=190).

[4]Tortolita southwest and west reduced to half the original estimate (table 8 at the back of the report).

[5]Altar Valley ground-water inflow was constant at rate estimated for steady-state calibrated model.

[6]Composite includes reduced Tortolita, Tucson northwest, and Brawley Wash recharge, and all three transmissivity alterations to southern part of Avra Valley.

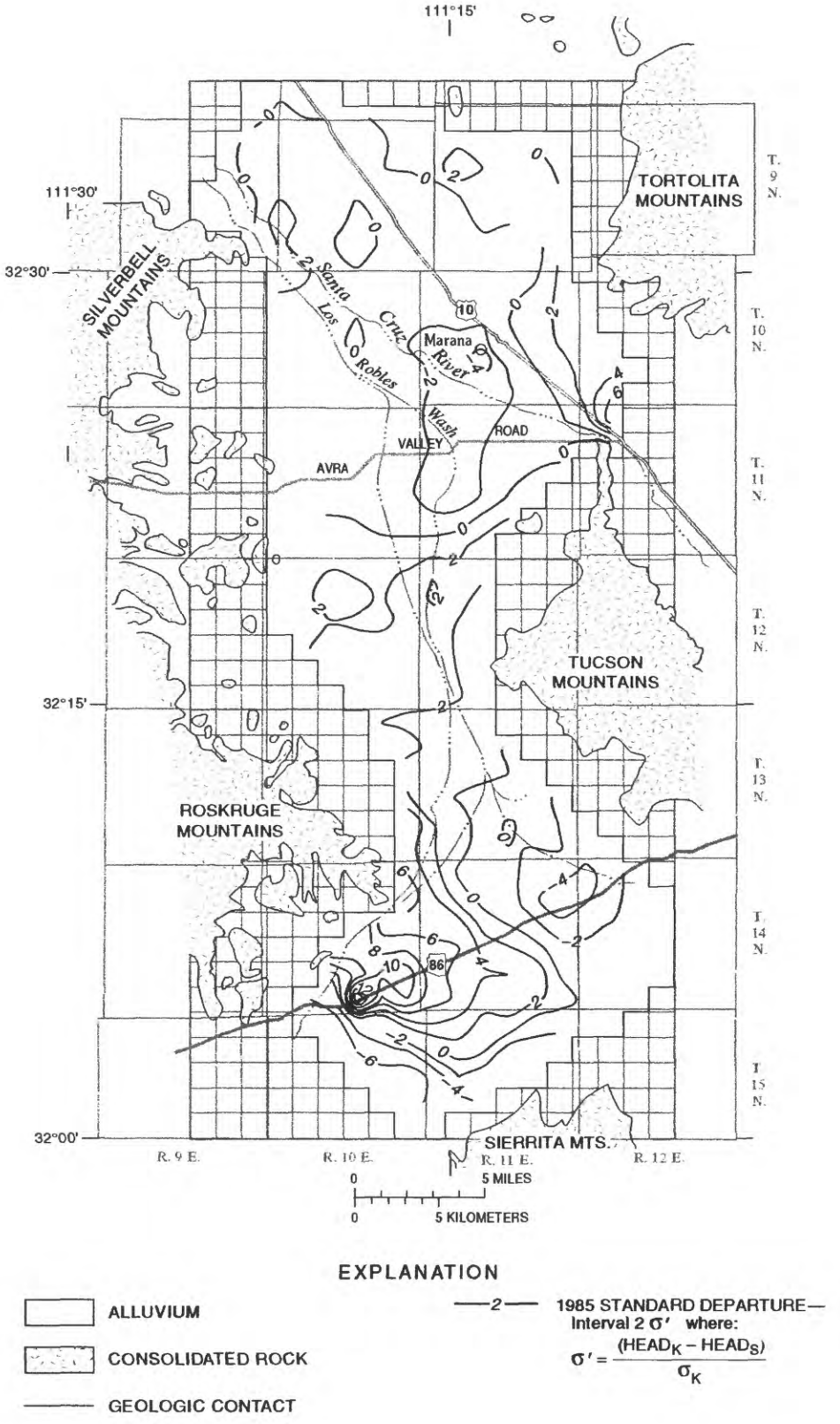

Figure 22. Standardized calibration error for steady-state model with alternate boundary conditions.

significant improvement in the measure of error for the model as a whole. This concept demonstrates that nonspatial statistics are necessary but are not sufficient for defining the fit of a model. Testing conceptual-model components that improve model fit locally may not have a significant regional effect on the whole model. This example also shows the utility of calibration-error maps for assessing residuals that are normalized with respect to the uncertainty in the estimated head surface. In the southern part of Avra Valley, the kriged surface may be questionable because of few measured predevelopment heads. Errors in point comparisons and kriged comparisons, however, are consistent where point data do exist in this area. Model-error comparisons would have been improved if cokriging with the land surface was used to estimate a more realistic kriged head surface.

The use of a parameter-estimation technique such as MODFLOWP (Hill, 1992) might be helpful in assessing the importance of alternate conceptual models for predeveloped and developed conditions. This approach was used successfully for testing alternate conceptual-model features for the regional Madison aquifer (Cooley and others, 1986). This regression technique (Cooley and Naff, 1989) was applied to conceptual models composed of 32 and 215 transmissivity zones. The technique had limited success in the Avra Valley model because of insensitivity to the large number of parameter zones in the model (Zimmerman and others, 1991, Appendix D). These insensitivities persisted even when Jacobson's (1985) method of supplementing the 100 measured comparison heads with 233 kriged heads was used. Even for a 32-zone case, insensitivities and strongly correlated transmissivity zones that were aligned with the sedimentary facies (Zimmerman and others, 1991, fig. D-2) precluded the use of this method for assessing alternate boundary conditions for Avra Valley (Zimmerman and others, 1991, Appendix D). This approach, however, warrants further investigation for steady-state and transient-state simulations of Avra Valley and could potentially allow the assessment of time-varying recharge such as streamflow infiltration along the Santa Cruz River and Brawley Wash.

Transient-State Models

Early predictive simulations using analog and digital models commonly overestimate projected ground-water declines (Konikow, 1986). In south-central Arizona, an electric-analog model was used to predict ground-water-level change from 1964 to 1985 in Avra Valley (Moosburner, 1972). The predicted change was as much as 50 to 100 ft larger (fig. 23) than the change that actually occurred (Cuff and Anderson, 1987) although the total amount of pumpage predicted generally was correct (Hanson, 1989b).

Predictive errors related to pumping and recharge resulted in Moosburner's overprediction of water-level declines by 50 to 100 ft in the north-central part of the basin where the retirement of agricultural land by the City of Tucson and the development of substantial recharge from irrigation return flow and streamflow infiltration occurred (fig. 23). Conversely, Moosburner correctly estimated the pumping rate of wells in the AV well field but predicted about half the number of wells that would be pumping by 1985. This resulted in underestimation of water-level declines by 50 to 100 ft in the southern part of the valley (fig. 23). Thus, predictive errors of future development with the analog model largely were related to misestimation of the spatial distribution and not the amount of future pumpage.

A one-layer regional model of Avra Valley and adjacent Tucson basin (Travers and Mock, 1984) and the current two-layer model of Avra Valley were used in this study for transient-state comparisons of potential model errors for simulation of historical development of the aquifer system. Both models indicate that the largest divergence from measured heads applies to transient periods after the calibration period. Initial analyses indicate that errors in total pumpage and lack of consideration of land subsidence prior to 1985 may not be the major cause of errors in the prediction from the electric-analog model and errors in the historical simulations from digital models. Overprediction of declines from the analog model and divergent rates of decline from the ADWR one-layer regional model may be more closely related to the inability of two-dimensional models to accurately simulate a three-dimensional system and to errors in estimating the spatial

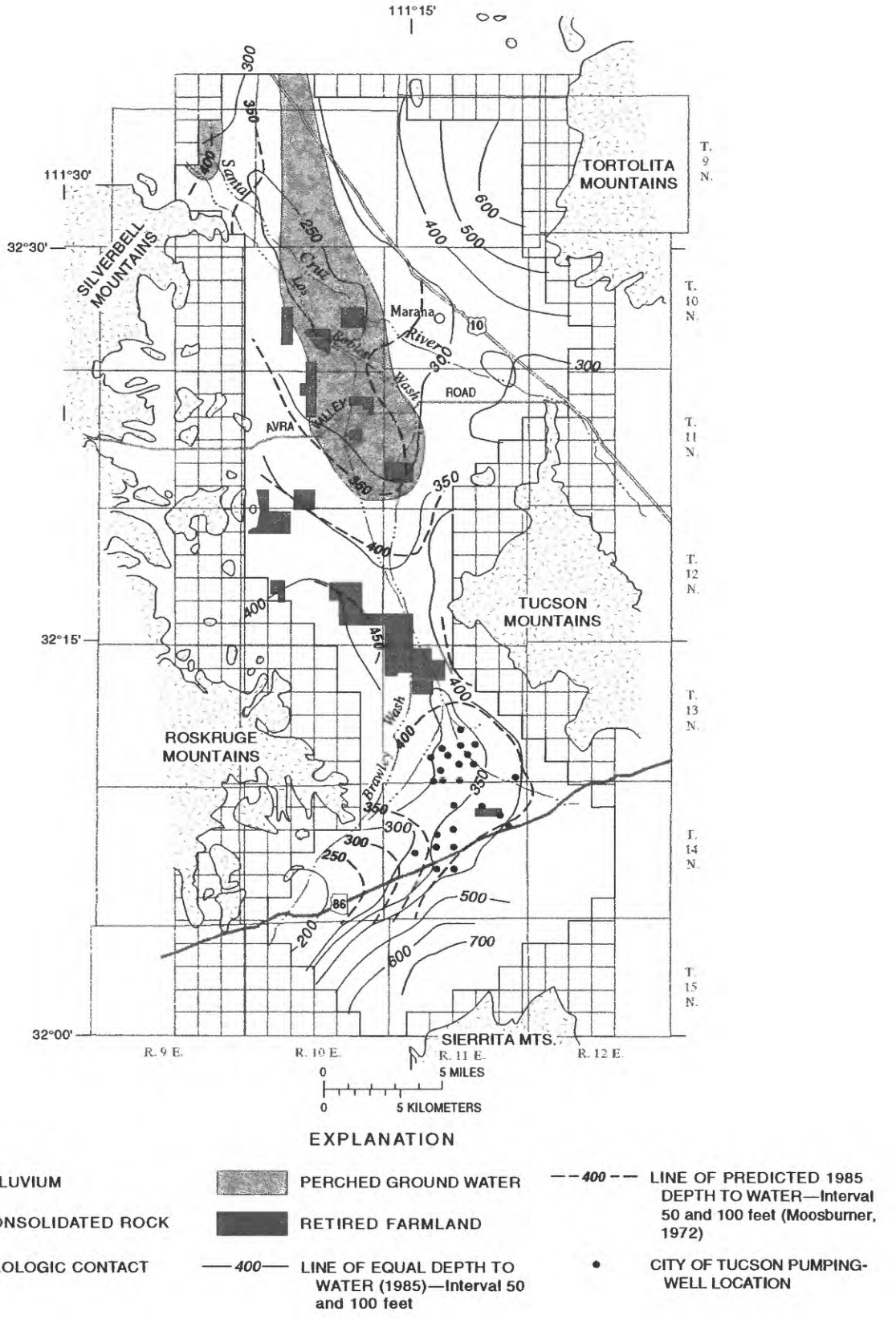

Figure 23. Difference between analog-model predicted and hand-contoured depths to water, 1985.

distribution of pumpage, aquifer recharge, storage, and transmissivity. Results from the two-layer model indicate that three-dimensional flow may be significant locally. In the two-layer model, about 20 percent of total simulated basin flow is occurring between layers, and the lower layer supplies between 3 and 9 percent of basin flow to the upper layer.

Contours of standardized-calibration error for simulated developed conditions for 1985 from the two-layer model (Hanson and others, 1990) indicate errors of less than twice the kriging error throughout most of the model area (fig. 24). Underestimation of simulated heads (positive errors) are related to areas of uncertainty of less than 10 ft. About 60 percent of this error is comparable to the intrinsic error in the kriged heads and, therefore, may be related to an unachievable match between the kriged and simulated surfaces or errors related to composite heads. Areas where the simulated heads are less than the kriged estimate occur southeast of Picacho Peak, south of the Santa Cruz River, and on the northwestern flank of the Tucson Mountains. The two larger areas are coincident with the suspected zone of perched water. Thus, the larger areas of underestimated head may indicate that even the most accurate depth-to-water measurements used to krige the developed heads for 1985 may be influenced by decades of areal recharge from irrigation return flow and streamflow infiltration that result in locally variable or composite heads. The northwestern flank of the Tucson Mountains is an area where simulated heads were underestimated in simulations of predevelopment and developed heads. This area also is where Clifton (1981) added an additional 500 acre-ft/yr of recharge for simulation of predevelopment ground-water flow. Simulated heads overestimate kriged heads (negative errors) by more than twice the kriging error in the southern part of the model and west of the Tortolita Mountains. The southern region is an area with kriging errors between 10 and 60 ft. As in the predevelopment comparison, this area may reflect a poor estimation of kriged heads (fig. 8), underestimation of hydraulic diffusivity, or overestimation of ground-water inflow from Altar Valley. Areas where the largest overestimation of simulated heads occur in the southern part of the model are roughly coincident with the same areas in the predevelopment calibration-error map (fig. 20). This persistent error may reflect areas of underestimated transmissivity or heads from deeper wells or public-supply wells (AV well field) that are less than the regional-head surface during basinwide winter water-level surveys (fig. 9). As with the predevelopment standardized calibration-error map, there is a lack of differences greater than twice the kriging errors along most of the flow-model boundary where uncertainty in the kriged-head surface generally is largest.

Hydrographs from both digital models indicate a divergence in simulation error throughout the period 1960–79 (fig. 25) in the northern and southern parts of Avra Valley. Overestimation of water-level declines in the 1970's and 1980's and similar decline rates in the 1940's through the 1960's is noted for the wells near the Santa Cruz River and the area of suspected perched ground water (fig. 25, wells A, B, C, D, F, H, and J). Development of a return-flow component in Avra Valley after about 1965 (Anderson, 1983) and increased streamflow after about 1960 (Webb and Betancourt, 1990) also may account for some degree of error between predicted and measured water levels. In the two-layer model, an average 40-percent reduction in pumping from 1965 through 1984 was required to account for the combined effects of irrigation return flow, above-average streamflow infiltration, sewage-effluent return flow, and decreased pumpage because of the retirement of agricultural lands (Hanson and others, 1990).

Hydrographs for wells E, G, I, M, and L in the central part of the basin indicate good matches between measured and simulated heads and rates of water-level decline for both models (fig. 25). Hydrographs for wells N, O, P, Q, R, S, and T generally show a good match to heads and rates of decline for the two-layer model in the southern part of the valley. The simulated hydrograph for well U shows overestimation of heads for the two-layer model. The simulated hydrograph from well V shows underestimation of head and overestimation of rate of water-level decline near the southern boundary of the valley for both models. The remainder of the simulated hydrographs for wells in the southern part of the valley show overestimated and underestimated heads and rates of

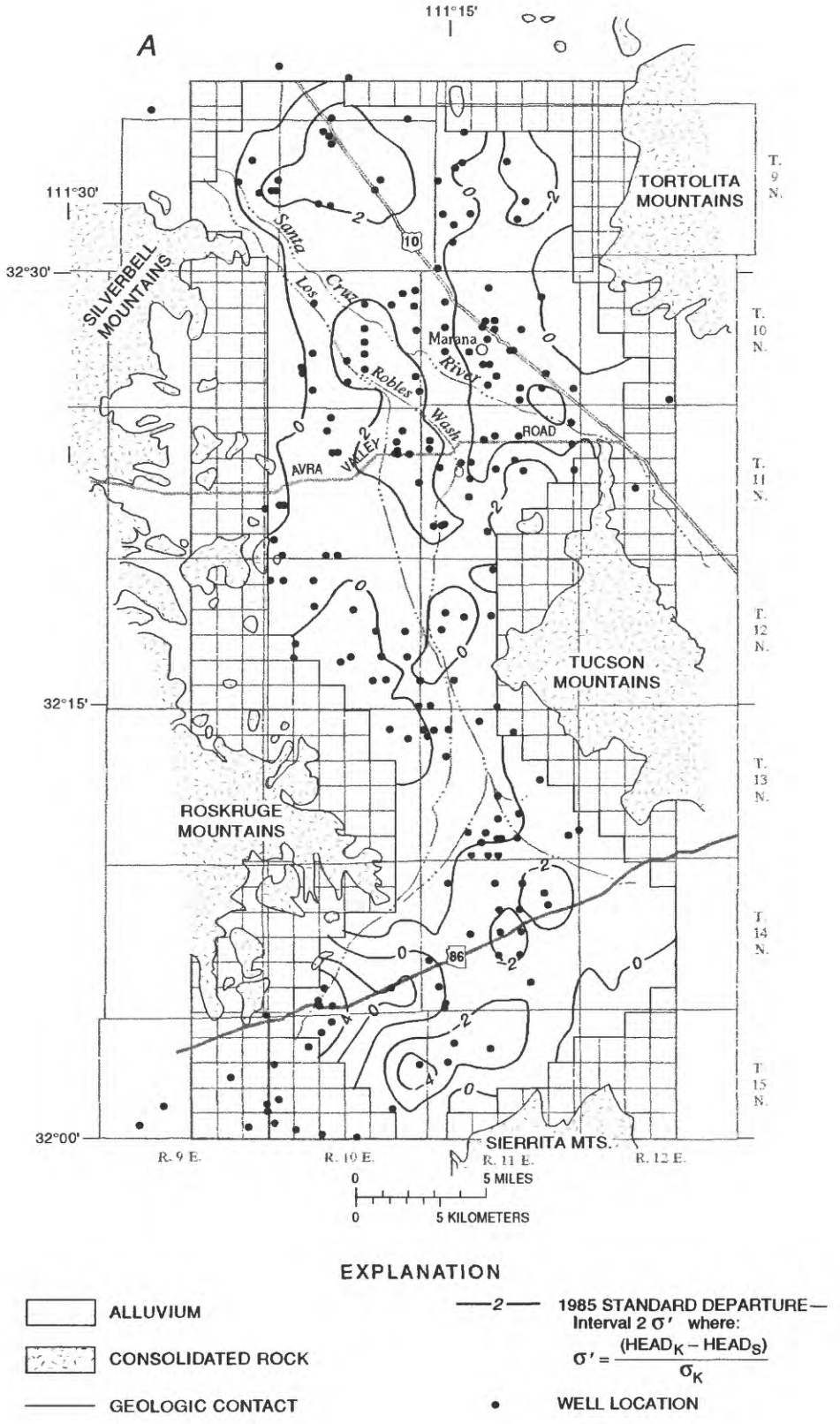

Figure 24*A*. Standardized transient-state calibration errors. *A*, Calibrated model.

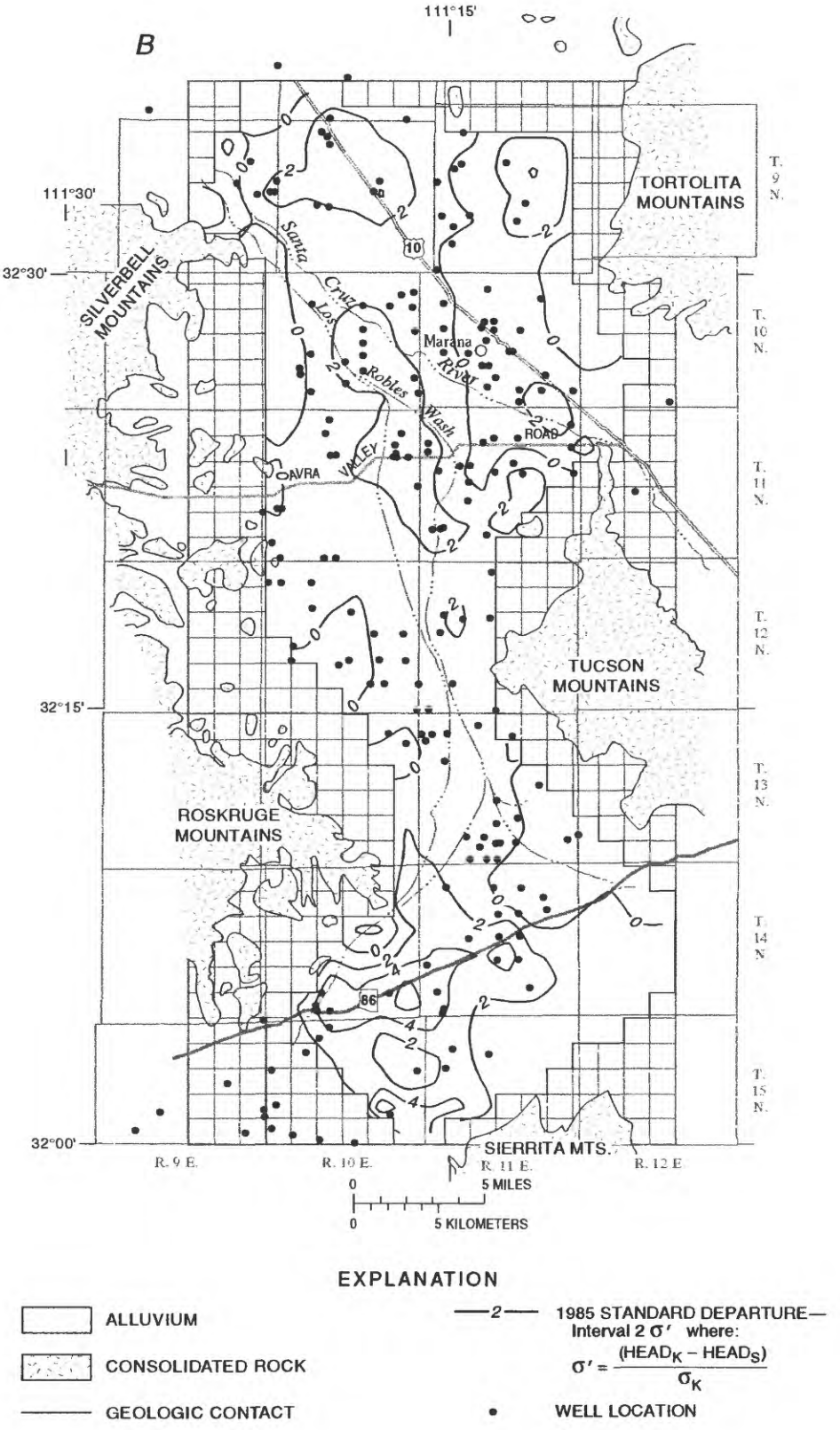

Figure 24*B*. Standardized transient-state calibration errors. *B*, Alternate-boundary conditions.

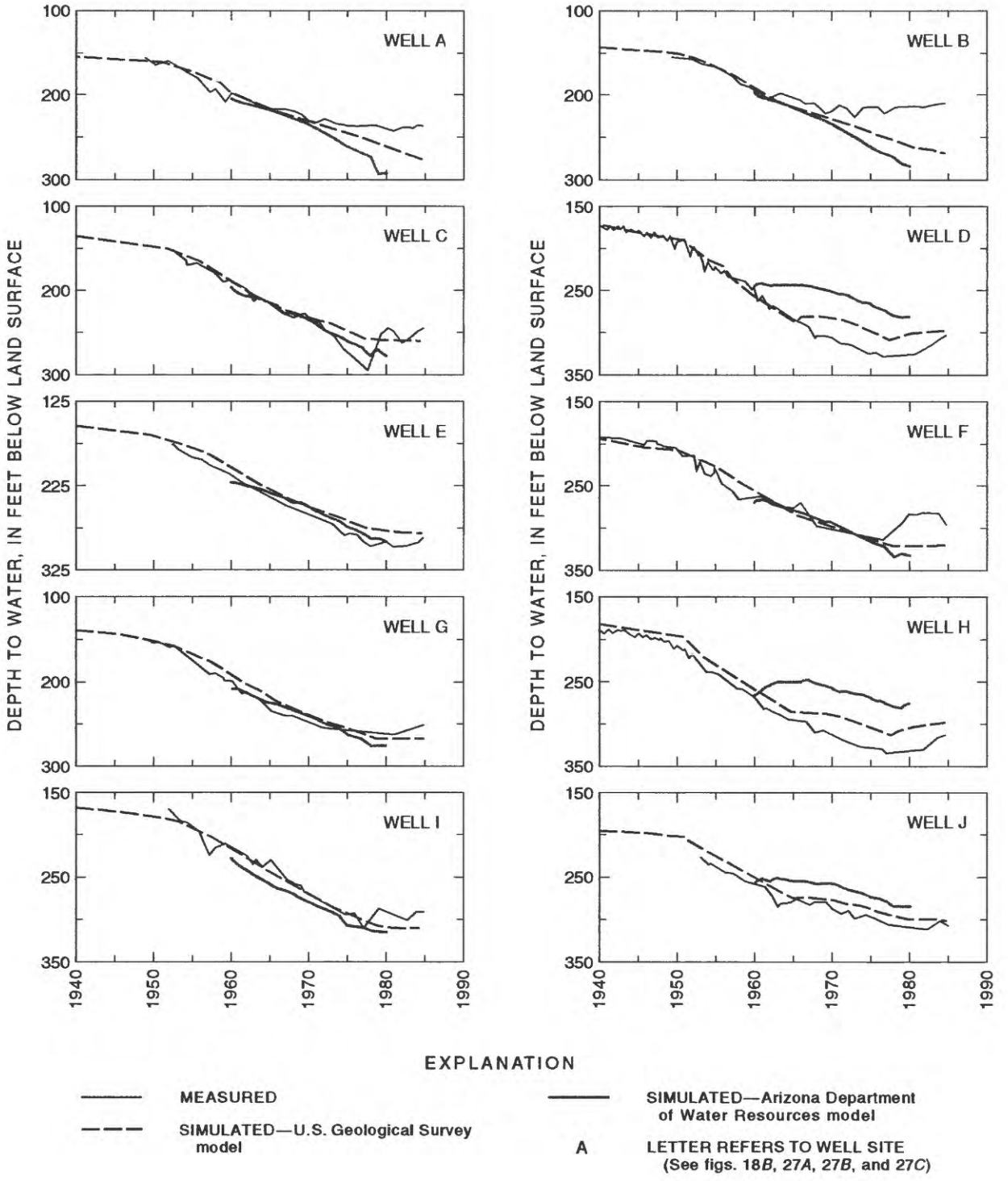

Figure 25. Measured and simulated depths to water in selected wells in Avra Valley, 1940–85.

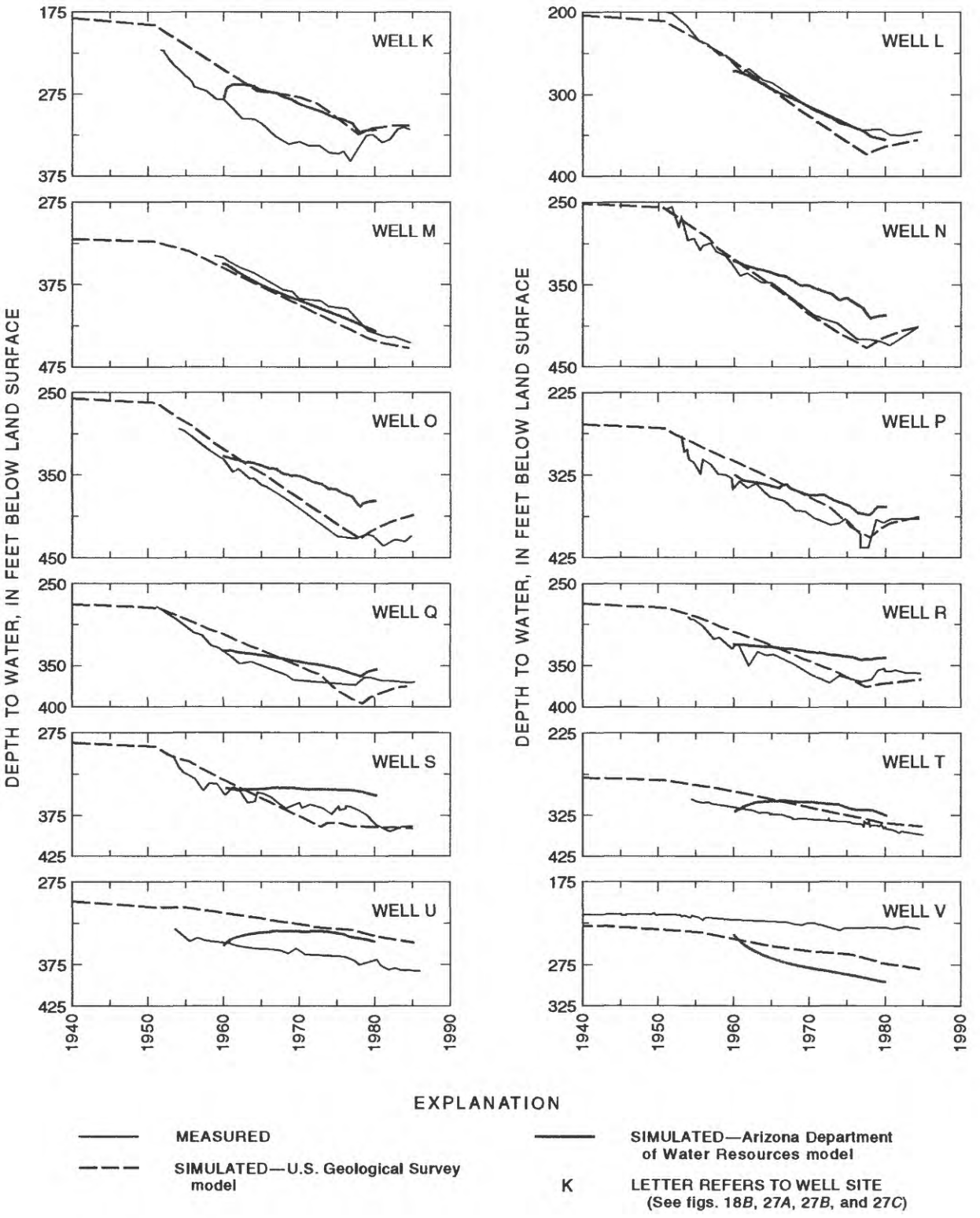

Figure 25. Continued.

water-level decline in the one-layer model. The difference between simulated hydrographs is because of a combination of differences in pumpage, recharge, and hydraulic diffusivity.

A comparison of the total net withdrawal between the two models indicates some differences in net withdrawal represented as pumpage minus recharge (fig. 26). This difference largely reflects the additional recharge used in the ADWR model. Thus, the spatial differences shown in hydrographs from the northern and southern parts of the valley are a combination of spatial differences in changes in storage and net withdrawals. Differences in specific yield between models indicate a smaller specific yield in the northern part of the basin and a larger specific yield in the southern part of the valley near the AV well field (fig. 27*A*) for the one-layer model compared to the upper layer of the two-layer model. A net change in storage because of differences in hydraulic diffusivity and net withdrawals indicate a similar pattern of smaller changes in storage in the northern part of the valley along the Santa Cruz River and along the flanks of the Roskruge Mountains and larger changes in storage in the southern part of the valley (fig. 27*B*) for the one-layer model. These model-parameter differences resulted in local differences in change of storage of as much as 4,000 acre-ft/mi^2 for the period 1960–79. The water-level difference between the two simulations indicates differences from larger values of more than 40 ft along parts of the Santa Cruz River and from the flanks of the Roskruge Mountains to the AV well field (fig. 27*C*). Differences from smaller values are greater than 40 ft along the Tortolita Mountains, Brawley Wash, Picacho Peak, and the Sierrita Mountains (fig. 27*C*).

The differences in hydraulic properties used (fig. 18*B* and 27*A*) along with the hydrographs (fig. 25) collectively indicate that the one-layer model used smaller values of specific yield and transmissivity along the Santa Cruz River and used larger values of specific yield and transmissivity south of the basin constriction, which includes the AV well field compared to the two-layer model. In contrast, hydrographs of simulated water-level declines match the measured declines for both models (fig. 25, wells E, G, I, M, and L) in the north-central parts of the basin where there is little difference in transmissivity, specific yield, and net change in storage. Differences in hydraulic properties and differences in recharge estimates,

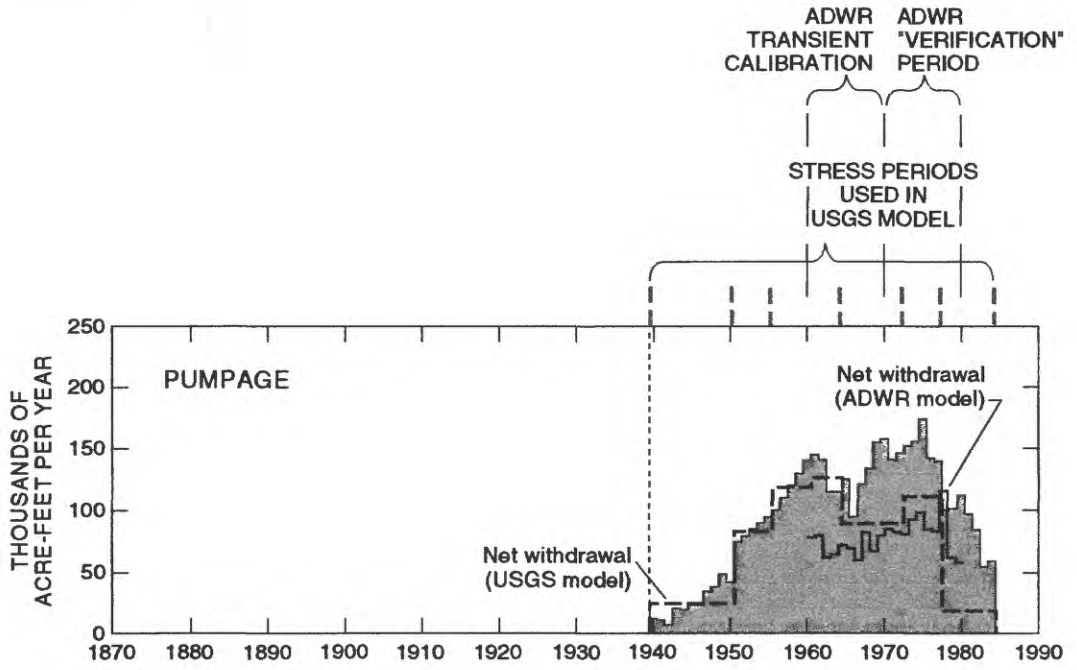

Figure 26. Annual estimated total pumpage and simulated net withdrawal, by simulation interval, Avra Valley, 1940–85.

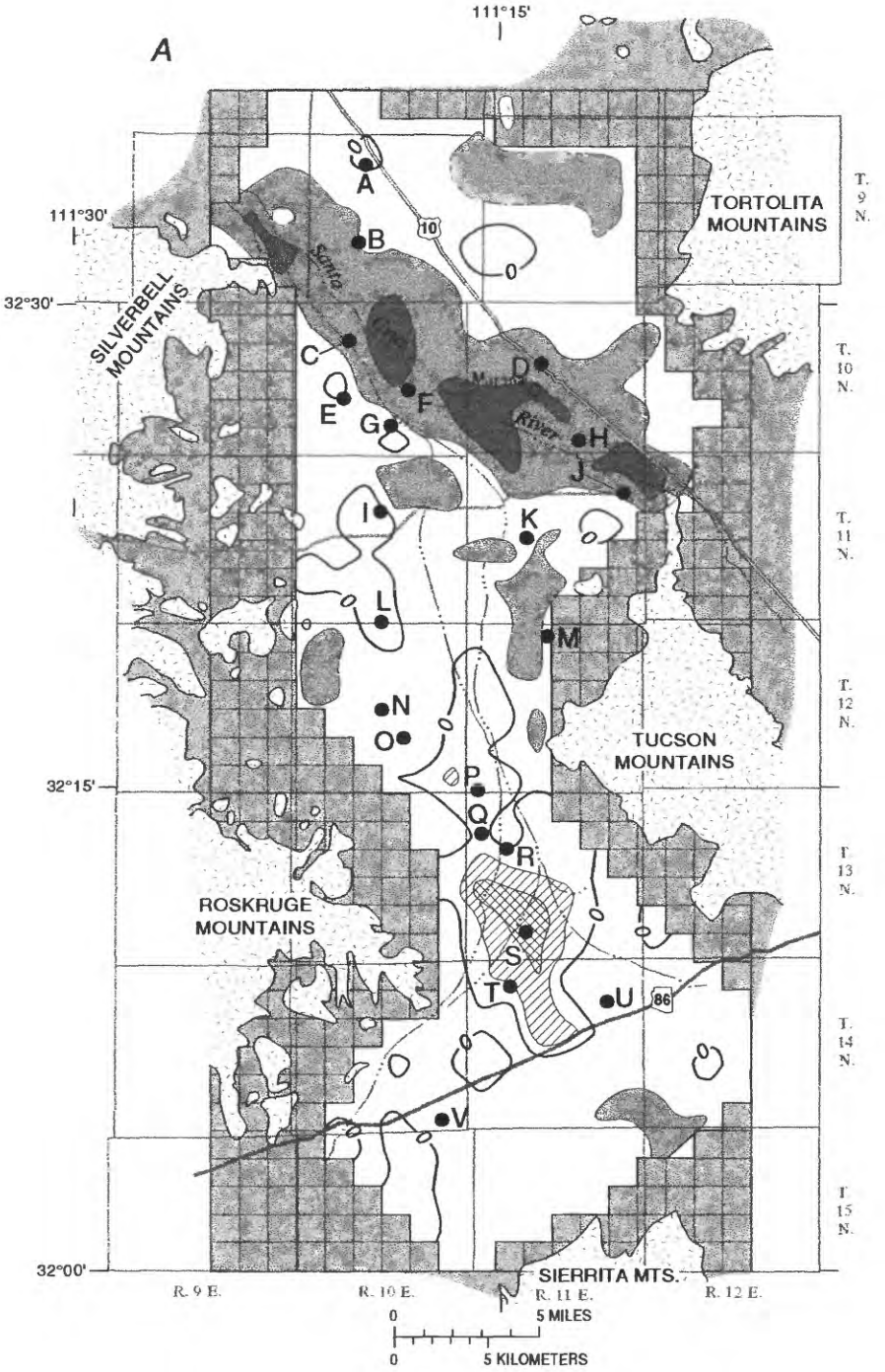

Figure 27*A*. Differences between trial-and-error model estimates of specific yield, 1960–79.

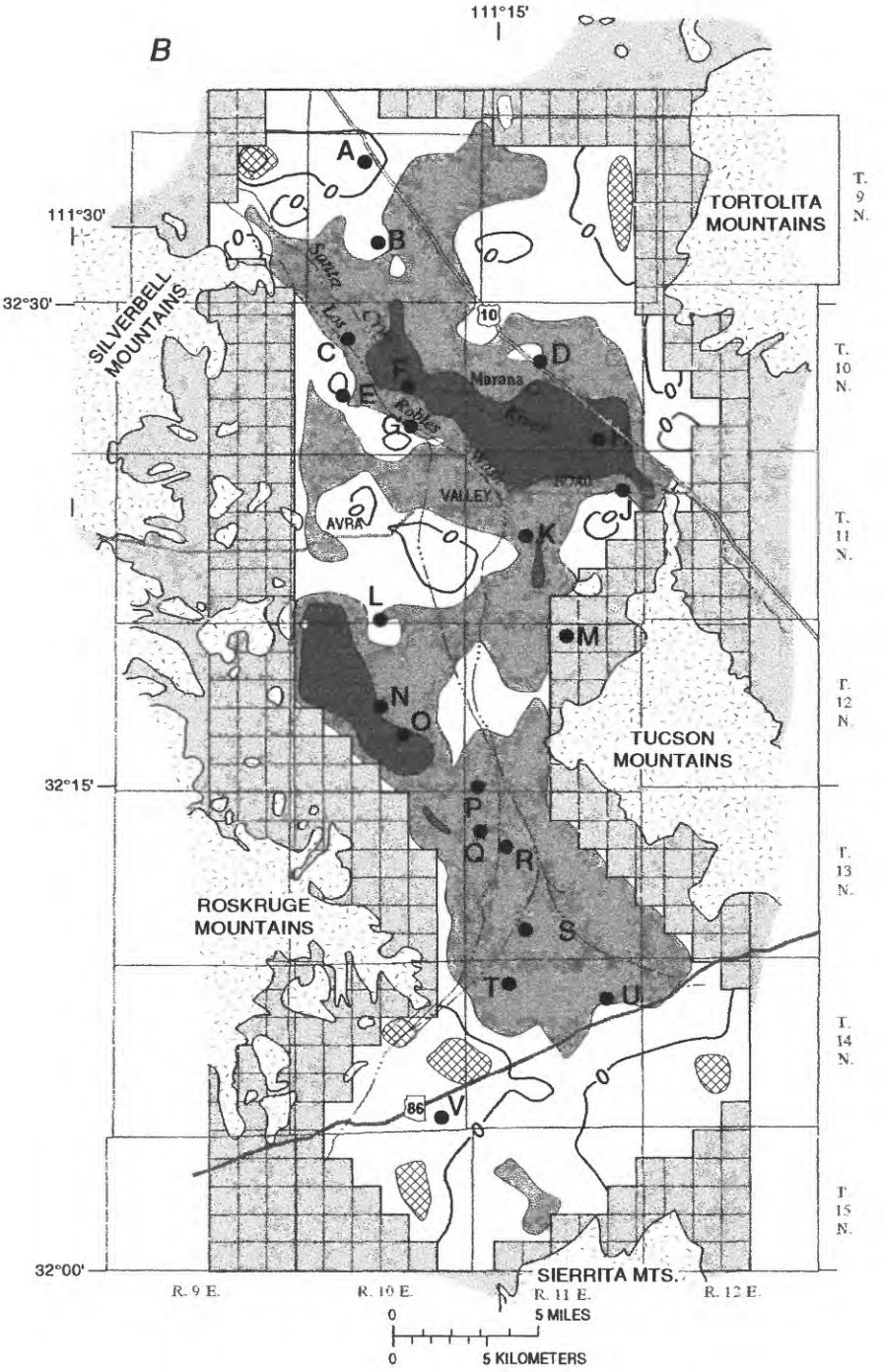

EXPLANATION

ALLUVIUM

CONSOLIDATED ROCK

GEOLOGIC CONTACT

— 0 — BOUNDARY BETWEEN POSITIVE AND NEGATIVE DIFFERENCE

DIFFERENCE IN WATER FROM STORAGE, IN ACRE-FEET PER MODEL CELL
[USGS minus ADWR model values]

Greater than 4,000

2,000 to 4,000

2,000 to −2,000

Greater than −2,000

● S WELL LOCATION—Letter indicates corresponding hydrograph. (See fig. 25)

Figure 27*B*. Differences between trial-and-error model estimates of water from storage, 1960–79.

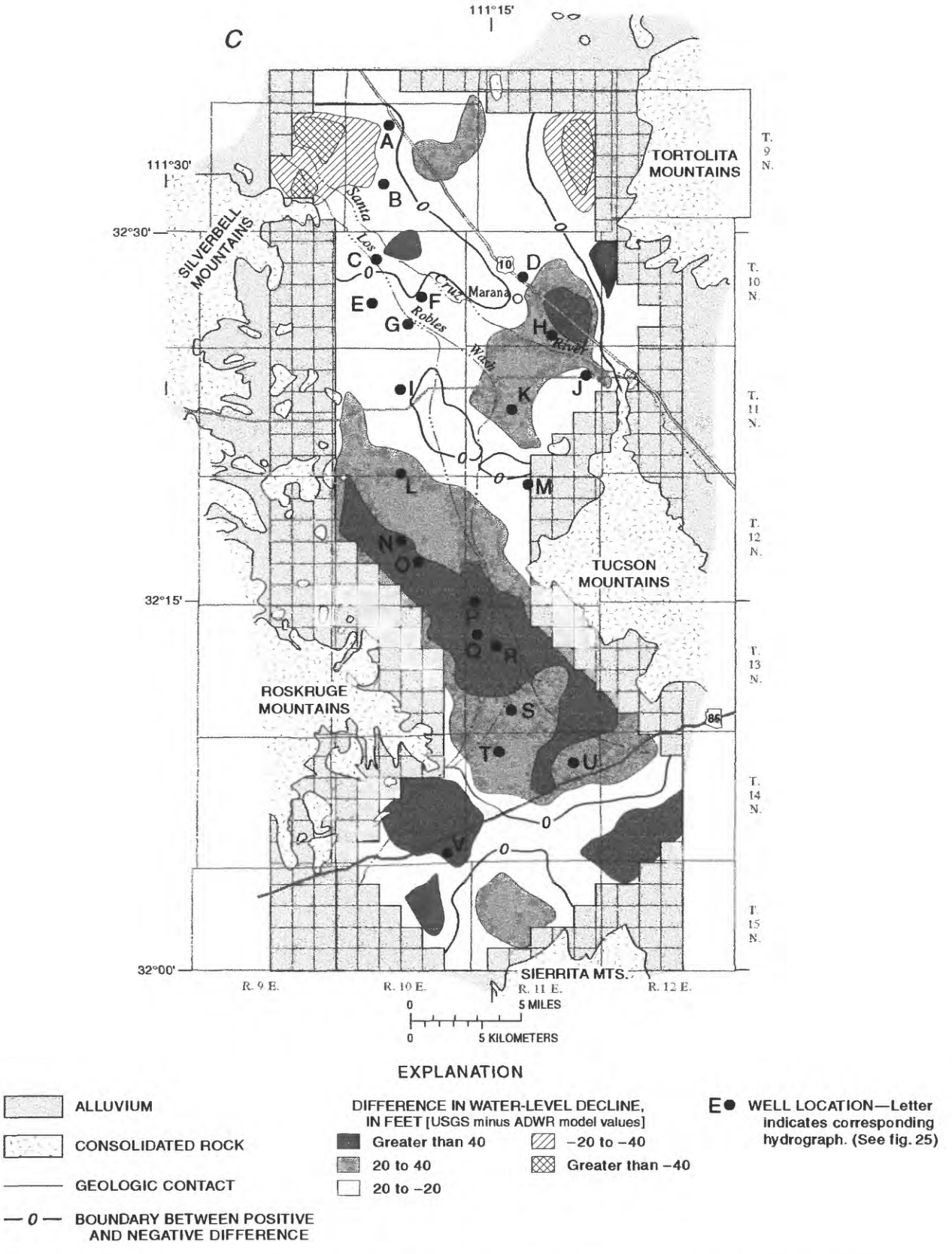

Figure 27C. Differences between trial-and-error model estimates of water-level decline, 1960–79.

therefore, appear to be the major sources of the historical predictive errors between these two models.

As a final comparison, the alternate conceptual model from the predevelopment comparison was used to simulate historical conditions to evaluate the persistence of predictive errors through time. The two-layer model had a mean error of 4.8 ft at the end of the historical transient simulation on the basis of 190 comparison points. The alternate conceptual model resulted in an increase of mean error to 9.4 ft and about the same variance on the basis of the 190 comparisons made for the developed heads for 1985. The comparison between standardized calibration-error maps for the original and alternate models indicate improvement near the AV well field in south-central Avra Valley and a pronounced underestimation of heads in southwestern Avra Valley (fig. 24). The southwestern region remains the largest area of comparison error and could potentially require additional simulated recharge through seasonal streamflow infiltration and ground-water inflow and a smaller increase in transmissivity for the south-central part of the valley. The remainder of the areas show slight improvement but are not discernable in the error maps at the contour interval shown. Returning the ground-water inflow from Altar Valley back to the original rate or treating the ground-water inflow boundary as a constant-head boundary did not improve the fit in the southwestern part of Avra Valley. The alternate conceptual model, therefore, improved the historical predictive errors in selected subregions, had little effect on other subregions, and degraded the fit in the southwestern part of the valley. Although the mean error is about twice the error of the calibrated model, the largest component of this error occurs in the southwestern part of the valley.

As of 1994, the aquifer system in Avra Valley has areas of perched ground water and areas of nonuniform vertical-head distribution, and is affected by variable recharge, pumpage, and land subsidence. These complexities may be unforeseen or overlooked during model conceptualization and calibration thereby increasing the chances for inadequate predictive simulations of future conditions. The scope of this study precludes a complete analysis of alternate conceptual models that could test the effects of varying these attributes of the developed aquifer system. Future studies could employ parameter-estimation techniques for a more complete, systematic, and quantitative analysis of alternate conceptual models for steady-state and transient-state conditions.

The potential effect on water-level declines and predictive errors from historical and future land subsidence was one alternate component of the conceptual model that was assessed from previous model simulations (Hanson and others, 1990). Water-level declines from 1940 to 1986 could be overestimated on the order of 7 ft (fig. 28*A*); whereas, the predicted water-level declines from 1985 to 2025 may be overestimated by as much as 40 ft if aquifer-system compaction is excluded from the conceptual model. Simulation of these projected declines indicated that as much as 10 percent of the simulated ground-water withdrawals may come from nonrecoverable storage, which indicates that aquifer-system compaction is a significant source of water and could potentially affect simulated water-level declines over parts of Avra Valley. This data would indicate that the potential for historical predictive errors was small and the potential for future predictive errors was large when subsidence is excluded from the simulation of ground-water flow in Avra Valley.

SUMMARY AND CONCLUSIONS

Ground water is the main source of water for irrigation, public supply, and industry in the Tucson basin and Avra Valley in southeastern Arizona. Since 1980, ADWR has been responsible for managing the ground-water resources within the active management areas of Arizona. Avra Valley is a 520-square-mile alluvial basin within the Tucson Active Management Area in southern Arizona. This report presents a postaudit of regional estimates of head and transmissivity and a postaudit of the ground-water flow models developed for Avra Valley.

The use of measured heads in model comparisons is becoming a common practice for evaluating and calibrating regional ground-water flow models. Direct comparison with point values of head and comparison with regional-geostatistical estimates of head can be used for

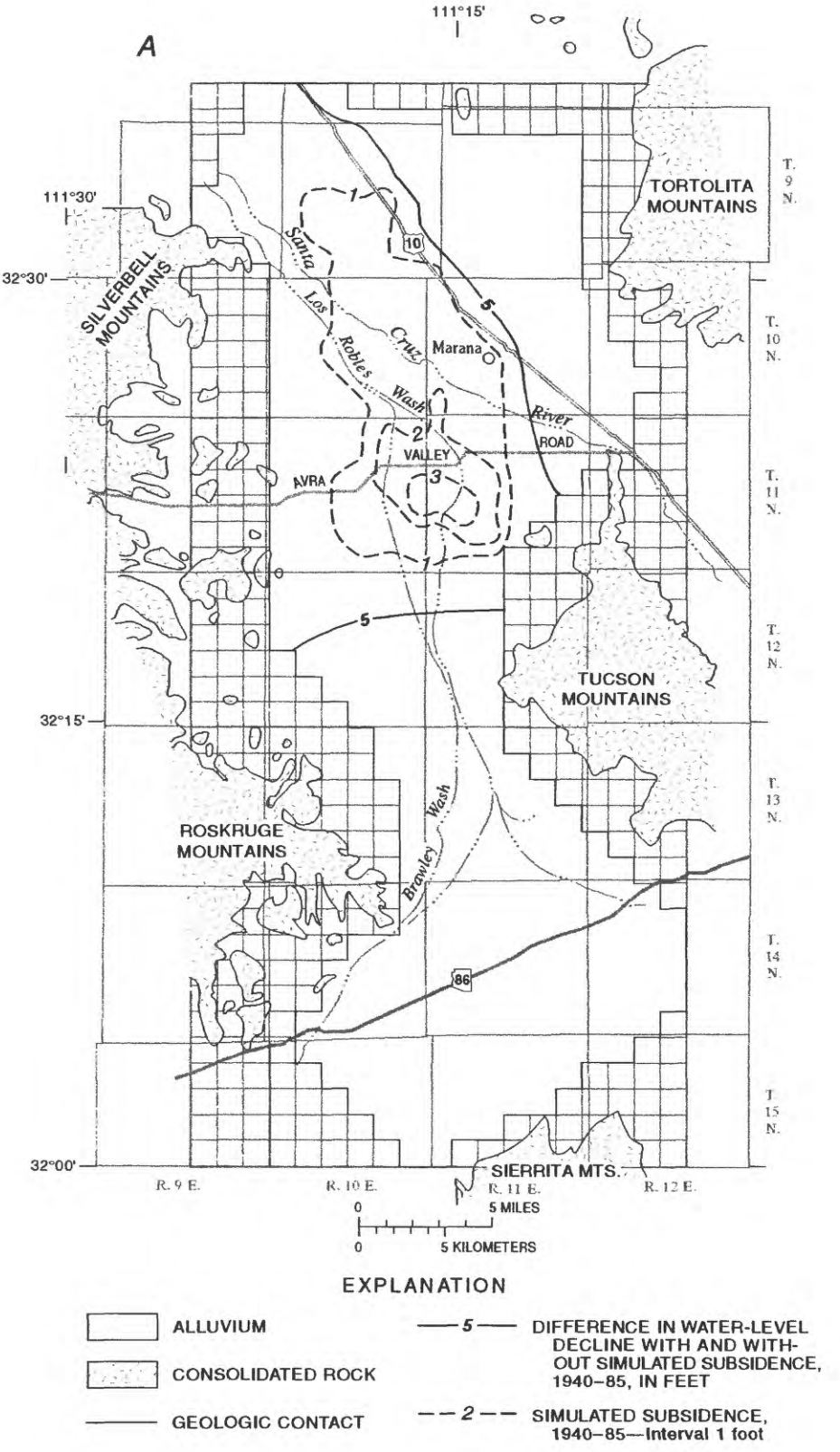

Figure 28*A*. Estimated subsidence and related water-level decline with and without simulated subsidence during historical simulation period, 1940–85.

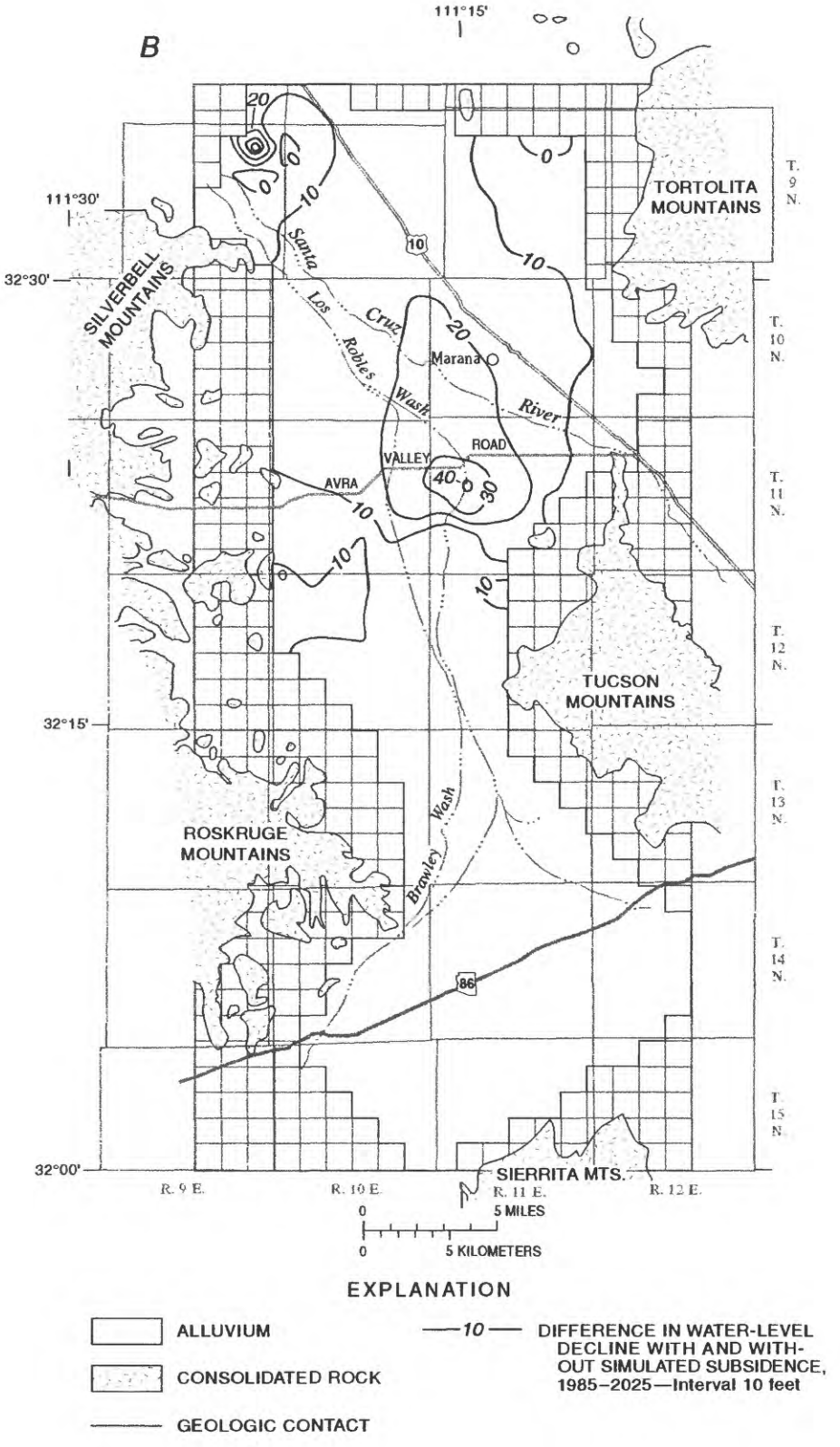

Figure 28*B*. Estimated difference in water-level decline with and without simulated subsidence as the difference between two trial-and-error estimates of predicted subsidence and related water-level decline, 1985–2025.

model calibration. Spatial comparisons provide additional information over nonspatial statistics for assessing the potentially localized effects from errors in model parameters. These comparisons, however, are only as good as the distribution and amount of measured data. Generally, head data become more variable and more plentiful as the aquifer system is developed. Regional estimates of head are affected mostly by measurement errors and to some lesser extent by interpretation errors. The significance of these errors is problem dependent and could become more significant during development when water use changes, vertical gradients develop, perched water increases in large areas, and land subsidence begins to occur.

Kriging of predevelopment heads for Avra Valley provided estimates comparable to previous estimates that had a kriging error that generally ranged from 4 to 10 ft. Kriging of developed heads also was comparable to previous estimates of regional heads in 1985 that had a kriging error that generally ranged from 10 to 14 ft. The developed head surface, therefore, is estimated with about 50 percent more uncertainty, half the measurement error, and about twice as many data points as were used to estimate the predevelopment heads. The greater uncertainty with less measurement error and more data reflects the greater local variability in heads that is typical of developed aquifer systems. Measurement errors did not substantially affect the distribution of uncertainty for either head estimate because most wellhead altitudes were surveyed accurately. The incorporation of heads from adjacent basins at the ground-water inflow and outflow boundaries reduced uncertainty locally for these boundary areas in the kriging of developed heads. Universal cokriging of heads with the strongly correlated land-surface altitudes may improve head estimates and model comparisons where head data are sparse.

Local and regional estimates of transmissivity were an integral part of previous models of Avra Valley. Local estimates of transmissivity can be subdivided into northern and south-central regions that are distributed along the valley axis and the Santa Cruz River. Regional estimates used for calibration of flow models are derived from local aquifer-test estimates. In turn, these initial estimates are susceptible largely to errors related to aquifer-test conditions, and to some extent, on related geologic data used to aid in well construction and test interpretation. Interpretation errors from violation of aquifer-test model assumptions may be more significant than measurement errors for transmissivity estimates. Transmissivity estimates may change systematically throughout the aquifer system and may not be comparable to estimates from previous decades as wells become older and less efficient and as the regional system is dewatered during development. Estimates of local aquifer-test uncertainty can be made through local weighted geometric means or through nonlinear regression of single or multiple tests.

Comparison of kriged transmissivities with trial-and-error model-derived transmissivities indicate a common pattern of smaller values along the Santa Cruz River and southeast of the Silverbell Mountains in the northern part of the valley and larger values in the northeastern part of the valley and in the AV well field with respect to the trial-and-error model-derived values. Cokriging transmissivities with specific capacities and average silt-and-clay content substantially reduced the difference in the northeastern part of the valley where only silt-and-clay data were available. Uncertainty in kriged estimates was substantially reduced by the incorporation of covarying properties through cokriging or ordinary kriging supplemented with linear regression. Cokriging provided the least uncertainty of all kriged estimates.

Predictive errors for the Avra Valley model were a different combination of factors that become significant in the simulation of ground-water flow for the periods representing predevelopment, historical development, and future development conditions. Predictive errors for simulation of predevelopment conditions are caused by potential systematic errors in local transmissivity estimates, uncertainty in long-term mountain-front recharge, and uncertainty in predevelopment heads along the margins of the basin where recharge and transmissivity estimates are constrained by heads during model calibration.

Comparison of other model-derived transmissivities with trial-and-error model transmissivities indicate a similar pattern as the kriged estimates. The previous inverse models contain the same pattern of smaller and larger values compared to

initial kriged estimates. The regional ADWR model that was based initially on drillers' log estimates also shows these same differences compared to the head-conditioned transmissivities of the trial-and-error model. These differences may be related to a systematic bias in aquifer-test conditions and an underestimation of specific capacity and transmissivity in the northern and central parts of the valley and with overestimation in the southern part of the valley. In turn, this bias may be related to more layering of alluvial units and well inefficiency in the northern and central parts of the valley and may be related to less layering, more variable well construction, and more pronounced delayed yield in the southern part of the valley.

Early predictive simulations of regional-aquifer systems commonly overestimate projected ground-water declines. These differences commonly are related to uncertainties in pumpage, two-dimensional representation of a three-dimensional system, and lack of consideration of land subsidence. The largest source of predictive errors is the assumed amount and distribution of future pumpage and recharge. In Avra Valley, historically predicted changes to 1985 were as much as 50 to 100 ft different than actual declines. The predictive errors from the analog model of Avra Valley were caused by the errors in the spatial distribution and not in the total amount of future pumpage. The two-dimensional simulation produced a small increase in predictive errors on the basis of digital-model comparisons. Omission of subsidence in simulations of historical ground-water flow were estimated to be small predictive errors (<7 ft) for 1940–85.

Predictive errors for simulation of historical development (1960–79) appear to be caused to a greater extent by combined errors in estimates of transmissivity and storage properties and to a lesser extent by the effects of recharge estimates on the estimates of net withdrawal and estimates of land subsidence. Predictive errors for simulation of future development were caused by misestimation of the spatial distribution and not by the total quantity of future pumpage for the analog model. Analog-model predictions of future development indicate that changes to 1985 were as much as 50 to 100 ft different from actual declines that were caused by errors in the distribution and not the total amount of future pumpage. Comparison of two digital models resulted in spatially variable differences in transmissivity of as much as 30,000 ft^2/d and differences in specific yield of as much as 0.1. These model-parameter differences resulted in local differences in change of storage of as much as 4,000 acre-ft/mi^2 for 1960–79, which is equivalent to historical predictive errors in water levels of as much as 40 ft. Areas that show no difference in these model parameters yield comparable simulated water-level declines that are similar to measured declines. The pattern of differences in aquifer parameters is similar to the pattern of differences from local and geostatistical-transmissivity estimates.

A postaudit of alternate conceptual models was explored on the basis of a well-by-well comparison of reduction in mean error and variance and standardized calibration-error maps for predevelopment heads (1940) and developed heads (1985). Calibration-error maps that compare simulated and kriged heads to the kriging uncertainty provide a useful tool for exploring potential errors in model structure. The spatial structure of model errors and the adequacy of model fit that are available in this method are not available from traditional methods of model comparison such as well-by-well, cell-by-cell, and single-value nonparametric-statistical measures. Calibration-error maps indicate higher heads in the southern part of Avra Valley and lower heads in the northern part. Increased transmissivity in the southern part of the lower layer of the model; decreased hydraulic conductivity in the southwestern part of the upper layer; reduced ground-water inflow from Altar Valley; and increased recharge along the Tortolita Mountains, Tucson Mountains, and Brawley Wash yielded a statistically better model for predevelopment but not for developed conditions (1940–85). Large changes in water use and climatic cycles, therefore, can be major contributing factors in the uncertainty of future stresses on the aquifer system. In addition, predictive errors for future simulations (1986–2025) also could potentially include errors of more than 40 ft from the omission of subsidence from the simulation of regional ground-water flow in Avra Valley. Refinement of the changing conceptual model of an aquifer system under development will require a variety of additional

field data. First and foremost would be the installation of piezometer nests for better vertical segregation of water-level and water-chemistry data. Long-term aquifer tests and better spatial and vertical distribution of water-level data in combination with extensometer, flowmeter, and isotope data would refine the effects of pumping on vertical flow, leakage, and subsidence. Additional data, such as isotope analysis and age-dating of ground waters and surface waters, wellbore-flowmeter logs and related depth-dependent water-chemistry samples, and areal microgravity and Global Positioning System measurements, will be needed to better assess the effects and extent of climatically variable recharge, three-dimensional distributions of pumpage and recharge, and the spatial distribution and magnitude of subsidence.

REFERENCES CITED

Aboufirassi, M., and Marino, M.A., 1984, Cokriging of aquifer transmissivities from field measurements of transmissivity and specific capacity: Journal of the International Association of Mathematical Geology, v. 16, no. 1, p. 19–35.

Ahmed, Shakeel, and De Marsily, Ghislain, 1987, Comparison of geostatistical methods for estimating transmissivity using data on transmissivity and specific capacity: American Geophysical Union, Water Resources Research, v. 23, no. 9, p. 1717–1737.

Ahmed, Shakeel, De Marsily, G., and Talbot, A., 1987, Combined use of hydraulic and electrical properties of an aquifer in a geostatistical estimation of transmissivity: Groundwater, v. 26, no. 1, p. 78–86.

Allen, T.J., 1981, The subsurface stratigraphy of Avra Valley, Pima County, Arizona: Kent, Ohio, Kent State University, unpublished master's thesis, 71 p.

Anderson, S.R., 1987, Cenozoic stratigraphy and geologic history of the Tucson basin, Pima County, Arizona: U.S. Geological Survey Water-Resources Investigations Report 87–4190, 20 p.

_____1988, Potential for aquifer compaction, land subsidence, and earth fissures in the Tucson basin, Pima County, Arizona: U.S. Geological Survey Hydrologic Investigations Atlas HA–713, 3 sheets.

_____1989, Potential for aquifer compaction, land subsidence, and earth fissures in Avra Valley, Pima and Pinal Counties, Arizona: U.S. Geological Survey Hydrologic Investigations Atlas HA–718, 3 sheets.

Anderson, S.R., and Hanson, R.T., 1987, Relation of aquifer compaction to Cenozoic depositional environments in the Tucson basin, Arizona [abs.], *in* Abstracts with Programs: Phoenix, Arizona, Geological Society of America Annual Meeting and Exposition, October 26–29, 1987, p. 573.

Anderson, T.W., 1972, Electrical-analog analysis of the hydrologic system, Tucson basin, southeastern Arizona: U.S. Geological Survey Water-Supply Paper 1939–C, 34 p.

_____1983, Implications of deep percolation to ground-water systems in south-central Arizona based on numerical-model studies, *in* Proceedings of the 1982 Deep Percolation Symposium, October 26, 1982: Arizona Department of Water Resources Report 4, p. 30–40.

_____1986, Geohydrology of the southwest alluvial basins, Arizona, *in* Anderson, T.W., and Johnson, I.A., eds., Regional Aquifer Systems of the United States, Southwest Alluvial Basins of Arizona: American Water Resources Association Monograph Series 7, p. 99–111.

Anderson, T.W., Freethey, G.W., and Tucci, Patrick, 1992, Geohydrology and water resources of alluvial basins in south-central Arizona and parts of adjacent States: U.S. Geological Survey Professional Paper 1406–B, 67 p.

Arizona Department of Water Resources, 1984, Proposed management plan—First management period 1980–1990: Tucson, Arizona Department of Water Resources, Tucson Active Management Area report, v.p.

_____1988, Draft management plan—Second management period, 1990–2000: Tucson, Arizona Department of Water Resources, Tucson Active Management Area report, 377 p.

Babcock, J.A., and Hix, G.L., 1982, Annual static water level basic data report, Tucson basin and Avra Valley, Pima County, Arizona, 1981: City of Tucson, Tucson Water Planning Division report, 21 p.

Babcock, J.A., Cameron, J.A., and Andrews, John, 1984, Annual static water level basic data report, Tucson basin and Avra Valley, Pima County, Arizona, 1983: City of Tucson, Tucson Water Planning Division report, 45 p.

Babcock, J.A., Cameron, J.A., and Brumbaugh, Lynn, 1985, Annual static water level basic data report, Tucson basin and Avra Valley, Pima County, Arizona, 1984: City of Tucson, Tucson Water Planning Division report, 47 p.

Babcock, J.A., Cameron, J.A., and Heidenreich, L.K., 1986, Annual static water level basic data report, Tucson basin and Avra Valley, Pima County,

Arizona, 1985: City of Tucson, Tucson Water Planning Division report, 57 p.

Babcock, J.A., Heidenreich, L.K., and Bergstrom, Jim, 1987, 1986 static water level basic data report, Tucson basin and Avra Valley, Pima County, Arizona: City of Tucson, Tucson Water Planning Division report, 223 p.

Babcock, J.A., Heidenreich, L.K., and Katz, L.K., 1988, Annual static water level basic data report Tucson basin and Avra Valley, Pima County, Arizona, 1987: City of Tucson, Tucson Water Planning Division report, 137 p.

Babcock, J.A., Miley, Terry, and Stevens, C.R., 1989, Annual static water level basic data report, Tucson basin and Avra Valley, Pima County, Arizona, 1988: City of Tucson, Tucson Water Planning and Technical Services Division report, 136 p.

Benjamin, J.R., and Cornell, C.A., 1970, Probability, statistics, and decision for civil engineers: New York, McGraw-Hill Book Company, Inc., 684 p.

Clifton, P.M., 1981, Statistical inverse modeling and geostatistical analysis of the Avra Valley aquifer: Tucson, Arizona, University of Arizona, unpublished master's thesis, 190 p.

Clifton, P.M., and Neuman, S.P., 1982, Effects of kriging and inverse modeling on conditional simulation of the Avra Valley aquifer in southern Arizona: American Geophysical Union, Water Resources Research, v. 18, no. 4, p. 1215–1234.

Conner, L.L., 1986, Geochemistry of groundwater in Avra Valley, Pima County, Arizona: Tucson, Arizona, University of Arizona, unpublished master's thesis, 72 p.

Cooley, R.L., and Naff, R.L., 1989, Regression modeling of ground-water flow: U.S. Geological Survey Techniques of Water-Resources Investigations, book 3, chap. B–4, 232 p.

Cooley, R.L., Konikow, L.F., and Naff, R.L., 1986, Nonlinear-regression groundwater flow modeling of a deep regional aquifer system: American Geophysical Union, Water Resources Research, v. 22, no. 13, p. 1759–1778.

Cuff, M.K., and Anderson, S.R., 1987, Ground-water conditions in Avra Valley, Pima and Pinal Counties, Arizona—1985: U.S. Geological Survey Water-Resources Investigations Report 87–4192, 3 sheets.

Davidson, E.S., 1973, Geohydrology and water resources of the Tucson basin, Arizona: U.S. Geological Survey Water-Supply Paper 1939–E, 81 p.

Davis, G.E., and Stafford, J.F., 1966, First annual report, June 1965–June 1966, Tucson Wastewater Reclamation Project: City of Tucson, Water and Sewers Department duplicated report, 70 p.

Delhomme, J.P., 1976, Application of the theory of regionalized variables from hydrology: Paris, France, School of Mines of Paris, doctoral dissertation, 94 p.

Dunlap, L.E., and Spinazola, J.M., 1981, Interpolating water-table altitudes in west-central Kansas using kriging techniques: U.S. Geological Survey Open-File Report 81–1062, 68 p.

Eberly, L.D., and Stanley, T.B., Jr., 1978, Cenozoic stratigraphy and geologic history of southwestern Arizona: Geological Society of America Bulletin, v. 89, no. 6, p. 921–940.

Freethey, G.W., Pool, D.R., Anderson, T.W., and Tucci, Patrick, 1986, Description and generalized distribution of aquifer materials in the alluvial basins of Arizona and adjacent parts of California and New Mexico: U.S. Geological Survey Hydrologic Investigations Atlas HA–663, 4 sheets.

Freethey, G.W., and Anderson, T.W., 1986, Predevelopment hydrologic conditions in the alluvial basins of Arizona and adjacent parts of California and New Mexico: U.S. Geological Survey Hydrologic Investigations Atlas HA–664, 3 sheets.

Goode, D.J., and Appel, C.A., 1992, Finite-difference interblock transmissivity for unconfined aquifers and for aquifers having smoothly varying transmissivity: U.S. Geological Survey Water-Resources Investigations Report 92–4124, 79 p.

Grundy, W.D., and Miesch, A.T., 1987, Brief discussion of STATPAC and related statistical programs for the IBM personal computer: U.S. Geological Survey Open-File Report 87–411A–C, v.p.

Hanson, R.T., 1987, One-dimensional modeling of aquifer-system compaction in south-central Arizona [abs.]: American Geophysical Union, EOS Transactions, v. 68, no. 44, p. 1300–1301.

_____1989a, Aquifer-system compaction, Tucson basin and Avra Valley, Arizona: U.S. Geological Survey Water-Resources Investigations Report 88–4172, 69 p.

_____1989b, Postaudit analyses of ground-water models of an alluvial aquifer system, Avra Valley, Arizona: Proceedings of the 28th International Geological Congress, July 9–19, 1989, v. 2, p. 26–27.

Hanson, R.T., Anderson, S.R., and Pool, D.R., 1990, Simulation of ground-water flow and potential land subsidence, Avra Valley, Arizona: U.S. Geological Survey Water-Resources Investigations Report 90–4178, 41 p.

Hill, M.C., 1992, A computer program (MODFLOWP) for estimating parameters of a transient, three-dimensional, ground-water flow model using

nonlinear regression: U.S. Geological Survey Open-File Report 91–484, 358 p.

Jacobson, E.M., 1985, A statistical parameter estimation method using singular value decomposition with application to Avra Valley aquifer in southern Arizona: Tucson, Arizona, University of Arizona, doctoral dissertation, 315 p.

Johnson, R.B., 1980, Proposed water supply augmentation for Tucson, Arizona: Tucson, Arizona, University of Arizona, unpublished master's thesis, 79 p.

Konikow, L.F., 1986, Predictive accuracy of a ground-water model—Lessons from a postaudit: Groundwater, v. 24, no. 2, p. 173–184.

Lohman, S.W., 1972, Ground-water hydraulics: U.S. Geological Survey Professional Paper 708, 70 p.

Matheron, G., 1975, The intrinsic random functions and their applications: Advanced Applications to Probability, v. 5, p. 439–468.

Matlock, W.G., and Morin, G.A.C., 1976, Groundwater in the Avra and Altar Valleys, Arizona: Tucson, University of Arizona Agricultural Experiment Station Technical Bulletin 232, 59 p.

McDonald, M.G., and Harbaugh, A.W., 1988, A modular three-dimensional finite-difference ground-water flow model: U.S. Geological Survey Techniques of Water-Resources Investigations, book 6, chap. A1, 586 p.

Moosburner, Otto, 1972, Analysis of the ground-water system by electrical-analog model, Avra Valley, Pima and Pinal Counties, Arizona: U.S. Geological Survey Hydrologic Investigations Atlas HA–215, 2 sheets.

Myers, D.E., 1982, Matrix formulation of cokriging: Journal of the International Association of Mathematical Geology, v. 14, no. 3, p. 249–257.

Neuman, S.P., and Jacobson, E.M., 1984, Analysis of nonintrinsic spatial variability by residual kriging with application to regional groundwater levels: Journal of the International Association of Mathematical Geology, v. 16, no. 5, p. 499–521.

Oppenheimer, J.M., and Sumner, J.S., 1981, Gravity modeling of the basins in the Basin and Range Province, Arizona: Arizona Geological Society Digest, v. 13, p. 111–115.

Osterkamp, W.R., 1973, Ground-water recharge in the Tucson area, Arizona: U.S. Geological Survey Miscellaneous Investigations Series Map I–844–E, 1 sheet.

Palumbo, M.R., and Khaleel, R., 1983, Kriged estimates of transmissivity in the Mesilla Bolson, New Mexico: Water Resources Bulletin, v. 19, no. 6, p. 929–936.

Pool, D.R., 1986, Aquifer geology of alluvial basins of Arizona, *in* Anderson, T.W., and Johnson, I.A., eds., Regional Aquifer Systems of the United States, Southwest Alluvial Basins of Arizona: American Water Resources Association Monograph Series 7, p. 25–36.

Reeter, R.W., and Cady, C.V., 1982, Maps showing ground-water conditions in the Avra/Altar area, Pima and Pinal Counties, Arizona: Arizona Department of Water Resources Hydrologic Map Series Report 7, 2 sheets.

Sampson, R.J., 1988, Surface III User's Manual: Lawrence, Kansas, Kansas Geological Survey, Interactive Concepts Incorporated, 277 p.

State of Arizona, 1980, Arizona Groundwater Management Act of 1980: Phoenix, State of Arizona, Arizona Revised Statutes, section 45–401 through 45–636 (supplement 1981–82), v.p.

Travers, B.C., and Mock, P.A., 1984, Groundwater modeling study of the upper Santa Cruz basin and Avra Valley in Pima and Santa Cruz Counties, southeastern Arizona: Arizona Department of Water Resources unnumbered report, 2 volumes, v.p.

Tucci, Patrick, and Pool, D.R., 1986, Use of geophysics for geohydrologic studies in the alluvial basins of Arizona, *in* Anderson, T.W., and Johnson, I.A., eds., Regional Aquifer Systems of the United States, Southwest Alluvial Basins of Arizona: American Water Resources Association Monograph Series 7, p. 37–56.

U.S. Environmental Protection Agency, 1984, Final determination of ground water system of the Upper Santa Cruz basin and Avra-Altar basin of Pima, Pinal, and Santa Cruz Counties, Arizona—Aquifer determination: Federal Register, v. 49, no. 16, OW–FRL–2511–3, p. 2948–2950.

Waddell, R.K., 1982, Two-dimensional steady-state model of ground-water flow, Nevada test site and vicinity, Nevada-California: U.S. Geological Survey Water-Resources Investigations Report, 82–4085, 77 p.

Webb, R.H., and Betancourt, J.L., 1992, Climatic variability and flood frequency of the Santa Cruz River, Pima County, Arizona: U.S. Geological Survey Water-Supply Paper 2379, 40 p.

Weiss, E.J., 1991, Regional ground-water flow in upper and middle Paleozoic rocks in southeastern Utah and adjacent parts of Arizona, Colorado, and New Mexico: U.S. Geological Survey Water-Resources Investigations Report 90–4079, 57 p.

Whallon, A.J., 1983, A geohydrologic study of the regional ground-water system in Avra Valley, Pima and Pinal Counties, Arizona: Tucson, Arizona,

University of Arizona, unpublished master's thesis, 68 p.

White, N.D., Matlock, W.G., and Schwalen, H.C., 1966, An appraisal of the ground-water resources of Avra and Altar Valleys: Arizona State Land Department Water-Resources Report 25, 66 p.

Williams, D., 1987, Geostatistical analysis and inverse modeling of the upper Santa Cruz basin, Arizona: Tucson, Arizona, University of Arizona unpublished master's thesis, 149 p.

Wrege, B.M., Schumann, H.H., and Wallace, B.L., 1985, Geohydrologic data along the Tucson Aqueduct of the Central Arizona Project in Pinal and Pima Counties, Arizona: U.S. Geological Survey Open-File Report 85–565, 77 p.

Yates, S.R., and Warrick, A.W., 1987, Estimating soil water content using cokriging: Journal of the Soil Science Society of America, v. 51, p. 23–30.

Zimmerman, D.A., Hanson, R.T., and Davis, P.A., 1991, A comparison of parameter estimation and sensitivity analysis techniques and their impact on the uncertainty in ground water flow model predictions: U.S. Nuclear Regulatory Commission, NUREG/CR–5522 (SAND90–1028), v.p.

BASIC DATA

Table 5. Predevelopment heads for Avra Valley, Arizona

[-999, no information. Other negative numbers are negative coordinates with respect to the southwest corner of the model grid. All values are in feet]

Local well number	X location[1]	Y location[1]	Altitudes		Well depth	Land-surface measurement error[2]
			Water level	Land surface		
(D-16-11)08ccc	52,980	16,200	2,216.00	2,906.00	2,152.00	1.0
(D-16-10)04bda	29,605	25,758	2,381.30	2,540.00	2,140.00	5.0
(D-15-12)17bbb	84,859	48,264	2,062.00	2,459.00	2,009.00	.5
(D-15-12)06dad	83,923	55,236	2,047.00	2,406.10	1,995.00	.1
(D-15-11)35bab	70,303	32,529	2,150.00	2,610.00	2,084.00	10.0
(D-15-11)32ddc	56,875	26,899	2,200.00	2,630.10	2,166.10	.1
(D-15-11)17dc	55,880	43,569	2,120.00	2,425.00	2,056.00	25.0
(D-15-11)17aab	56,835	47,910	2,084.00	2,388.50	1,888.50	.5
(D-15-11)12dcd	77,381	48,881	2,057.00	2,420.00	1,918.00	5.0
(D-15-11)12dca1	77,382	49,386	2,056.00	2,416.00	1,866.20	.5
(D-15-11)11ddd	73,341	48,585	2,060.00	2,408.00	1,929.00	1.0
(D-15-11)09dab	62,858	50,524	2,069.00	2,375.00	2,034.00	25.0
(D-15-11)09da	62,514	50,322	2,066.00	2,373.00	-999	.5
(D-15-11)05cdd	54,786	53,774	2,058.00	2,365.30	1,637.00	.1
(D-15-10)35aab	40,463	31,164	2,315.00	2,530.00	-999	5.0
(D-15-10)35aaa	41,491	31,482	2,316.00	2,530.00	2,180.00	1.0
(D-15-10)34dbb	34,259	28,977	2,366.00	2,530.00	2,330.00	5.0
(D-15-10)33cac	27,891	27,884	2,378.40	2,530.00	2,324.00	1.0
(D-15-10)29aab	24,907	36,379	2,376.13	2,521.50	2,251.50	.1
(D-15-10)16dad	30,948	43,532	2,379.57	2,496.00	2,096.00	12.5
(D-14-11)32ab	56,011	63,569	2,035.00	2,325.00	1,925.00	5.0
(D-14-11)24aad	78,537	73,426	2,020.00	2,450.00	1,855.00	1.0
(D-14-11)09dba	61,290	82,145	1,982.00	2,255.00	1,820.00	5.0
(D-14-10)25caa	44,160	66,022	2,023.00	2,331.00	1,931.00	1.0
(D-14-10)25bcd	42,699	65,925	2,022.00	2,331.60	1,943.60	.1
(D-13-11)29cc	52,992	95,498	1,948.00	2,188.00	1,943.00	1.0
(D-13-11)18ddd	51,815	106,208	1,921.00	2,151.90	1,746.90	.1
(D-13-11)10bb	63,721	116,144	1,894.00	2,255.00	-999	1.0
(D-13-11)09aad	63,199	115,843	1,894.00	2,242.00	1,876.00	1.0
(D-13-11)08aa	57,243	116,197	1,898.00	2,168.80	1,854.00	.1
(D-13-11)07aaa	51,753	116,007	1,903.00	2,113.00	1,703.00	20.0
(D-13-11)07aba	50,895	116,009	1,907.00	2,107.80	1,707.80	.1
(D-13-11)06cb	47,814	118,946	1,885.00	2,096.00	1,696.00	1.0
(D-13-11)04dab	61,624	118,814	1,890.00	2,200.00	-999	1.0
(D-13-11)04cab	59,565	118,616	1,883.00	2,168.70	1,804.70	.1
(D-13-11)04aa	63,173	121,235	1,888.00	2,187.00	1,839.00	1.0
(D-13-10)10bb	31,852	116,565	1,880.00	2,092.00	1,823.00	1.0
(D-12-12)08abd	88,423	147,963	1,971.00	2,070.00	1,820.00	5.0
(D-12-12)07bcc	79,680	146,763	1,880.00	2,073.00	-999	5.0
(D-12-12)06bad	81,661	153,327	1,887.00	2,041.00	1,861.00	10.0
(D-12-12)05cbb	84,914	151,302	1,942.00	2,058.00	-999	5.0
(D-12-12)05bdd	86,800	152,006	1,950.00	2,064.00	1,876.00	5.0

See footnotes at end of table.

Table 5. Predevelopment heads for Avra Valley, Arizona—Continued

Local well number	X location[1]	Y location[1]	Altitudes		Well depth	Land-surface measurement error[2]
			Water level	Land surface		
(D-12-11)35cb	70,211	124,252	1,884.00	2,230.00	1,860.00	10.0
(D-12-11)34ddd	68,415	119,841	1,884.00	2,188.50	1,863.10	.5
(D-12-11)34dda	68,665	122,639	1,889.00	2,225.00	1,873.00	25.0
(D-12-11)34ccb	64,033	122,344	1,888.00	2,188.50	1,871.30	.5
(D-12-11)33bb	58,726	127,204	1,870.00	2,097.70	1,767.70	.1
(D-12-11)29aad	58,050	132,055	1,834.00	2,062.50	1,662.30	.5
(D-12-11)19aac	51,975	137,221	1,821.00	2,020.00	1,545.00	20.0
(D-12-11)18ddd	52,835	138,633	1,824.00	2,014.00	1,796.00	.5
(D-12-11)08cba	54,137	145,600	1,807.00	1,988.00	1,588.00	.5
(D-12-11)05ad	58,007	151,754	1,800.00	2,005.00	1,795.00	5.0
(D-12-11)01acd	77,202	151,818	1,872.00	2,035.00	1,859.00	5.0
(D-12-10)30bbc	15,862	129,250	1,848.00	2,080.00	1,575.00	20.0
(D-12-10)29abb	23,668	132,249	1,837.00	2,020.80	1,600.80	.5
(D-12-10)27dad	36,176	128,776	1,850.00	2,042.90	1,442.00	.1
(D-12-10)26bba	37,901	132,307	1,838.00	2,040.00	1,804.00	20.0
(D-12-10)26aad	41,328	131,388	1,842.00	2,039.10	1,720.10	.1
(D-12-10)26aab	40,730	132,198	1,839.00	2,030.00	1,717.00	20.0
(D-12-10)20dd	25,299	133,052	1,834.00	2,020.00	1,781.00	20.0
(D-12-10)14ccc	37,060	138,068	1,824.00	2,007.00	1,622.00	20.0
(D-12-10)14bcc	36,810	140,695	1,828.28	2,004.10	1,402.1	.1
(D-12-10)09bbb	26,064	147,525	1,802.00	1,964.50	1,796.30	.5
(D-12-10)03daa	36,151	149,889	1,799.00	1,970.00	1,715.00	.5
(D-12-10)01daa	46,693	150,568	1,799.00	1,970.00	1,770.00	20.0
(D-12-09)23ddd	10,207	132,497	1,840.00	2,120.00	1,708.00	20.0
(D-11-12)31ddd	84,148	154,737	1,925.00	2,056.00	1,636.00	.1
(D-11-11)34add	68,643	157,086	1,818.11	2,008.00	1,498.00	1.0
(D-11-11)30aaa	52,556	165,505	1,784.00	1,957.00	1,707.00	1.0
(D-11-11)28dbb	61,456	161,747	1,791.00	1,975.00	1,791.00	25.0
(D-11-11)22ccb	63,948	167,446	1,801.00	1,980.00	1,658.00	.5
(D-11-11)19caa	49,819	167,229	1,775.00	1,945.00	1,675.00	10.0
(D-11-11)16ddd	63,187	170,533	1,798.00	1,980.00	1,643.00	10.0
(D-11-11)16cdd	60,960	170,335	1,791.13	1,966.00	1,428.00	.1
(D-11-10)36ddb1	51,244	154,194	1,796.17	1,959.40	1,784.00	.1
(D-11-10)32dad	25,801	155,982	1,783.11	1,940.00	1,440.00	1.0
(D-11-10)32daa1	25,629	155,982	1,784.00	1,941.00	1,701.00	1.0
(D-11-10)27bac	32,933	163,032	1,775.24	1,916.00	1,752.00	1.0
(D-11-10)24ad	46,908	167,741	1,775.00	1,935.00	-999	10.0
(D-11-10)23ddd	41,674	164,421	1,774.00	1933.10	1,563.00	.1
(D-11-10)22add	36,285	166,962	1,774.34	1,915.00	1,315.00	1.0
(D-11-10)20dcc	23,087	164,577	1,761.00	1,921.00	1,563.00	1.0
(D-11-10)20acc	22,157	168,318	1,760.00	1,915.00	1,725.00	10.0
(D-11-10)17add	25,767	172,347	1,748.00	1,884.00	1,384.00	1.0
(D-11-10)09ddd	31,085	175,059	1,755.00	1,895.00	1,305.00	.1

See footnotes at end of table.

Table 5. Predevelopment heads for Avra Valley, Arizona—Continued

Local well number	X location[1]	Y location[1]	Altitudes		Well depth	Land-surface measurement error[2]
			Water level	Land surface		
(D-11-10)08dad	25,780	176,590	1,744.80	1,883.00	1,678.00	1.0
(D-11-10)08aad	25,702	179,015	1,730.00	1,878.00	-999	1.0
(D-11-09)36cd	12,257	154,310	1,785.00	2,040.00	1,608.00	20.0
(D-10-11)35dbd	74,774	185,361	1,800.00	2,280.00	1,637.00	20.0
(D-10-11)30caa	52,451	193,488	1,751.00	2,037.00	1,711.00	12.5
(D-10-11)30bcd	50,740	193,896	1,744.00	2,020.10	1,670.10	.1
(D-10-11)29bcc	55,505	193,945	1,755.00	2,090.00	1,540.00	10.0
(D-10-11)18da	55,212	203,281	1,750.00	2,100.00	1,742.00	20.0
(D-10-11)17cab	57,010	203,883	1,755.00	2,130.00	1,684.00	10.0
(D-10-10)34cdd	36,587	182,821	1,745.24	1,896.00	-999	12.5
(D-10-10)34cbb	34,623	184,544	1,751.00	1,893.90	1,389.00	.1
(D-10-10)20dcd	27,203	193,255	1,720.00	1,863.00	-999	.1
(D-10-10)05daa	28,968	210,625	1,700.00	1,858.40	1,378.40	.1
(D-10-10)04cac	30,506	209,913	1,700.00	1,870.40	1,540.40	.1
(D-10-09)36ddd3	17,924	182,880	1,721.00	1,859.00	1,640.00	1.0
(D-10-09)36dbd	16,815	183,894	1,715.00	1,857.80	1,357.00	.1
(D-10-09)36cdd	15,108	182,778	1,710.00	1,857.00	1,627.00	12.5
(D-10-09)33ddc	1,486	182,738	1,724.00	1,945.00	-999	10.0
(D-10-09)24ddd1	18,387	193,283	1,700.00	1,844.90	1,527.00	.1
(D-10-09)23ddd	12,996	193,504	1,695.00	1,839.30	1,317.00	.1
(D-10-09)23cad	10,091	194,626	1,695.00	1,830.80	1,439.00	.1
(D-10-09)23ada	12,921	196,434	1,692.00	1,829.40	1,595.00	.1
(D-10-09)16ccc	-2,302	198,715	1,635.00	1,785.00	1,433.00	5.0
(D-10-09)13dda	18,240	198,956	1,695.00	1,822.00	-999	10.0
(D-10-09)12ccb	13,549	204,514	1,670.00	1,816.10	1,584.00	.1
(D-10-09)10dba1	6,111	205,956	1,655.00	1,798.80	1,610.00	.1
(D-10-09)08dda	-3,049	204,577	1,636.00	1,773.00	-999	.1
(D-10-09)05dcc	-4,911	209,333	1,611.00	1,759.10	1,601.10	10.0
(D-09-10)31aab	22,305	218,678	1,688.00	1,827.90	-999	.1

[1]All values are in feet from lower left-hand corner (31°59'58", 111°25'13") of U.S. Geological Survey ground-water flow model (Hanson and others, 1990).

[2]Land-surface altitude-measurement error.

Table 6. Developed aquifer heads for Avra Valley, Arizona

[-999, no information. Other negative numbers are negative coordinates with respect to the southwest corner of the model grid. All values are in feet]

Local well number	X location[1]	Y location[1]	Altitudes		Well depth	Land-surface measurement error[2]
			Water level	Land surface		
(D-16-10)34bab	34,176	188	3,095.80	2,491.30	875.00.	0.1
(D-16-10)30dda	21,442	1,944	2,787.00	2,505.30	500.00	5.0
(D-16-09)25cbc	11,803	2,482	2,685.00	2,528.80	437.00	10.0
(D-16-09)E30aad	-10,920	2,974	2,945.00	2,567.21	425.00	10.0
(D-16-10)30cbb	16,885	3,474	2,690.00	2,500.10	405.00	5.0
(D-16-09)24ddc	15,431	6,206	2,652.60	2,502.30	-999	.1
(D-16-10)23dcd	41,424	6,430	3,056.90	2,410.30	714.00	.1
(D-16-10)19cca	17,242	7,514	2,652.00	2,499.20	180.00	1.0
(D-16-09)20dab	-5,739	7,094	2,825.00	2,558.50	355.00	10.0
(D-16-09)24dac	15,521	7,519	2,651.20	2,499.80	240.00	.1
(D-16-10)19cab	18,020	8,319	2,645.00	2,494.30	-999	5.0
(D-16-09)14dbc	8,225	12,899	2,658.20	2,511.70	250.00	.1
(D-16-10)18bbd	17,183	15,494	2,607.00	2,453.30	500.00	5.0
(D-16-10)13adb	47,127	15,507	2,851.00	2,244.10	800.00	10.0
(D-16-10)18bbc	16,926	15,697	2,604.00	2,454.50	300.00	5.0
(D-16-11)08ccc	52,980	16,200	2,907.70	2,215.60	754.00	.1
(D-16-10)08bdd	24,252	19,612	2,581.80	2,425.50	232.00	.1
(D-16-11)08bdb	54,537	19,934	2,822.75	2,203.15	802.00	.1
(D-16-11)09aca	61,762	19,009	2,900.00	2,174.00	1,200.00	10.0
(D-16-10)05ddd	26,841	22,231	2,571.70	2,406.20	295.00	.1
(D-15-09)36ddd	15,239	25,703	2,601.00	2,441.20	-999	5.0
(D-15-11)31ddd	52,489	27,010	2,622.00	2,205.40	528.00	5.0
(D-15-10)33dbc	29,009	27,780	2,530.00	2,366.70	616.00	1.0
(D-15-10)33cbc	26,428	27,788	2,539.60	2,374.30	783.00	.1
(D-16-10)04bdc	28,740	24,346	2,550.00	2,383.10	-999	10.0
(D-15-11)31dad	52,578	28,525	2,596.00	2,200.60	550.00	5.0
(D-15-10)33bcc	26,002	28,900	2,531.45	2,364.65	710.00	.1
(D-15-10)35aaa	41,491	31,482	2,529.60	2,297.80	350.00	1.0
(D-15-10)28cdc	27,300	31,523	2,528.90	2,360.90	640.00	.1
(D-15-11)31aba	51,038	31,761	2,543.00	2,201.70	526.00	5.0
(D-15-11)35bab	70,303	32,529	2,613.00	2,126.60	526.00	.1
(D-15-11)30bac	48,986	36,817	2,487.00	2,181.90	500.00	5.0
(D-15-11)22ccc	63,434	37,997	2,502.00	2,117.20	1,130.00	5.0
(D-15-11)20aaa	57,684	42,756	2,433.93	2,078.03	895.00	1.0
(D-15-11)12ccc	73,771	48,685	2,412.00	2,014.30	1,475.00	10.0
(D-15-11)11add	73,174	51,313	2,387.90	2,007.90	588.00	.1
(D-15-11)11bbb	68,708	53,240	2,360.64	2,002.04	1,120.00	1.0
(D-15-11)09aaa	62,691	53,252	2,348.00	2,000.30	1,472.00	5.0
(D-15-11)05ccd	52,980	53,576	2,369.50	2,020.20	712.00	.1
(D-14-11)34ccc	63,477	59,008	2,322.00	1,984.90	620.00	.1
(D-14-11)33dcd	61,414	59,012	2,328.80	1,984.80	670.00	.1
(D-14-11)33ccc	58,149	59,019	2,336.00	1,987.40	712.00	1.0
(D-14-11)33bdd	60,131	61,641	2,319.00	1,975.10	1,330.00	10.0

See footnotes at end of table.

Table 6. Developed aquifer heads for Avra Valley, Arizona—Continued

Local well number	X location[1]	Y location[1]	Altitudes		Well depth	Land-surface measurement error[2]
			Water level	Land surface		
(D-14-11)34aad	67,952	62,737	2,319.60	1,978.20	512.00	0.1
(D-14-11)34bbc1	63,398	62,746	2,311.30	1,974.10	535.00	.1
(D-14-11)34bbc2	63,914	62,846	2,309.00	1,973.10	1,266.00	5.0
(D-14-11)28dcc	60,823	64,064	2,316.70	1,970.90	495.00	.1
(D-14-11)29ddd	57,386	64,071	2,319.90	1,969.80	542.00	.1
(D-14-12)30cdc	80,585	64,534	2,407.80	1,987.90	566.00	.1
(D-14-11)27bcc	63,406	66,887	2,311.78	1,972.88.	1,150.00	1.0
(D-14-11)27aad	67,875	67,788	2,312.60	1,964.60	516.00	.1
(D-14-11)22cbb	63,416	71,433	2,283.00	1,942.70	1,239.00	5.0
(D-14-10)12aba	45,149	83,294.	2,236.00	1,842.20	485.00	5.0
(D-14-11)08ccc	52,955	79,840	2,258.00	1,898.90	590.00	.1
(D-14-11)07bad	49,186	83,688	2,241.30	1,870.98	700.00	.1
(D-14-11)07bba	48,244	84,902	2,234.20	1,864.10	1,260.00	.1
(D-14-11)06ccd	48,331	85,205	2,234.10	1,862.70	635.00	.1
(D-14-11)05ccd	53,483	85,294	2,236.20	1,878.80	616.00	.1
(D-14-11)06dcc	50,220	85,301	2,235.40	1,866.10	-999	.1
(D-14-10)02ddd	41,376	85,324	2,245.10	1,844.80	1,015.00	.1
(D-14-11)04cda	59,842	87,401	2,263.20	1,883.10	581.00	.1
(D-13-11)34ccc	63,282	90,222	2,336.00	1,867.50	555.00	10.0
(D-13-11)31cdd	49,546	90,556	2,212.20	1,844.30	705.00	.1
(D-13-11)31ccc1	47,657	90,561	2,214.30	1,838.60	736.00	.1
(D-13-10)26dcd	40,202	95,631	2,190.20	1,801.00	705.00	.1
(D-13-10)26ccd	37,627	95,638	2,190.20	1,791.00	700.00	.1
(D-13-11)30ccc	47,585	95,814	2,187.80	1,816.70	682.00	.1
(D-13-10)22ccc	31,374	100,101	2,163.00	1,734.30	-999	5.0
(D-13-10)22cdd	33,436	100,903	2,168.50	1,745.40	1,100.00	.1
(D-13-10)24dcc	45,023	100,972	2,163.33	1,789.43	575.00	1.0
(D-13-10)23dcc	39,444	100,987	2,168.40	1,779.70	700.00	.1
(D-13-10)20ccd	21,421	101,041	2,147.10	1,726.70	515.00	.1
(D-13-10)20cab	21,858	103,464	2,126.90	1,723.60	627.00	.1
(D-13-11)18ddc1	51,816	106,309	2,151.93	1,786.93	370.00	1.0
(D-13-11)16adc	62,290	109,216	2,295.00	1,792.80	567.00	10.0
(D-13-10)08ddd	25,574	111,635	2,110.00	1,726.30	600.00	.1
(D-12-10)12bcd	42,996	145,830	1,990.40	1,728.10	1,010.00	.1
(D-13-10)06ddd	19,586	116,806	2,086.40	1,715.40	-999	.1
(D-13-10)05ddd1	25,591	116,989	2,090.10	1,717.40	587.00	.1
(D-13-11)04daa	62,482	118,812	2,203.90	1,759.80	430.00	.1
(D-12-10)33cdd	28,009	122,133	2,062.30	1,707.40	1,255.00	.1
(D-12-10)31dcc	19,261	122,161	2,061.30	1,721.50	757.00	.1
(D-12-10)33ddd	30,926	122,225	2,068.10	1,718.90	940.00	.1
(D-12-10)33cdc	27,924	122,234	2,069.00	1,711.00	1,900.00	.1
(D-12-10)31bda	17,299	125,502	2,066.70	1,690.90	528.00	.1
(D-11-11)31cbc	47,479	156,425	1,969.00	1,690.70	650.00	1.0
(D-12-11)30ddd1	51,953	128,129	2,056.20	1,750.10	686.00	.1
(D-12-11)30cdd	50,409	128,133	2,053.80	1,751.70	639.00	.1

See footnotes at end of table.

Table 6. Developed aquifer heads for Avra Valley, Arizona—Continued

Local well number	X location[1]	Y location[1]	Altitudes		Well depth	Land-surface measurement error[2]
			Water level	Land surface		
(D-12-11)30ddd2	52,725	128,329	2,058.30	1,751.60	725.00	0.1
(D-12-10)30abb	18,523	132,367	2,055.00	1,690.20	698.00	20.0
(D-12-10)30bbc3	15,606	131,771	2,074.30	1,688.00	547.00	.1
(D-12-10)30aba	19,638	132,363	2,045.00	1,679.60	810.00	20.0
(D-12-11)W19aad	47,517	137,232	2,018.80	1,729.70	790.00	.1
(D-12-11)20aaa	57,891	137,914	2,017.10	1,701.40	375.00	.1
(D-12-11)16dad	63,468	140,024	2,028.70	1,700.00	512.00	.1
(D-12-12)18cbc	79,583	139,793	2,078.00	1,766.80	550.00	10.0
(D-12-11)E18dab	51,896	140,352	2,003.00	1,698.30	600.00	20.0
(D-12-11)15aca	67,415	141,936	2,039.00	1,750.60	550.00	.1
(D-12-11)17add	58,070	141,349	2,004.70	1,700.60	560.00	1.0
(D-12-11)17acc	56,270	141,353	2,004.00	1,701.40	1,000.00	5.0
(D-12-10)12dcd	45,646	143,095	1,998.50	1,714.10	430.00	.1
(D-12-10)12ccd1	43,417	143,202	1,993.50	1,718.30	-999	.1
(D-12-10)09dcd	29,532	143,343	1,988.80	1,691.50	1600.00	.1
(D-12-10)12ccd2	42,818	143,406	1,997.50	1,720.70	-999	.1
(D-12-10)09ddd	30,904	143,440	1,986.80	1,689.60	508.00	.1
(D-12-10)12cdb2	43,161	143,506	1,995.00	1,705.20	1,295.00	.1
(D-12-11)07cdd	49,591	143,995	1,995.80	1,721.30	606.00	.1
(D-12-11)12dad	79,335	145,249	2,072.20	1,775.00	555.00	.1
(D-12-11)07bdd	49,682	146,419	1,986.00	1,704.10	550.00	.1
(D-12-11)09acc	60,910	146,494	2,013.40	1,693.80	585.00	.1
(D-12-11)09add	63,226	147,298	2,020.60	1,695.60	520.00	.1
(D-12-10)01dcc	44,117	148,453	1,980.90	1,702.29	414.00	.1
(D-12-10)04dcc	28,348	148,599	1,967.00	1,680.80	1,600.00	.1
(D-11-12)34ddc	99,142	154,518	2,390.00	2,002.40	490.00	10.0
(D-11-11)34ddd	68,553	154,561	2,012.30	1,700.70	492.00	1.0
(D-11-10)32daa3	25,631	156,488	1,940.50	1,659.20	501.00	.1
(D-11-11)35adc	73,098	156,876	2,019.80	1,706.10	860.00	.5
(D-11-11)34add2	68,729	156,985	2,008.00	1,695.20	787.00	5.0
(D-11-10)27cdc1	33,007	159,092	1,923.20	1,674.40	550.00	.1
(D-11-11)28ddd2	63,422	159,723	1,991.00	1,684.90	768.00	5.0
(D-11-10)25dda2	46,888	159,761	1,953.20	1,694.10	600.00	.1
(D-11-11)26ddd	73,961	160,208	2,012.00	1,706.50	-999	10.0
(D-11-10)29dbc	23,759	160,433	1,939.80	1,645.80	500.00	.1
(D-11-10)27daa	36,526	161,304	1,935.50	1,672.40	3,212.00	.1
(D-11-11)28acc2	61,029	162,253	1,981.00	1,679.80	980.00	5.0
(D-11-11)28acc1	62,057	162,352	1,980.00	1,679.90	500.00	.5
(D-11-10)27bac	32,933	163,032	1,915.60	1,693.60	-999	.1
(D-11-10)22ddd2	36,278	164,335	1,918.10	1,680.40	638.00	.1
(D-11-10)22ddd1	36,278	164,436	1,923.20	1,678.80	375.00	.1
(D-11-10)20ddd	25,656	164,569	1,904.70	1,639.00	529.00	.1
(D-11-11)20ccc2	53,068	164,898	1,953.00	1,671.50	965.00	10.0
(D-11-11)22dcd	67,116	165,070	1,998.00	1,688.40	503.00	5.0
(D-11-11)20ddd	58,036	164,886	1,967.00	1,675.30	840.00	1.0

See footnotes at end of table.

Table 6. Developed aquifer heads for Avra Valley, Arizona—Continued

Local well number	X location[1]	Y location[1]	Altitudes		Well depth	Land-surface measurement error[2]
			Water level	Land surface		
(D-11-10)22add	36,285	166,962	1,915.00	1,670.00	600.00	1.0
(D-11-11)21acd	61,725	167,505	1,977.00	1,675.70	702.00	5.0
(D-11-10)24aaa	47,083	169,357	1,935.00	1,669.70	500.00	1.0
(D-11-11)21aaa2	63,100	169,624	1,979.00	1,672.00	588.00	1.0
(D-11-11))21aaa1	63,271	169,724	1,978.00	1,670.70	375.00	1.0
(D-11-10)15ddd	36,293	169,790	1,909.30	1,673.20	515.00	.1
(D-11-11)16cdd2	60,789	170,235	1,968.00	1,669.40	906.00	5.0
(D-11-11)16cdd1	60,960	170,335	1,966.00	1,669.10	538.00	.1
(D-11-11)18ddd	52,909	170,151	1,949.00	1,668.20	596.00	1.0
(D-11-11)16dbd	61,477	171,647	1,968.00	1,667.90	512.00	1.0
(D-11-11)16dad	63,275	171,745	1,969.00	1,661.50	700.00	1.0
(D-11-10)13aaa2	46,583	174,611	1,925.00	1,669.10	1,002.00	20.0
(D-11-10)12ccc	42,045	174,724	1,911.00	1,661.00	883.00	20.0
(D-11-10)08ddd	25,690	175,075	1,885.30	1,642.80	443.00	.1
(D-11-11)07ddd	52,922	175,404	1,941.00	1,663.50	680.00	1.0
(D-11-10)12dbb	44,534	177,142	1,914.00	1,661.70	-999	20.0
(D-11-10)12add	46,847	177,641	1,920.00	1,664.60	800.00	20.0
(D-11-11)11dcd	72,875	176,171	2,148.20	1,694.00	505.00	.1
(D-10-11)S31cdc	51,483	182,580	1,963.00	1,652.40	565.00	5.0
(D-10-10)21bcc	29,093	195,774	1,865.00	1,612.20	725.00	5.0
(D-10-10)20acc	26,698	195,984	1,859.00	1,606.60	1,010.00	2.5
(D-10-09)14caa	10,454	200,484	1,814.60	1,535.70	800.00	.1
(D-10-09)13daa	18,584	200,758	1,837.20	1,586.90	542.00	.1
(D-10-10)09bbb	29,561	208,704	1,859.00	1,618.00	500.00	5.0
(D-10-10)05dad	28,882	210423	1,855.00	1,617.80	580.00	1.0
(D-10-10)05dba	27,772	211,235	1,850.00	1,614.20	603.00	2.5
(D-10-09)12cbc	13,295	205,121	1,816.00	1,543.10	442.00	.1
(D-12-11)20dda	57,969	134,176	2,048.10	1,706.80	695.00	.1
(D-13-10)14cdd	38,172	106,344	2,143.32	1,765.20	596.00	.1
(D-13-10)24abb	44,607	106,024	2,143.00	1,778.60	1,000.00	10.0
(D-15-11)15aaa	68,096	47,887	2,405.20	2,020.10	800.00	.1
(D-15-11)15bbb	63,626	47,795	2,391.80	2,020.60	993.00	.1
(D-15-11)15ccc	63,703	43,249	2,437.50	2,057.50	1,000.00	.1
(D-15-11)15ddd	68,087	43,241	2,452.40	2,054.00	900.00	.1
(D-15-11)22ddd	68,164	38,089	2,515.30	2,104.90	1,000.00	.1
(D-16-10)29ddd	26,604	1,018	2918.00	2,505.20	1,000.00	5.0
(D-13-10)05ddd2	25,506	116,989	2,087.40	1,717.00	-999	.1
(D-11-10)27cdc2	32,957	159,042	1,923.40	1,674.25	550.00	.1
(D-13-11)31ccc2	47,486	90,561	2,214.00	1,841.10	736.00	2.0
(D-12-10)04acd	29,384	151,021	1,964.20	1,657.40	1,200.00	.1
(D-10-10)04bbb	29,577	213,856	1,864.00	1,613.00	1,004.00	.1
(D-10-10)01bbb	45,485	213,609	2,010.00	1,645.20	1,460.00	.1
(D-10-11)19bdb	51,612	200,764	2,040.00	1,654.10	1,500.00	.1
(D-10-11)31add	55,005	187,724	2,024.00	1,650.20	1,200.00	.1
(D-11-11)09acd	61,919	178,213	2,043.00	1,671.90	1,193.00	.1

See footnotes at end of table.

Table 6. Developed aquifer heads for Avra Valley, Arizona—Continued

Local well number	X location[1]	Y location[1]	Altitudes		Well depth	Land-surface measurement error[2]
			Water level	Land surface		
(D-11-11)23bbb	68,924	169,713	2,045.00	1,682.90	1,105.00	0.1
(D-11-11)31bcc	79,610	157,068	2,043.00	1,767.60	1,115.00	.1
(D-12-11)01dda	79,342	149,896	2,041.00	1,765.70	984.00	.1
(D-12-11)10ada	68,282	147,490	2,035.00	1,698.70	1,400.00	.1
(D-12-11)14cbc	69,125	139,811	2,055.00	1,765.70	850.00	.1
(D-12-11)33bbc	61,469	126,997	2,102.00	1,750.90	998.00	.1
(D-13-11)17bcb	52,597	110,045	2,135.00	1,766.80	1,200.00	.1
(D-13-11)17adc	56,798	108,924	2,193.00	1,775.60	1,106.00	.1
(D-13-11)29cdd	54,709	95,696	2,194.00	1,833.60	790.00	.1
(D-14-11)10aab	67,135	84,760	2,370.00	1,894.10	1,000.00	.1
(D-14-11)14dcd	72,527	74,749	2,374.00	1,938.80	1,006.00	.1
(D-14-11)36aac	78,436	63,426	2,379.00	1,986.60	1,410.00	.1
(D-10-09)13ddd	18,320	198,638	1,837.20	1,589.30	401.00	.1
(D-10-09)13dcd	16,951	198,643	1,835.00	1,583.00	320.00	.1
(D-10-09)13ccd	14,297	198,349	1,829.00	1,570.70	401.00	.1
(D-10-11)17cab	57,010	203,883	2,130.00	1,662.60	-999	10.0
(D-11-10)10ddd	36,308	174,942	1,906.00	1,653.90	590.00	1.0
(D-10-11)18da	55,212	203,281	2,103.20	1,659.50	500.00	.1
(D-10-11)08bac	57,197	210,954	2,150.00	1,668.35	-999	2.5
(D-10-11)15bcb	66,337	204,874	2,260.00	1,683.55	-999	2.5
(D-10-11)22ddc	70,000	196,381	2,320.00	1,695.35	-999	5.0
(D-10-11)27cad	68,453	192,646	2,280.00	1,681.10	-999	2.5
(D-10-11)29aac	58,443	194,182	2,155.00	1,675.10	-999	2.5
(D-10-11)30ddd	55,184	191,259	2,075.00	1,667.50	-999	2.5
(D-10-11)30caa2	52,451	193,488	2,041.60	1,659.20	450.00	.1
(D-11-10)29acc	23,505	161,545	1,935.00	1,646.50	-999	20.0
(D-11-11)33aca	61,619	157,908	1,992.00	1,688.10	-999	20.0
(D-13-10)06ccd	16,584	116,917	2,092.10	1,712.20	382.00	0.1
(D-13-10)15abb	33,809	110,903	2,122.00	1,717.70	-999	20.0
(D-11-11)22dcc	66,774	165,171	1,994.00	1,684.40	-999	25.0
(D-10-10)15add	39,549	201,199	1,930.00	1,653.00	2,510.00	10.0
(D-10-10)15dac	38,516	198,878	1,910.00	1,627.00	714.00	10.0
(D-12-12)21bdd	92,437	136,038	2,105.00	2,004.80	-999	5.0
(D-09-10)28adc	33,451	222,330	1,910.00	1,603.50	1,500.00	.1
(D-09-10)19ccc2	19,094	224,800	1,810.00	1,535.00	640.00	.1
(D-09-09)31dad	-7,622	215,608	1739.00	1,253.40	1,017.00	2.5

[1]All values are in feet from lower left-hand corner (31°59'58", 111°25'13") of U.S. Geological Survey ground-water flow model (Hanson and others, 1990).

[2]Land-surface altitude-measurement error.

Table 7. Transmissivity estimates from aquifer tests and related data from selected wells in Avra Valley, Arizona

[ft, foot; ft^2/d, foot squared per day; (gal/min)/ft, gallons per minute per foot; -999, no information]

Local well number	X location (ft)[1]	Y location (ft)[1]	Trans-missivity (ft^2/d)[2]	Specific capacity [(gal/min)/ft][2]	Average silt-and-clay content[2,3]	Land-surface altitude (ft)
NONAME	41,674	164,421	17,111	46.0	0.57	1,933
AF-5	33,007	159,091	8,822	14.4	.69	1,922
W-5	30,904	143,440	2,138	16.0	-999	1,984
AF-12	42,654	144,906	5,079	23.5	.75	1,994
AF-16	27,924	122,234	2,219	12.2	.54	2,068
AF-17	30,926	122,225	850	6.2	-999	2,068
AF-18	50,863	138,638	3,448	12.9	.63	2,010
AF-21?	51,953	128,129	1,069	23.5	.57	2,056
AF-20	50,409	128,133	855	8.3	.75	2,052
AF-22	52,725	128,329	1,163	4.1	.75	2,055
AF-23	25,591	116,989	3,529	10.4	.54	2,100
AF-27	39,444	100,987	5,480	22.1	-999	2,167
AF-30	40,202	95,631	5,173	17.5	-999	2,190
AF-31	47,585	95,814	10,560	114.0	.57	2,168
AF-32	47,657	90,561	10,079	23.1	.57	2,211
AF-34	49,546	90,556	7,753	39.2	.57	2,213
AF-35?	59,842	87,401	35,291	15.9	.37	2,250
AF-37	48,082	85,181	5,347	17.9	.22	2,230
AF-39	49,186	83,688	8,261	25.6	.22	2,242
AF-40	52,955	79,840	7,419	24.1	.51	2,257
AV-18	63,416	71,433	37,163	36.4	.18	2,280
AV-17	67,875	67,788	31,147	39.5	-999	2,312
AV-19	63,406	66,887	28,072	41.6	.13	2,300
AV-21	66,066	64,761	36,895	64.0	.09	2,310
AV-20	58,081	67,504	24,998	60.6	.16	2,305
AV-14	60,823	64,064	11,229	38.6	.14	2,325
AV-13	57,386	64,071	5347	25.8	.16	2,318
AV-22	60,131	61,641	22,458	38.5	.14	2,320
AV-24	61,414	59,012	8,916	28.2	-999	2,328
AV-15	63,914	62,846	11,362	27.5	.17	2,309
AV-25	63,476	59,008	12,298	27.6	-999	2,322
AV-12	62,691	53,252	33,928	28.4	.24	2,350
AV-8	73,174	51,313	19,878	37.5	-999	2,388
AV-11	68,708	53,240	41,775	38.0	.03	2,370
AV-9	73,753	51,096	37,002	29.3	.11	2,410
AV-6	68,096	47,887	3,943	14.5	.58	2,400
AV-5	63,626	47,795	7,675	18.5	.62	2,400
AV-1	63,703	43,249	7,218	18.8	.43	2,450
AV-2	68,087	43,241	10,915	15.6	.56	2,450
AV-7	57,684	42,756	7,740	13.0	.48	2,450
AV-4	63,434	37,997	1,403	6.6	.19	2,500
AV-3	68,164	38,089	3,181	14.0	.51	2,510
AF-001	36,646	173,527	12,700	71.2	.60	1,906

See footnotes at end of table.

Table 7. Transmissivity estimates from aquifer tests and related data from selected wells in Avra Valley, Arizona—Continued

Local well number	X location (ft)[1]	Y location (ft)[1]	Trans-missivity (ft^2/d)[2]	Specific capacity [(gal/min)/ft][2]	Average silt-and-clay content[2,3]	Land-surface altitude (ft)
AF-002	36,278	164,436	7,941	40.3	0.57	1,923
AF-013	42,818	143,406	4,706	23.4	.75	1,998
AF-029	37,627	95,638	1,700	14.1	-999	2,190
AF-036	53,483	85,294	6,684	30.5	.43	2,236
AF-038	50,200	85,301	15,374	19.7	.22	2,235
AF-041	45,531	98,344	25,294	56.8	.56	2,180
AF-042	43,557	98,349	7,380	27.8	-999	2,177
AF-044	38,172	106,344	7,299	25.5	-999	2,143
AF-045	36,198	106,350	10,615	29.7	-999	2,143
AF-046	45,023	100,972	16,618	166.0	-999	2,165
AF-048	57,969	134,176	4,104	17.8	-999	-999
AF-049	36,183	100,996	13,503	14.5	-999	2169
AF-050	36,284	106,350	4,104	17.0	.80	2,143
AF-053	28,336	116,980	8,623	18.8	.54	2,188
AF-054	30,910	116,972	6,085	32.3	-999	2,190
AF-055	27,300	31,523	6,484	29.8	-999	2,528
AF-056	26,002	28,900	3,106	11.4	.36	2,531
AF-058	36,293	169,790	25,013	99.4	-999	1,909
AF-060	44,248	132,896	6,631	25.1	-999	2,036
AF-062	29,605	25,758	47,380	111.9	-999	2,541
AF-063	26,841	22,231	34,198	83.8	.06	2,565
AF-064	24,252	19,612	38,422	58.2	-999	2,575
AF-065	66,052	12,940	201	2.5	-999	2,610
AF-067	18,020	8,319	80,548	85.1	-999	2,643
A-58	80,671	64,433	5,160	11.1	.06	2,420
A-59	80,585	64,534	3,075	6.3	.06	2,410

[1]All values are in feet from lower left-hand corner (31°59'58", 111°25'13") of U.S. Geological Survey ground-water flow model (Hanson and others, 1990).

[2]Number of significant figures for transmissivity, specific capacity, and average silt-and-clay content may not reflect the precision of the various estimates.

[3]Silt-and-clay fraction determined as total sample weight minus weight of sand-and-gravel fractions. Average silt-and-clay content is thickness-weighted average for sediment samples from the upper Tinaja beds.

Table 8. Specific-capacity estimates and related data for selected wells in Avra Valley, Arizona

[ft, foot; (gal/min)/ft, gallons per minute per foot; -999, no information]

Local well number	X location (ft)[1]	Y location (ft)[1]	Specific capacity [(gal/min)/ft][2]	Average silt-and-clay content[2,3]	Local well number	X location (ft)[1]	Y location (ft)[1]	Specific capacity [(gal/min)/ft][2]	Average silt-and-clay content[2,3]
(D-16-11)09aaa2	62,884	20,825	8.7	0.25	(D-12-11)09bdd	61,253.	146,494	51.0	0.26
(D-16-11)08bdb	54,537	19,934	11.3	.21	(D-12-11)07dcc	49,591	143,995	46.0	-999
(D-16-10)29ddd	26,604	1,018	56.4	.19	(D-12-11)07bdd	49,682	146,419	44.3	-999
(D-15-11)05cdd	54,786	53,774	74.6	-999	(D-12-11)04bab	59,993	153,409	104.1	-999
(D-15-11)05ccd	52,980	53,576	74.6	-999	(D-12-11)01caa	76,602	151,112	55.9	-999
(D-14-11)34aad	67,952	62,737	36.3	.17	(D-12-10)32ddd	25,608	122,242	9.9	-999
(D-14-11)33dcc	60,084	59,019	32.5	.14	(D-12-10)29bbb	21,181	132,156	53.9	-999
(D-14-11)33ccc	58,149	59,019	40.9	-999	(D-12-10)29acb	23,663	130,734	29.9	-999
(D-14-11)29ccc	53,120	63,677	39.7	-999	(D-12-10)29abb	23,087	130,953	63.7	-999
(D-14-11)07dcc	50,326	80,079	33.3	.22	(D-12-10)28bcc	26,491	130,219	20.8	-999
(D-13-11)04cad	59,993	118,211	7.0	-999	(D-12-10)27dad	36,176	128,776	22.1	-999
(D-13-10)25dcc	44,752	95,720	107.3	.56	(D-12-10)26add	41,410	129,974	15.2	-999
(D-13-10)25adc	46,260	98,344	49.3	-999	(D-12-10)23ddc	40,818	133,006	13.2	-999
(D-13-10)22dcc	34,366	100,996	14.5	-999	(D-12-10)23acd	40,396	135,331	39.7	.65
(D-13-10)22cdd	33,436	100,903	12.2	-999	(D-12-10)21ddc	30,958	132,832	14.1	-999
(D-13-10)20ccd	21,421	101,041	7.1	.40	(D-12-10)20ddd	25,299	133,052	26.9	-999
(D-13-10)14bcc	36,806	108,874	11.2	.80	(D-12-10)20add	25,564	135,273	22.7	-999
(D-13-10)16ddd	30,878	106,365	31.2	-999	(D-12-10)14cbd	36,810	140,695	14.1	.65
(D-13-10)14bdc	37,544	109,216	10.4	-999	(D-12-10)12dcd	45,646	143,095	17.0	.75
(D-13-10)09ddd	30,980	111,618	39.7	-999	(D-12-10)12bad	42,654	147,593	46.0	-999
(D-13-10)08ddd	25,499	111,618	38.0	.57	(D-12-10)11ccd	37,767	143,095	19.0	-999
(D-13-10)08ada	25,499	114,969	16.3	.57	(D-12-10)11bcd	37,767	145,743	17.9	-999
(D-13-10)06ddd	19,586	116,806	21.6	-999	(D-12-10)09dcd	29,532	143,343	7.4	-999
(D-13-10)06ddc	18,541	116,806	32.9	-999	(D-12-10)04ddc	30,320	148,795	16.8	.44
(D-13-10)06ccd	17,785	116,812	13.4	-999	(D-12-10)04acd	29,817	152,535	26.7	.44
(D-12-11)29add	57,961	130,742	11.3	-999	(D-12-10)03dad	35,119	149,911	14.1	-999
(D-12-11)20aaa	57,891	137,914	35.5	-999	(D-12-10)01dcc	45,474	148,453	22.5	-999
(D-12-11)19bbc	47,259	137,131	13.6	-999	(D-12-10)01cdd	44,011	148,453	19.2	-999
(D-12-11)19aac	51,978	137,025	24.3	.63	(D-11-11)35ddd	74,315	154,583	131.9	-999
(D-12-11)18ddc	51,978	138,736	19.0	.63	(D-11-11)35adc	73,480	157,192	146.5	-999
(D-12-11)18dab	51,896	140,352	26.4	.63	(D-11-11)34add	68,643	157,086	153.1	.28

See footnotes at end of table.

Table 8. Specific-capacity estimates and related data for selected wells in Avra Valley, Arizona—Continued

Local well number	X location (ft)[1]	Y location (ft)[1]	Specific capacity [(gal/min)/ft][2]	Average silt-and-clay content[2,3]	Local well number	X location (ft)[1]	Y location (ft)[1]	Specific capacity [(gal/min)/ft][2]	Average silt-and-clay content[2,3]
(D-12-11)18cbc	47,523	139,959	15.9	-999	(D-11-11)31dad	52,532	155,302	79.5	-999
(D-12-11)16dad	63,468	140,024	27.3	-999	(D-11-11)31cbc	47,406	127,433	83.1	.42
(D-12-11)15dbd	66,982	139,613	36.3	.30	(D-11-11)28ddd	63,368	159,761	111.6	.34
(D-12-11)15acd	66,552	141,328	73.4	.30	(D-11-11)28acd	62,188	162,509	124.1	-999
(D-12-11)14cbd	70,411	140,011	51.4	.30	(D-11-11)26bdc	70,728	162,509	85.5	.27
(D-12-11)14bcd	70,622	141,328	69.0	.30	(D-11-11)21aaa	63,574	169,853	20.3	.28
(D-12-11)12dad	78,905	144,542	66.5	-999	(D-11-11)20ddd	57,785	165,099	121.0	-999
(D-12-11)12bcd	75,566	146,568	79.5	-999	(D-11-11)20ccc	53,326	165,099	117.1	.45
(D-11-11)18ddd	52,426	170,335	201.3	0.33	(D-11-10)20ddd	25,656	164,569	109.2	-999
(D-11-11)17baa	54,786	175,175	129.1	-999	(D-11-10)20dcc	23,087	164,577	59.6	-999
(D-11-11)16cdd	60,960	170,335	105.3	.28	(D-11-10)17add	25,767	172,347	126.8	-999
(D-11-10)33bcb	25,114	156,453	42.6	-999	(D-11-10)15aad	36,304	173,528	60.4	.60
(D-11-10)31dad	19,375	155,196	48.9	-999	(D-11-10)13aaa	46,753	174,207	93.4	.46
(D-11-10)28bac	28,136	163,046	83.9	-999	(D-11-10)12ccc	42,474	175,026.	59.6	.48
(D-11-10)27bac	32,933	163,032	20.8	.69	(D-11-10)09dcc	29,076	174,969	41.8	-999
(D-11-10)26add	41,667	161,694	65.3	-999	(D-11-10)09cdd	28,453	174,969	36.7	-999
(D-11-10)25dda	46,888	159,761	112.0	-999	(D-11-10)08ddd	25,690	175,075	32.7	-999
(D-11-10)24aaa	46,826	169,055	92.2	.44	(D-11-10)08add	25,702	179,015	42.8	-999
(D-11-10)22add	36,285	166,962	81.5	.57	(D-10-10)34cbb	34,366	184,444	27.7	-999

[1]All values are in feet from lower left-hand corner (31°59'58", 111°25'13") of U.S. Geological Survey ground-water flow model (Hanson and others, 1990).

[2]Number of significant figures shown for specific capacity and silt-and-clay content may not reflect precision of the various estimates.

[3]Silt-and-clay fraction determined as total sample weight minus weight of sand-and-gravel fractions. Average silt-and-clay content is thickness-weighted average for sediment samples from the upper Tinaja beds.

Table 9. Specific-capacity estimates from various sources for City of Tucson wells in Avra Valley, Arizona

[-999, no information. All values are in feet]

Local well number	Local well name	Latitude	Longitude	Average silt-and-content[1,2]	Specific capacity, in gallons per minute per foot[1]					
					(A)[3]	(B)[4]	(C)[5]	(D)[6]	(E)[7]	(F)[8]
(D-11-10)15add	AF-001	32°28'37"	111°18'13"	-999	71.2	-999	-999	-999	60.7	-999
(D-11-10)22ddd	AF-002	32°27'07"	111°18'17"	.57	40.3	-999	46	45.6	46	-999
(D-11-10)27bac	AF-003	32°26'53"	111°18'56"	.69	20.8	14.5	-999	20.8	-999	-999
(D-11-10)27cdc1	AF-004	32°26'14"	111°18'55"	.69	-999	-999	-999	-999	-999	-999
(D-11-10)27cdc	AF-005	32°26'14"	111°18'55"	.69	14.4	-999	-999	14.4	-999	-999
(D-11-10)29dbc	AF-007	32°26'27"	111°20'43"	-999	-999	-999	-999	-999	-999	-999
(D-11-10)24bda	AF-047	32°27'39"	111°16'43"	.44	-999	-999	-999	-999	-999	-999
(D-11-10)15cdd	AF-057	32°27'59"	111°18'44"	.60	-999	-999	-999	-999	-999	-999
(D-11-10)15ddd	AF-058	32°28'00"	111°18'17"	.60	99.4	-999	100	99.4	100	-999
(D-11-10)22add	AF-059	32°27'32"	111°18'17"	.57	81.5	-999	-999	81.5	-999	-999
(D-11-10)20dcc	W-002	32°27'08"	111°20'51"	-999	59.6	-999	60	59.6	60	11.8
(D-11-10)20ddd	W-003	32°27'08"	111°20'21"	-999	109.2	-999	110	109.2	110	16
(D-12-10)04dcc	AF-009	32°24'30"	111°19'49"	.44	-999	-999	-999	-999	-999	-999
(D-12-10)04ddc	AF-010	32°24'32"	111°19'26"	.44	16.8	13.7	-999	16.8	-999	-999
(D-12-10)09dcd	AF-011	32°23'38"	111°19'35"	-999	7.4	7.5	-999	7.4	-999	-999
(D-12-10)12bcd	AF-012	32°18'53"	111°16'58"	.75	-999	-999	-999	-999	-999	-999
(D-12-10)12ccd1	AF-013	32°23'39"	111°17'00"	.75	23.4	-999	-999	23.4	45.0	-999
(D-12-10)12ccd2	AF-014	32°23'37"	111°16'53"	.75	-999	-999	-999	-999	-999	-999
(D-12-10)31bda	AF-015	32°20'41"	111°21'57"	.28	-999	-999	-999	-999	-999	-999
(D-12-10)33cdc	AF-016	32°20'09"	111°19'53"	.54	8.4	11.5	-999	8.4	-999	-999
(D-12-10)33ddd	AF-017	32°20'09"	111°19'18"	-999	6.2	13.5	28	6.2	28.4	-999
(D-12-10)26add	AF-043	32°21'26"	111°17'16"	-999	15.2	14.6	-999	15.2	26.7	-999
(D-12-10)24cdd1	AF-060	32°21'55"	111°16'43"	-999	25.1	41.3	33	16.5	-999	-999
(D-12-10)24cdd	AF-061	32°21'57"	111°16'44"	-999	-999	-999	-999	-999	-999	-999
(D-12-10)04acd	W-004	32°25'09"	111°19'32"	.44	26.7	-999	-999	-999	-999	26.7
(D-12-10)09ddd	W-005	32°23'39"	111°19'19"	-999	10.3	16.1	26	10.3	26	15.5
(D-13-10)05ddd	AF-023	32°19'17"	111°20'20"	.54	10.4	10.4	60	10.4	60	-999
(D-13-10)06ddd	AF-024	32°19'15"	111°21'30"	-999	21.6	22.5	-999	21.6	20	-999
(D-13-10)20ccd	AF-025	32°16'39"	111°21'08"	.40	7.1	-999	-999	-999	7.7	-999
(D-13-10)22cdd	AF-026	32°16'38"	111°18'48"	-999	12.2	12.2	-999	-999	-999	-999
(D-13-10)23dcc	AF-027	32°16'39"	111°17'38"	-999	22.1	37.3	56	22.1	56	-999
(D-13-10)25dcc	AF-028	32°15'47"	111°16'36"	56	107.3	-999	108	107.3	108	-999
(D-13-10)26ccd	AF-029	32°15'46"	111°17'59"	-999	14.1	13.1	-999	14.1	43.6	-999
(D-13-10)26dcd	AF-030	32°15'46"	111°17'29"	-999	17.5	36.7	100	17.5	100	-999
(D-13-10)25acd	AF-041	32°16'13"	111°16'27"	-999	89.5	56.8	90	89.5	90.3	-999
(D-13-10)25bdc	AF-042	32°16'13"	111°16'50"	-999	24.5	27.8	71	24.5	71.4	-999
(D-13-10)14cdc	AF-044	32°17'32"	111°17'53"	.80	64.5	-999	-999	64.5	-999	-999
(D-13-10)24abb	AF-045	32°17'32"	111°18'16"	-999	29.7	-999	-999	-999	-999	-999
(D-13-10)24dcc	AF-046	32°16'39"	111°16'33"	-999	49.7	-999	50	49.7	50	-999
(D-13-10)22ddd	AF-049	32°16'39"	111°18'16"	.80	14.5	13.4	-999	14.5	-999	-999
(D-13-10)15ddd	AF-050	32°17'32"	111°18'15"	.80	17.0	-999	-999	-999	29.0	-999
(D-13-10)14bcc	AF-051	32°17'57"	111°18'09"	.80	11.2	11.2	-999	-999	-999	-999
(D-13-10)14bcd	AF-052	32°17'55"	111°18'02"	.80	-999	-999	-999	-999	-999	-999

See footnotes at end of table.

Table 9. Specific-capacity estimates from various sources for City of Tucson wells in Avra Valley, Arizona—Continued

Local well number	Local well name	Latitude	Longitude	Average silt-and-content[1,2]	Specific capacity, in gallons per minute per foot[1]					
					(A)[3]	(B)[4]	(C)[5]	(D)[6]	(E)[7]	(F)[8]
(D-13-10)04cdd	AF-053	32°19'17"	111°19'48"	0.54	9.0	9.1	-999	9.0	-999	-999
(D-13-10)04ddd	AF-054	32°19'17"	111°19'18"	-999	14.1	15.8	-999	14.1	-999	-999
(D-13-10)22ccc	IL-001	32°16'30"	111°19'12"	-999	-999	-999	-999	-999	-999	-999
(D-15-10)28cdc	AF-055	32°05'11"	111°19'57"	.32	29.8	23	-999	-999	68.8	-999
(D-15-10)33bcc	AF-056	32°04'45"	111°20'12"	.36	11.4	8.9	9	-999	12.7	-999
(D-16-10)04bda	AF-062	32°04'14"	111°19'30"	-999	111.9	-999	-999	-999	-999	-999
(D-16-10)05ddd	AF-063	32°03'39"	111°20'02"	-999	83.8	-999	-999	-999	-999	-999
(D-16-10)08bdd	AF-064	32°03'13"	111°20'32"	-999	58.2	58.2	-999	-999	-999	-999
(D-16-10)18dba	AF-065	32°02'08"	111°12'26"	-999	2.5	-999	-999	-999	-999	-999
(D-16-10)18dba	AF-066	32°02'08"	111°12'26"	-999	-999	-999	-999	-999	-999	-999
(D-16-10)19cab	AF-067	32°01'21"	111°21'44"	-999	85.1	-999	-999	-999	-999	-999
(D-16-10)29ddd	F-002	32°00'09"	111°20'04"	..19	56.4	-999	-999	-999	-999	56.4
(D-11-11)31cbc	W-001	32°21'01"	111°16'06"	.42	83.1	-999	-999	-999	-999	83.1
(D-12-11)18dcc	AF-018	32°22'52"	111°15'26"	.63	12.9	-999	-999	12.9	-999	-999
(D-12-11)18ddc	AF-019	32°22'53"	111°15'13"	.63	19.0	-999	18	19.0	28.3	-999
(D-12-11)30dcc	AF-020	32°21'08"	111°15'31"	.75	8.3	-999	-999	-999	-999	-999
(D-12-11)30ddd2	AF-021	32°21'08"	111°15'13"	.75	23.5	-999	-999	23.5	23.5	-999
(D-12-11)30ddd1	AF-022	32°21'10"	111°15'04"	.75	4.1	-999	-999	4.1	-999	-999
(D-12-11)20dda	AF-048	32°22'08"	111°14'03"	.53	17.8	-999	-999	-999	-999	-999
(D-13-11)30ccc	AF-031	32°15'48"	111°16'03"	.57	114	-999	114	114	114	-999
(D-13-11)31ccc1	AF-032	32°14'56"	111°16'02"	.57	23.1	22.0	-999	22.8	15.4	-999
(D-13-11)31cdd1	AF-034	32°14'56"	111°15'40"	.57	39.2	-999	-999	39.2	34.4	-999
(D-14-11)04cad	AF-035	32°14'25"	111°13'40"	.37	15.9	14.9	-999	15.9	-999	-999
(D-14-11)05ccd	AF-036	32°14'04"	111°14'54"	.43	46.0	28.4	-999	46.0	-999	-999
(D-14-11)06ccd	AF-037	32°14'03"	111°13'54"	.22	17.9	-999	46	18.6	45.7	-999
(D-14-11)06dcc	AF-038	32°14'04"	111°15'32"	.22	19.7	21.5	-999	30.3	30.1	-999
(D-14-11)07bad	AF-039	32°13'48"	111°15'44"	.22	25.6	33.4	34	25.6	34	-999
(D-14-11)08ccc	AF-040	32°13'10"	111°15'00"	.51	24.1	22.4	-999	22.4	-999	-999
(D-14-11)29ddd	AV-013	32°10'34"	111°14'08"	.16	25.8	26.3	54	26.3	54	-999
(D-14-11)28dcc	AV-014	32°10'34"	111°13'28"	.14	38.6	-999	55	38.6	55	19.9
(D-14-11)34bbc1	AV-015	32°10'21"	111°12'58"	.17	-999	-999	31	-999	31	-999
(D-14-11)34bbc2	AV-015	32°10'22"	111°12'52"	.17	27.5	-999	-999	27.5	-999	28.8
(D-14-11)34aad	AV-016	32°10'21"	111°12'05"	-999	36.3	37.7	29	36.3	29.5	31.2
(D-14-11)27aad	AV-017	32°11'11"	111°12'06"	-999	39.5	39.5	-999	39.5	-999	22.0
(D-14-11)22cbb	AV-018	32°11'47"	111°12'58"	.18	36.4	-999	-999	36.4	-999	30.6
(D-14-11)27bcc	AV-019	32°11'02"	111°12'58"	.13	41.6	-999	-999	41.6	-999	40.6
(D-14-11)28bcb	AV-020	32°11'08"	111°14'00"	.16	60.6	-999	-999	60.6	-999	19.3
(D-14-11)27dcb	AV-021	32°10'41"	111°12'27"	.09	-999	-999	-999	-999	-999	51.0
(D-14-11)33bdd	AV-022	32°10'10"	111°13'36"	.14	38.5	-999	-999	38.5	-999	-999
(D-14-11)33ccc	AV-023	32°09'44"	111°13'59"	-999	41	-999	41	41	41	-999
(D-14-11)33dcd	AV-024	32°09'44"	111°13'21"	-999	28.2	-999	50	28.2	50	-999
(D-14-11)34ccc	AV-025	32°09'44"	111°12'57"	-999	27.6	34.1	49	27.6	49	-999
(D-15-11)15ccc	AV-001	32°07'08"	111°12'54"	.43	18.8	19.3	-999	18.8	-999	13.1
(D-15-11)15ddd	AV-002	32°07'08"	111°12'03"	.56	-999	-999	-999	-999	-999	10.8

See footnotes at end of table.

Table 9. Specific-capacity estimates from various sources for City of Tucson wells in Avra Valley, Arizona—Continued

Local well number	Local well name	Latitude	Longitude	Average silt-and-content[1,2]	Specific capacity, in gallons per minute per foot[1]					
					(A)[3]	(B)[4]	(C)[5]	(D)[6]	(E)[7]	(F)[8]
(D-15-11)22ddd	AV-003	32°06'17"	111°12'02"	0.51	-999	-999	-999	-999	-999	9.7
(D-15-11)22ccc	AV-004	32°06'16"	111°12'57"	.19	6.6	-999	-999	6.6	-999	5.5
(D-15-11)15bbb2	AV-005	32°07'53"	111°12'55"	.62	18.5	-999	-999	18.5	-999	13.1
(D-15-11)15aaa	AV-006	32°07'54"	111°12'03"	.58	-999	-999	-999	-999	-999	10.0
(D-15-11)20aaa	AV-007	32°07'03"	111°14'04"	.48	13.0	-999	-999	13.0	-999	9.8
(D-15-11)11add	AV-008	32°08'28"	111°11'04"	-999	37.5	36.2	32	37.5	32.0	32.8
(D-15-11)12ccc	AV-009	32°08'02"	111°08'24"	.11	29.3	-999	-999	29.3	-999	-999
(D-15-11)11bbb	AV-011	32°08'47"	111°11'56"	.03	38.0	-999	-999	38.0	-999	41.0
(D-15-11)09aaa	AV-012	32°08'47"	111°13'06"	.24	28.4	-999	-999	28.4	-999	26.8
(D-15-11)12dca	RF-001	32°08'08"	111°10'14"	.03	-999	-999	-999	-999	-999	-999
(D-15-11)12dca	RF-002	32°08'08"	111°10'14"	.03	-999	-999	-999	-999	-999	-999
(D-15-11)12dca	RF-003	32°08'09"	111°10'15"	.03	-999	-999	-999	-999	-999	-999
(D-16-11)08bdb	F-001	32°03'17"	111°14'40"	.21	11.3	-999	-999	-999	-999	11.3
(D-16-11)09aca	F-003	32°03'26"	111°13'03"	.25	8.7	-999	-999	-999	-999	8.7

[1]Number of significant figures for average silt-and-clay content and specific capacity may not reflect precision of various estimates.

[2]Silt-and-clay fraction determined as total sample weight minus weight of sand-and-gravel fractions. Average silt-and-clay content is thickness-weighted average for sediment samples from the upper Tinaja beds.

[3]Value accepted as representative for this study. Priority in choice of value was aquifer test, Clifton (1981), and other sources, respectively.

[4]University of Arizona Soils, Water, and Engineering Department data base or the 1966–68 average seasonal value.

[5]White and others (1966).

[6]Clifton (1981).

[7]Average pre-1960 value.

[8]Average pre-1988 Tucson Water well-efficiency value.

Table 10. Average silt-and-clay content for upper Tinaja bed sediments for selected wells in Avra Valley, Arizona

[ft, foot; -999, no information]

Local well name	X location (ft)[1]	Y location (ft)[1]	Average silt-and-clay content[2,3]	Land-surface altitude (ft)	Local well name	X location (ft)[1]	Y location (ft)[1]	Average silt-and-clay content[2,3]	Land-surface altitude (ft)
TA-16	13,602	243,307	0.12	1,858	GARCIA	47,298	118,240	0.46	2,093
TA-17	25,736	243,165	.11	1,853	CONEHO	52,864	114,186	.47	2,125
TA-18	29,129	235,173	.42	1,878	REIKER	71,394	114,249	.41	2,393
TA-19	26,635	230,332	.66	1,854	NELSON	62,290	109,216	.28	2,295
TA-20	26,605	220,634	.43	1,849	PRATT	61,602	108,308	.30	2,280
TA-2	33,451	222,330	.61	1,910	TA-51	56,798	108,924	.27	2,193
TA-15	29,577	213,856	.36	1,864	YECKLEY	52,330	106,308	.38	2,149
TA-13	37,016	213,228	.23	1,920	WR-45	52,331	106,409	.67	2,154
TA-14	45,485	213,609	.37	2,010	NEWELL	56,445	104,480	.45	2,190
LAB.2617	3,297	208,290	.30	1,785	TA-48	55,408	101,048	.20	2,198
APS	37,407	200,296	.47	1,908	TA-33	54,709	95,696	.27	2,194
TA-21	51,612	200,764	.09	2,040	COLEMAN	57,717	97,406	.73	2,230
MCLAUGHLIN	69,908	192,542	.35	2,290	WR-24	55,394	95,189	.45	2,202
PACKER	56,471	192,772	.36	2,090	LARSON	61,315	94,166	.32	2,305
TA-22	55,005	187,724	.35	2,024	TA-49	59,594	92,149	.11	2,274
MESSINA	69,634	183,350	.21	2,210	MCFARLAND	62,685	92,446	.26	2,330
BUCK	74,089	185362	.32	2,280	NONAME.2	63,282	90,222	.35	2,336
VALLES	41,518	169,877	.49	1,920	WR-29	41,376	85,324	.40	2,242
SOUTHWEST	30,979	168,493	.60	1,910	TA-42	67,135	84,760	.04	2,370
SILVERBELL	29,692	167,789	.78	1,910	TA-43	72,527	74,749	.10	2,374
STARKEY	31,200	156,369	.58	1,945	TA-46	84,530	59,477	.10	2,404
TA-23	61,919	178,213	.10	2,043	CLAUSE	94,073	63,405	.35	2,512
TA-24	68,924	169,713	.03	2,045	WR-33	36,790	42,000	.30	2,460
TA-25	79,610	157,068	.24	2,043	WR-34	41,928	34,410	.20	2,505
WR-43	31,230	137,882	.70	2,004	BATISTE	25,160	34,762	.32	2,530
NONAME.1	20,343	138,119	.50	2,020	WORDEN	24,463	31,734	.44	2,537
LAB.2407	18,523	132,367	.05	2,080	MCKINNEY	39,425	30,780	.31	2,532
TA-38	79,342	149,896	.14	2,041	HAYNIE	63,382	54,664	.38	2,335
TA-47	72,228	149,200	.31	2,035	WR-32	56,222	42,659	.43	2,434
TA-39	68,282	147,490	.24	2,035	LONGFELLOW	53,599	26,960	.33	2,620
HIGH.SCHOOL	62,683	133,257	.53	2,080	TA-45	89,427	58,663	.14	2,429
RICHINS	49,803	125,710	.67	2,062	WR-35	36,918	26,444	.21	2,570
TA-32	61,469	126,997	.13	2,102	WR-37	32,339	19,588	.20	2,647
RILLITO	82,941	150,092	.45	2,056					

[1]All values are in feet from lower left-hand corner (31°59'58", 111°25'13") of U.S. Geological Survey ground-water flow model (Hanson and others, 1990).

[2]Silt-and-clay fraction determined as total sample weight minus weight of sand-and-gravel fractions. Average silt-and-clay content is thickness-weighted average for sediment samples from the upper Tinaja beds.

[3]Number of significant figures for average silt-and-clay content may not reflect precision of various estimates.